NORTHWESTERN UNIVERSITY

Spontaneous and Catalyzed Nucleosome Accessibility

A DISSERTATION

SUBMITTED TO THE GRADUATE SCHOOL IN PARTIAL FULFILLMENT

OF THE REQUIREMENTS

For the Degree

DOCTOR OF PHILOSOPHY

Field of Biochemistry, Molecular Biology, and Cellular

Biology/ Interdepartmental Biological Sciences Program

By

Hannah Suzanne Tims

EVANSTON, IL

December 2007

ABSTRACT

Spontaneous and Catalyzed Nucleosome Accessibility

Hannah Suzanne Tims

Packaging of DNA into nucleosomes and chromatin not only enables DNA to fit within the nucleus, but it also protects and organizes DNA. However, the wrapping of DNA around histones occludes DNA from binding proteins in solution. Proteins that regulate, express and repair DNA are able to function only when occluded DNA is unwrapped to make it accessible. There are two mechanisms by which buried and occluded DNA is exposed to solution. These are: spontaneous transient unwrapping of DNA from the nucleosome, and catalyzed movement of nucleosomes by chromatin remodelers.

To study spontaneous accessibility we used fluorescence resonance energy transfer (FRET) systems to monitor structural changes in the nucleosome. We developed and improved a method for stopped flow FRET studies and used it to probe the rate of unwrapping DNA from the nucleosome. Sites far inside the nucleosome become accessible spontaneously only on very long timescales of minutes or tens of minutes as equilibrium accessibility and rates of unwrapping buried DNA are reduced by orders of magnitude. This delay could have a direct affect on gene activation for targets buried deeply inside nucleosomes. We show that binding of a protein to a target site inside the nucleosome destabilizes the wrapping of DNA further inside that nucleosome, increasing the equilibrium accessibility and, potentially, the rate of unwrapping. This mechanism appears to be in broad use at promoters, where important regulatory binding sites often occur multiple times in close proximity.

Another mechanism for increasing nucleosome accessibility is through chromatin remodeling complexes that catalytically move nucleosomes to expose buried target sites. Our

studies focus on the mechanism of the chromatin remodeling enzyme Imitation SWItch (ISWI) alone and in complex with Acf-1 (ACF). Earlier studies suggested that the active forms of ISWI and ACF were likely dimers. Here we show that although ISWI and ACF cooperatively bind to nucleosomes, their ATPase enzymatic activity is not dependent on dimerization, suggesting that they can function as monomers in ATP-dependent chromatin remodeling. Finally, we have developed a new high resolution mapping procedure that will allow the step size of ISWI induced nucleosome movement to be measured.

Acknowledgements

First and foremost, I would not have begun this journey, much less gotten this far, or had as much fun with out God. He has been feeding me ideas of all sorts for the last 27 years, and I trust He will continue to be my source of hope, joy, peace, love, and scientific thoughts.

I must thank my Family for their constant support and dedication to me, for their blind faith in my choices, and for pushing me to be more than I thought I could be.

I owe a debt of gratitude to all of the folks with GCF, who have been my family in grad school, and taught me to integrate faith, learning and practice. Thanks to Kristen for reminding me that God knows the answers to everything, including any questions my committee asks.

To all my labmates who are my other family here. Thanks for making it worthwhile day to day. You have made working fun, challenging, and rewarding. Special thanks to Gu who made it all begin, and continues to be a source of inspiration. Extra Especially thanks to Karissa, without whom nothing would have ever worked, and who is a constant friend and support, and an invaluable source of encouragement. Thanks scientifically and (especially) otherwise to Michael, Dan, Yvonne, Irene, Gabe (for help at the end and beyond! To ensure that histones continue to live a cold, dark existance), Annie (for reprieve from all the sciency stuff), Kristen, Amy, Erbay, and Georgette- who kept me sane, is a friend, confidant, encouragement, friend (did I already say that?), and who will be missed oh, so much!, it has been pure joy to sit next to you and work with you the last four years. You are all excellent scientists, and I have learned much from you.

Special thanks to PHDcomics.com for hours of entertainment. They have been eerily true to life, and a blessed assurance that it's not just me who feels this way.

Thanks to Gamma, Delta, Epsilon and Zeta Beta for hours of entertainment, and for loaning me money when I really needed a snack.

Thanks to all the 'tea time' folks, you have made staying that extra hour just that much easier. Thanks too, to all the Mondragon lab people for being good neighbors.

I thank my committee members for helpful suggestions on my project, and their genuine support and interest both in me and my project.

And finally, thanks to Jon who has been an excellent boss. I can only hope to be as ingenious one day! Thank you for the hours spent thinking about my papers, projects, and mistakes. Thank you for being a good teacher, challenging my speakin' and writin' skills, and for being patient with me when explaining the same thing for the tenth time. Thank you for helping me to see the bigger picture, both in research, and in grad school, I have enjoyed learning and working with you.

This thesis is dedicated, with love, to my Grandfather, LeRoy Broberg, who was a big thinker, excellent craftsman, and changed the world with an 8th grade education. He was a man of God, a loving father and grandfather, and he believed in me.

List of abbreviations

FRET Fluorescence Resonance Energy Transfer

TE 10 mM Tris 1mM EDTA pH 8.0

TBE 90 mM Tris-Borate 2 mM EDTA

DTT Dithiothreotol

PMSF Phenylmethylsulfonyl Floride

BZA Benzamadine

βME 2-mercaptoethanol

MPA 3-Mercaptopropionic Acid

OP 1-10 phenanthroline

ISWI Imitation Switch

ACF ATP-dependent Chromatin-assembly Factor

SWI/SNF Switch/Sucrose Non Fermenting

DO Donor only

DA Donor acceptor

Nuc. nucleosome

bp basepair

PCR Polymerase chain reaction

Table of Contents

List of Figures

Chapter 5 **Methods for Mapping Nucleosome Dyad Position with Basepair Resolution**

Chapter 6 **Chromatin Remodeling by ISWI/ACF**

Chapter 1

Introduction

Introduction

In vivo, genomic DNA is packaged and organized into chromatin to protect it from damage and regulate access. The basic unit of chromatin is the nucleosome, 147bp of DNA wrapped ~1.6 times around an octameric histone core made of two copies each of H3, H4, H2A and H2B [1]. Through interactions that are not fully understood, strings of nucleosomes are condensed by favorable internucleosomal contacts with DNA and/or histone tails, and with additional packaging proteins, to form closely spaced, folded, and packed chromatin fibers (Figure 1) [2]. Nevertheless, chromatin in vivo is not a homogenous assembly of tightly packaged and condensed nucleosomes. Rather, it has regions of condensed heterochromatin that are transcriptionally silenced by the addition of linker histones and modifications on DNA and histones that mark silenced regions. Other regions of DNA are less densely packaged into euchromatin, which is marked by an extended nucleosome packing structure and histone acetylation (for review see [3-5]). Although euchromatin regions are less compact than heterochromatin, the euchromatic DNA remains nucleosome bound and compacted when not actively transcribed.

The crystal structure of the nucleosome [1] reveals that DNA wrapped into nucleosomes is sterically occluded, by the histone octamer and by the adjacent gyre of DNA, from proteins whose DNA target binding sites are buried in the nucleosome (Figure 2). Additional biochemical data prove that access to nucleosomal DNA is reduced by many orders of magnitude compared to naked DNA [6, 7]. Since genomic DNA is packaged into nucleosomes throughout the cell cycle, target sites buried in nucleosomes are inaccessible until the DNA is unwrapped from the nucleosome [8]. How proteins involved in DNA replication, expression, repair, recombination,

Figure 1

DNA is organized in vivo into nucleosomes that compact by internucleosomal contacts to form a 30nm fiber, and higher compacted chromatin structures. Depiction from Felsenfeld and Groudine (2003) [2] of the many levels of compaction of DNA into chromatin.

Figure 1

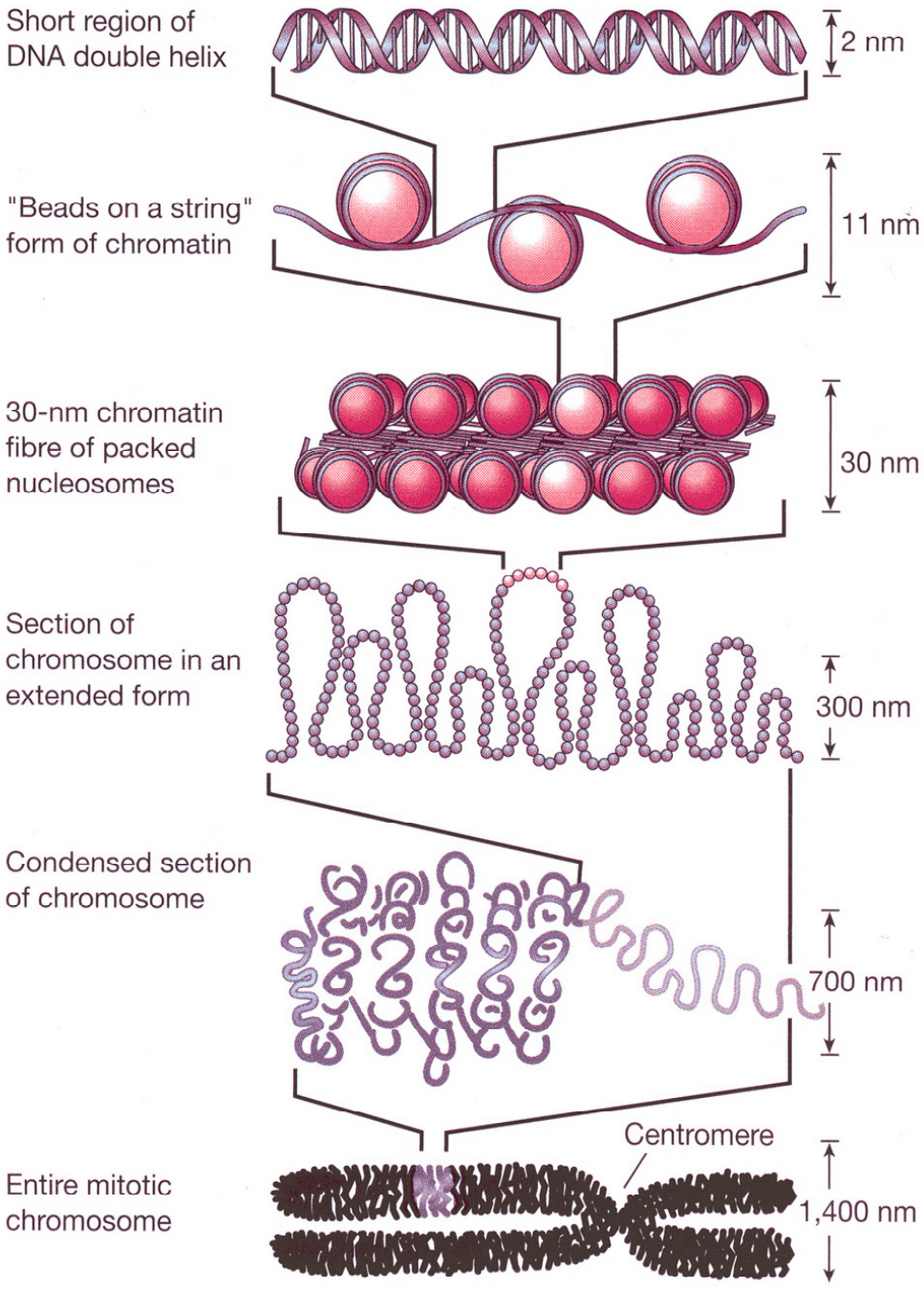
Short region of DNA double helix
2 nm
"Beads on a string" form of chromatin
11 nm
30-nm chromatin fibre of packed nucleosomes
30 nm
Section of chromosome in an extended form
300 nm
Condensed section of chromosome
700 nm
Centromere
Entire mitotic chromosome
1,400 nm

Figure 2

The crystal structure from Luger and Richmond at 2.8Å resolution [1]. Histones (colored center) are wrapped by 1.7 turns of DNA (shown in white). Binding the histone octamer and the adjacent gyre of DNA occludes DNA from binding proteins in solution.

Figure 2

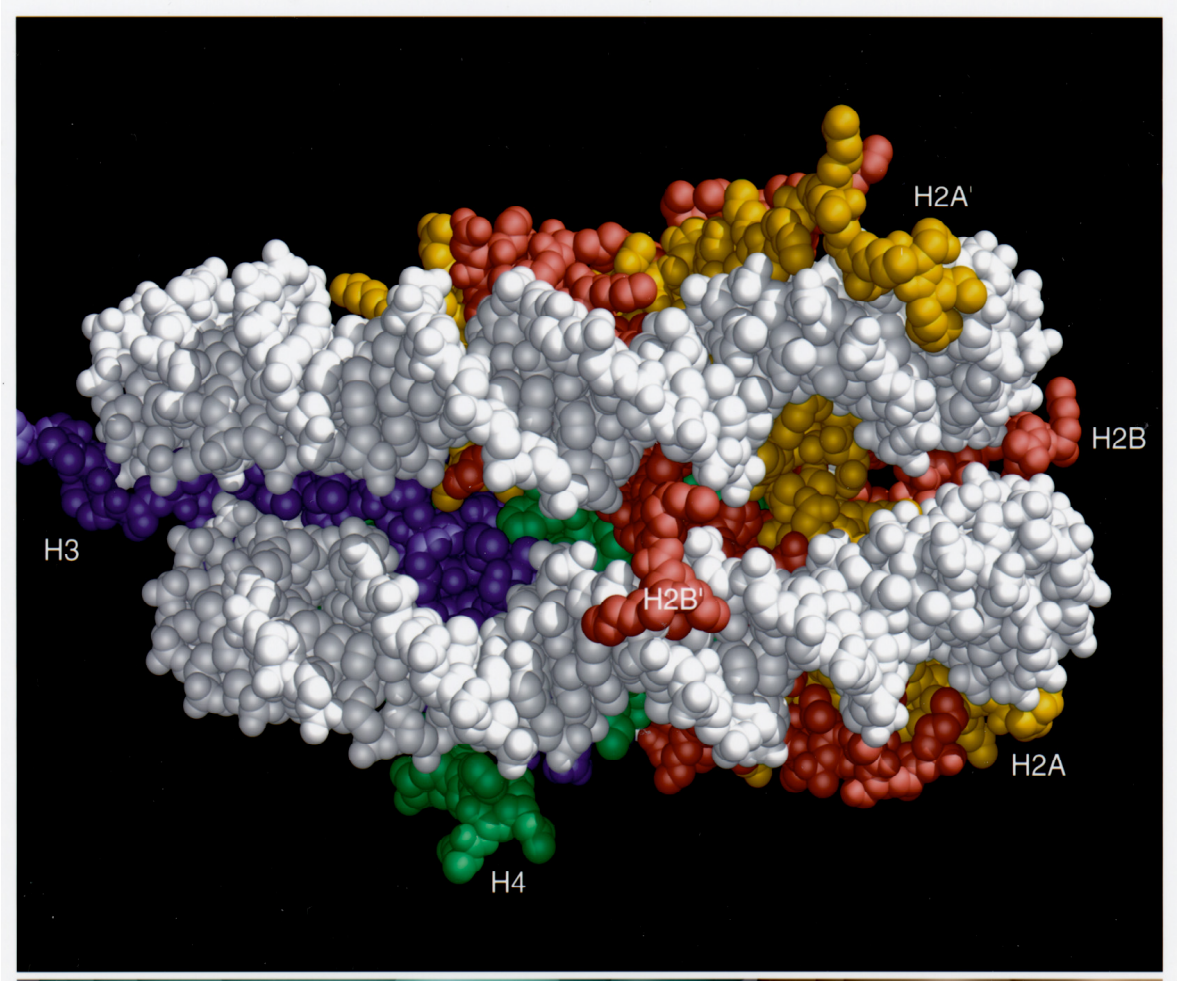

and gene regulation are able to function in an environment where their primary substrate is occluded from binding is not understood. It is clear that although genomic DNA is tightly packaged, there are mechanisms to make the DNA accessible to target proteins in a timely manner [9]. These are: spontaneous unwrapping of DNA from the histone core [8], and enzyme catalyzed remodeling of nucleosomes (Figure 3) [10]. My thesis research investigated both of these mechanisms.

Spontaneous accessibility of nucleosomal DNA occurs by a partial unwrapping of DNA from the histone octamer core, providing access to previously buried regions of both DNA and histones [6, 8, 11]. This partial unwrapping makes DNA near nucleosome edges easily accessible, but access to DNA buried further in the nucleosome remains severely restricted [7, 11]. The binding of multiple proteins to sites within a single nucleosome occurs cooperatively and increases occupancy of the proteins beyond what they can achieve acting individually [12]. In contrast, catalyzed exposure of buried targets occurs through the action of ATP-dependent remodeling enzymes. These enzymes move nucleosomes to new locations, or remodel the nucleosome structure, in either case making DNA that was previously buried more accessible (Figure 3) [10, 13, 14].

Histone Exchange

The protein core of the nucleosome comprises an octameric assembly of histone proteins. One ordinarily expects protein assemblies to be in continuous dynamic exchange equilibrium with free (unassembled) protein monomers. This expectation, however, raises a problem for chromatin function. Heterochromatin and euchromatin depend in part on modifications carried

Figure 3

Exposure of buried nucleosomal DNA occurs through spontaneous unwrapping, or catalyzed movement of the nucleosome. Spontaneous unwrapping allows fast access to DNA sites near nucleosome edges, but very slow access to sites buried further inside. Collaborative competition of binding proteins for targets inside the nucleosome increase accessibility to buried targets. Catalyzed movement of nucleosome position along DNA occurs through the activity of chromatin remodeling complexes, and can both expose buried sites, and bury accessible sites, thus regulating access.

Figure 3

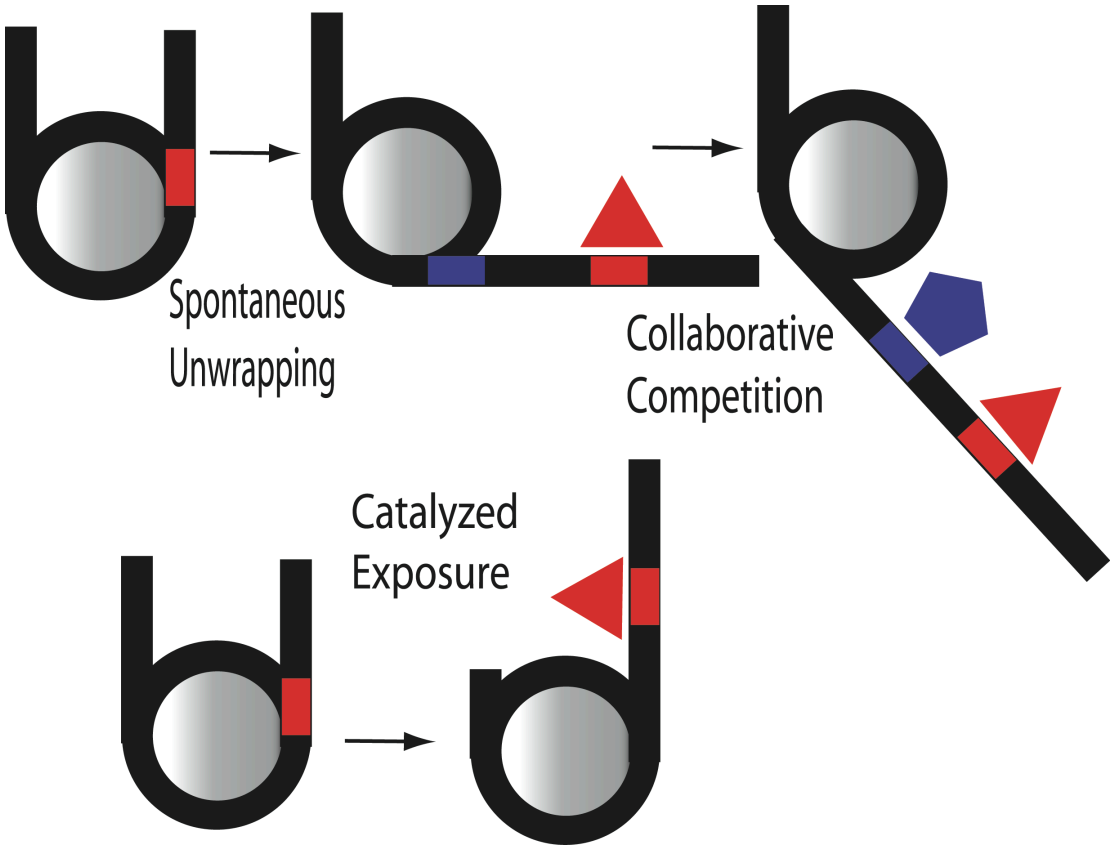
Spontaneous
Unwrapping
Collaborative
Competition
Catalyzed
Exposure

on the histone tails [3-5]. These epigenetic marks are inherited from one generation to the next, and must be maintained within a defined region of DNA to maintain silenced or active chromatin in appropriate DNA regions. If the histones carrying these critical epigenetic marks were in continuous free exchange, it is difficult to understand how epigenetic states could remain stable over time and through generations.

The simplest way that these epigenetic marks could be maintained on a given stretch of DNA is by stable association of the histones on that stretch of DNA – that is, if the histones simply do not exchange. The DNA wrapped around each nucleosome protein core might act as a cage to prevent spontaneous histone exchange. However, exposing buried target sites requires unwrapping DNA from the histone core, which in turn exposes the histone octamer to solution, thereby potentially allowing the expected histone exchange to occur. Additionally, the activity of polymerases and chromatin remodeling complexes disrupt nucleosome structure completely, further exposing and potentially destabilizing the histone octamer [15]. Indeed, even native nucleosomes show some characteristics of a system in a dynamic assembly/disassembly exchange equilibrium [16].

We used a FRET assay to test how stably the histones are associated with a given nucleosome under various increasingly extreme perturbations of the nucleosome structure. We show that histones manage to remain stably associated with their original nucleosome over long times, even despite complete transient disruption of nucleosome-DNA contacts by RNA polymerases. This remarkable property of the octameric histone complex facilitates the maintenance of stable epigenetic marks on nucleosomes, and thereby also the maintenance of stably inherited epigenetic states.

Spontaneous Accessibility

Site exposure, the unwrapping of nucleosomal DNA starting from one end and proceeding inward, was proposed and studied extensively in our lab (Figure 3) [6-8, 11, 17]. Using an indirect assay of restriction enzyme accessibility to buried nucleosomal DNA vs. naked DNA, the equilibrium unwrapped state of the nucleosome was observed. These studies revealed that DNA buried far inside the nucleosome remains accessible, but much less so than for DNA near the ends of nucleosomes, and up to 10^4- to 10^5-fold less accessible than naked DNA [7, 18]. Using FRET dye pairs on the nucleosome to measure structural changes allows a direct detection of which parts of the nucleosome move to allow access to buried sites, and provides access to rates of unwrapping. Further tests of nucleosome accessibility used FRET to directly test accessibility of nucleosomal DNA near the edges, yielding results that agree with the enzymatic assays [11]. Subsequent assays show that spontaneous DNA fluctuations occur with similar probability for individual nucleosomes and for test nucleosomes in the middle of long strings of nucleosomes (M.G. Poirier, J. Widom unpublished observations).

These unwrapping conformational fluctuations that make buried DNA transiently accessible are fast and allow proteins to bind target sites near the nucleosomal ends ~2-5 sec^{-1} [19]. However, enzymatic studies show that, as DNA target sites are moved further into the nucleosome, the sites become progressively less accessible, decreasing by 2–4 orders of magnitude, suggesting that the rate of spontaneous unwrapping of sites far inside the nucleosome might be similarly decreased. Such a decrease in rate of spontaneous accessibility at sites deep inside the nucleosome might result in significant temporal delays in gene expression. Recent single cell studies of gene activation events show that there is indeed a large diversity in response

time between different genetically identical cells in a population [20, 21]. This delay in response time could be due to variation between individual cells in the exact locations of nucleosomes that occlude a critical binding site in one cell, but not in another.

To answer these questions, our experiments extend the previous analyses of spontaneous accessibility to sites buried deep inside the nucleosome. Using FRET dye pairs probing structural fluctuations in the interior of the nucleosome, and with nucleosomes containing buried target sites for site specific DNA binding proteins, we monitor nucleosome structural rearrangements during partial DNA unwrapping, and measure the rate of unwrapping buried DNA.

Our experiments show that for proteins to access target sites, even when buried deep inside the nucleosome, DNA must unwrap from the octamer from one end and proceed inward, as previously hypothesized by the site exposure model [6, 8]. We developed an improved procedure for stopped flow FRET measurements, allowing detection of two color changes in FRET to be measured simultaneously from nM solutions on the sub-second timescale. This robust method was used to determine the rate of DNA unwrapping as DNA target sites were moved further inside the nucleosome. We find that the reduced accessibility of buried targets corresponds to a similarly reduced rate of unwrapping to expose the buried target sties. The rate of unwrapping decreases by at least an order of magnitude for each 10 base pairs that the target site is pushed further inside the nucleosome. The rate of this resulting very slow unwrapping corresponds well with what has been observed on the single cell level for the time delay in activation of a gene for two genetically identical cells [21]. Thus we conclude that the detailed nucleosome positioning can strongly affect gene regulation and activation, and that relatively minor (e.g., 10 bp) changes in nucleosome location can cause significant changes in gene response times.

One mechanism that cells can use to increase accessibility of buried targets is cooperative binding of proteins to target sites buried inside the same nucleosome. This cooperative binding, or collaborative competition, of target proteins inside a nucleosome has been shown to occur both in vitro and in vivo [12, 22]. The model implies that occupancy by a protein of a DNA target site inside a nucleosome destabilizes the DNA wrapping in that nucleosome, thereby facilitating binding of a second protein. Evidence of collaborative competition as a mechanism used by cells to increase accessibility of target sites is shown at promoters where important regulatory sites occur multiple times in close proximity (for example [23]). However, this coupling of the binding of one protein to the destabilization of the rest of the wrapped DNA in that nucleosome has never been directly observed. Using FRET-labeled nucleosome constructs, we show directly that binding a protein to a target site near the nucleosome edges destabilizes the wrapping of DNA further inside.

The discovery of chromatin remodeling proteins proves that spontaneous unwrapping, while contributing significantly to accessibility, is not the end of the story [10, 24]. Chromatin remodelers function to catalytically expose, or bury, critical DNA target sites, and are implicated at many promoters as contributing to gene regulation. However, they too are not the end of the story, as recent studies on accessibility of damaged DNA in yeast, show that DNA repair enzymes can access and repair damaged DNA on timescales faster than remodelers have been shown to function [9]. Thus, cells maintain a carefully regulated and balanced accessibility of their nucleosomal DNA, using both spontaneous and catalyzed mechanisms.

Catalyzed accessibility: chromatin remodelers

Chromatin remodelers were initially identified by the inability of mutants in the swi2 protein to appropriately activate genes for sucrose fermentation when their carbon source was switched [25-27]. Further studies showed that chromatin remodelers are integral to proper activation of gene expression at many promoters [28-30]. Chromatin remodelers assemble or disassemble, move or remove, and rearrange nucleosomes in an ATP-dependent manner. This is a key regulatory mechanism at many promoters which functions by making DNA target binding sites more, or less accessible, by changing positioning of nucleosomes. In vivo studies of nucleosome site accessibility catalyzed by remodeling factors have looked at the gene regions affected by the remodelers, as well as the net affect remodelers have on gene expression [30-32]. Through antibody staining of specific remodeling complexes, the cell or life cycle timing during which the remodelers act have also been studied [33].

Chromatin remodelers, notwithstanding the similarity of their functions, exist in a diverse set of remodeling complexes, and are differentially recruited to specific genes or regions to perform various tasks [34]. There are three main classes of SWItching/Sucrose Non Fermenting (SWI/SNF) remodelers involved in positively or negatively regulating gene expression, related by the sequence and activity similarities of their ATPase domains [35]. The SWI/SNF family are transcription activators that function by remodeling or disrupting nucleosomes. ISWI (Imitation SWItch) containing complexes are involved in transcription regulation through chromatin assembly and nucleosome mobilization. Mi2/CHD complexes are transcription repressors, functioning by nucleosome mobilization and by complexing with histone deacteylases to promote transcriptional silencing [34, 36-38]. These remodelers exist in the context of complexes consisting of a central enzymatic ATPase core protein closely related to the original swi2 mutant, together with additional proteins that modify the activity of the motor domain. The catalytic

subunits of remodeling complexes are also closely related by sequence to the larger DEAD box family of ATPases [39-41]. Although very little is known about the detailed mechanism of SWI/SNF related proteins, much information can be gained by structural and mechanical comparisons of the larger family of ATPases, and can help to shed light on the mechanism of remodeler activity.

Mechanistic studies of remodeling complexes show that these highly related enzymes have diverse structural effects on nucleosome structure, which likely stem from variations on a shared mechanism of nucleosome modification [34]. Generally, remodeling complexes are proposed to function by anchoring on a nucleosome, translocating along that nucleosome's DNA to pull in a loop or bulge of DNA, which can then propagate through the nucleosome to effectively move the nucleosome to a new location [24]. Such a translocation could be accomplished by two distinct potential mechanisms: introducing twist defects, or longer bulges of DNA, into the nucleosome [42]. (Twist defects may also be considered to be one base pair long bulges.) Assays with gaps and nicks in the DNA have shown that the torsional strain required for twisting is not required for remodeling [43, 44]. These same assays revealed a DNA translocation activity of remodelers, since gaps on one side of the remodeler, but not the other, stall nucleosome movement [45]. Together these results argue against the twisting mechanism for remodeling. DNA translocating activity is also conserved in the larger family of DEAD box ATPases, many of which are DNA translocating enzymes [39-41]. Thus studies of this broader class of enzymes may reveal aspects of chromatin remodeling mechanisms.

We have studied Drosophila Imitation switch (ISWI) chromatin remodeler, which exists in vivo in the context of several different protein complexes, the simplest of which is ACF [46-49]. Although ISWI exists only in complex with other proteins in vivo, it has been shown to

maintain catalytic nucleosome moving activity when functioning alone in vitro [46]. Thus ISWI alone is a useful simplified system for study of remodeler mechanism. Moreover it provides an opportunity to compare activity of ISWI alone or in complex with Acf-1 (ACF). Understanding the mechanism of ISWI remodeling activity will help us to understand what aspects of nucleosome structure are modified, and whether any inherent characteristics of nucleosomes (such as spontaneous DNA site exposure) are harnessed during remodeling activity. We will also gain a fuller understanding of the mechanistic steps in ISWI-induced nucleosome movement, as well as the role of remodelers in making nucleosomal DNA more or less accessible.

We used a series of biochemical assays to test the enzymatic activity and nucleosome mobility output of ISWI and ACF. To conserve precious reagents, and because we need to simultaneously measure ATPase activity and nucleosome moving, we developed a simple small scale assay for ATPase activity, using buffers that can also be used for nucleosome mobility assays. We used thin layer chromatography (TLC) to separate free phosphate from ATP for quantification of the ATPase activity of ISWI. We find that ISWI and ACF are highly activated by natural chromatin and nucleosomes and, to a lesser extent, by naked DNA. ACF shows an intrinsic spacing activity in vitro and in vivo, which, together with data showing cooperativity of ACF and ISWI binding DNA and nucleosomes, suggests that ISWI may be a functional dimer [50-52]. We test the dependence of ISWI and ACF ATPase activity on ISWI and ACF concentration, and prove that their ATPase activities are not linked to dimerization. Thus our results suggest that these remodelers can function as monomers, notwithstanding their ability to dimerize.

A critical goal of our work is to elucidate what these nucleosome remodeling enzymes accomplish with the hydrolysis of a single ATP. Specifically, we chose to ask, how far along the DNA is a nucleosome translocated when a remodeler undergoes a single ATPase cycle. To address this question, we developed a method for high resolution mapping of nucleosome positions before and after ISWI induced nucleosome movement. Mapping takes advantage of a histone H4 S47C mutation located near the nucleosome dyad, to which we attach a chemical that allows for hydroxyl radical mapping chemistry. We map the location of the nucleosome dyad axis with basepair resolution, by monitoring the hydroxyl radical cleavage sites, which flank the dyad symmetrically. This method is also very useful in other nucleosome mapping experiments.

Our studies of the ISWI and ACF ATPase activities define the binding constants of ISWI and ACF to nucleosomes, and the conditions in which single enzymatic turnovers may be observed. Thus, we can pre-bind ISWI or ACF to a nucleosome, rapidly add ATP, wait for a short time such that each remodeler undergoes zero or one ATPase cycles, then quench the reactions, and map the new locations of the nucleosomes chemically, at single basepair resolution. In this way, we will determine how far ISWI and ACF can move a nucleosome in one ATP turnover step.

Access to buried nucleosomal target sites is tightly regulated by the intrinsic structural characteristics of the nucleosome, as well as by chromatin remodeling complexes. Our studies of the mechanisms used to make buried target sites more accessible show that, while spontaneous fluctuations of DNA away from the histone core provides rapid access to sites near nucleosomal edges, access to sites further inside the nucleosome is possible only after long times. Accessibility can be increased by cooperative binding of proteins to targets inside the

nucleosome making buried DNA more available by first binding a protein near the edges. We also show that the activity of ISWI and ACF are not dependent on dimerization, and we provide a method for detailed analysis of ISWI induced nucleosome movement.

Chapter 2

Fluorescence Resonance Energy Transfer (FRET) and Stopped-flow FRET for Analyses of Nucleosome Conformational Changes and Dynamics

Fluorescence Resonance Energy Transfer (FRET) and Stopped-flow FRET for Analyses of Nucleosome Conformational Changes and Dynamics

Introduction

The packaging of DNA in chromatin creates obstacles that occlude the binding of regulatory proteins to their DNA target sites, and occlude the access of polymerases, repair, and recombination enzymes to their DNA substrates. These obstacles occur with even the lowest level of chromatin organization, the wrapping of DNA locally around a histone protein octamer into a nucleosome. How these obstacles are overcome in vivo, allowing these many multi-protein complexes access to their target sites and substrates when needed, is not known.

Our laboratory has been investigating one possible answer to this question, which involves a dynamic accessibility that is intrinsic to nucleosomes themselves. Early studies using restriction enzymes as probes of accessibility of nucleosomal DNA showed that nucleosomes exist in a dynamic conformational equilibrium in which the wrapped nucleosomal DNA spontaneously partially unwraps, such that stretches of the buried DNA are constantly, but transiently, fully accessible, as though they are naked DNA. We refer to this behavior as "site exposure". The equilibrium constant for site exposure – the fraction of time that a given stretch of DNA acts as though it is freely-accessible naked DNA – can be surprisingly large: as much as 0.01–0.1 (i.e., 1–10%) of the time (depending on the DNA sequence) for sites just inside from the end of the nucleosome, decreasing progressively to 10^{-4}–10^{-5}, for sites in the middle of the nucleosomal DNA. These results suggested a mechanism for site exposure in which the wrapped nucleosomal DNA spontaneously unwraps starting from one end of the nucleosome, and

progressing inward, likely in steps of DNA helical turns (~10 bp). Subsequent biochemical studies proved that site exposure occurred not by nucleosome sliding, as some had imagined, but by partial unwrapping, leaving the remainder of the wrapped DNA fixed on the histone octamer. Recent studies suggest that not only is site exposure an intrinsic property of nucleosomes in vitro, but it appears to be functionally important in vivo. A remarkable cooperative binding behavior predicted by the site exposure model occurs in vivo [22]; and studies on UV photodamage repair by photolyase in vivo suggest that the rate is too fast to be consistent with remodeling factor action and must instead reflect intrinsic nucleosome dynamics [9].

Biochemical studies revealed the existence of intrinsic nucleosomal site exposure, but are unable on their own to test the hypothesis that nucleosomal DNA unwraps from an end, and they did not provide access to the rates of site exposure and re-wrapping. The fluorescence resonance energy transfer (FRET) experiment provides an ideal solution to these needs [53]. FRET represents the nonradiative transfer of energy from a fluorescence donor (D) to an acceptor (A), whose absorption spectrum must overlap partially with the emission spectrum of D. The hallmark of FRET is that when one excites D, one observes less fluorescence emission from D than would otherwise be expected (in the absence of A), and, if A is itself a fluorophore, one detects excess emission intensity from A owing to the transfer of excitation energy from D to A ("sensitized emission"). The efficiency of FRET depends on the sixth power of the actual distance (R) between D and A, relative to a characteristic transfer distance, R_0 (the distance between D and A at which FRET occurs with 0.5 probability). Changes in FRET may be monitored, among other ways, by detecting changes in quenching of the donor or changes in sensitized emission of the acceptor. A beauty of the FRET experiment is that R_0 values for common dye pairs are in the several nm range, and thus the FRET efficiency is a sensitive

function of nm-scale *changes* in distance between D and A. A second important feature of FRET is that it is a nanosecond timescale process; and thus may be continuously read to report on slower timescale molecular dynamics.

In earlier work our laboratory used steady-state FRET to show that nucleosomal DNA unwraps starting from one end [11]; and we and others have used it to characterize the relative stability of nucleosomes (Chapter 3) [54] and the conformational changes that result upon binding of a site specific DNA binding protein [11, 55]. In subsequent work we used FRET in conjunction with fluorescence correlation spectroscopy (FCS) and stopped-flow mixing, to measure the rates of unwrapping and re-wrapping of nucleosomal DNA [19]. Current studies investigate the rates of site accessibility at sites further inside the nucleosome (Chapter 4), and the dynamic nucleosome conformational changes that are driven by ATP-dependent [50] or ATP-independent nucleosome remodeling factors and chaperones. These processes can occur on the hundreds of milliseconds to many seconds timescale, and thus may be too slow for conventional free solution FRET-FCS. However, this same timescale is ideal for analysis by stopped flow mixing coupled with FRET, which gives convenient access to timescales from a few milliseconds on up. Thus we expect that the basic procedures that others and we have developed will prove to be of broad utility in studies of nucleosome dynamics. Here we describe how to design, set up, and execute such a stopped-flow FRET study on nucleosomes.

Experimental design

Overall strategy

This broad approach to analysis of conformational dynamics has several requirements that must be met. One must have a way to drive the dynamics to be studied, so that there will be

a significant change in the average state of the system between the beginning and end of the experiment. Moreover, it must be possible to rapidly turn on this driving force by mixing two reagents together. Finally, one must have a way of quantitatively monitoring the evolution of the system in real time, as the system progresses through the reaction.

In our case, we wish to study spontaneous nucleosome unwrapping. We create a driving force by coupling nucleosome unwrapping to the binding of a site specific DNA binding protein that would like to bind to a nucleosomal target site, but can't – until the nucleosome unwraps to make the previously buried site accessible. This process can be initiated by mixing together two solutions, one containing the nucleosomes in buffer, the other containing the site-specific binding protein in buffer. Studies of ATP-dependent proteins can often initiate reactions by rapid addition of ATP. Again in our case, since we wish to study specific conformational changes, FRET provides an ideal real-time readout.

In the studies described here, we use the *Escherichia coli* repressor protein LexA as an arbitrarily chosen site specific DNA binding protein that can only bind to its target site when that stretch of DNA has been unwrapped from the surface of the histone core of the nucleosome (Figure 1A). Even at the lowest LexA concentrations that suffice to yield a detectable FRET change (i.e., that trap and stabilize a significant fraction of nucleosomes in the unwrapped state), the LexA binding is fast and stable in comparison to DNA unwrapping-rewrapping times [19]; thus, LexA binding can be used to trap nucleosomes in a partially unwrapped conformation. At the start of the reaction, most nucleosomes have fully wrapped DNA (small equilibrium constant for unwrapping); after addition and binding of LexA at sufficient concentrations, most nucleosomes have significantly unwrapped their DNA and have been trapped in this state by LexA binding.

Figure 1

System used for analysis of nucleosome conformational dynamics. A. The site exposure model. Donor and acceptor fluorophore locations are indicated by D and A respectively. The location of a binding site for LexA protein is shown hatched. DNA unwrapping from the nucleosome must precede LexA binding, and is rate limiting. B. Crystal structure of the nucleosome [16]. Dye-labeled residues shown in space filling representation. The DNA region containing the LexA binding site is shown in red as sticks. The FRET donor dye Cy3 (cyan) is attached to the DNA at the 5' end. The FRET acceptor dye Cy5 (magenta) is attached to V35 of histone H3 V35C, C110A. Since there are two copies of histone H3 in the nucleosome, there are two sites of attachment of Cy5: one close to Cy3 giving efficient FRET, and one that is too far away from Cy3 to give significant FRET.

Figure 1

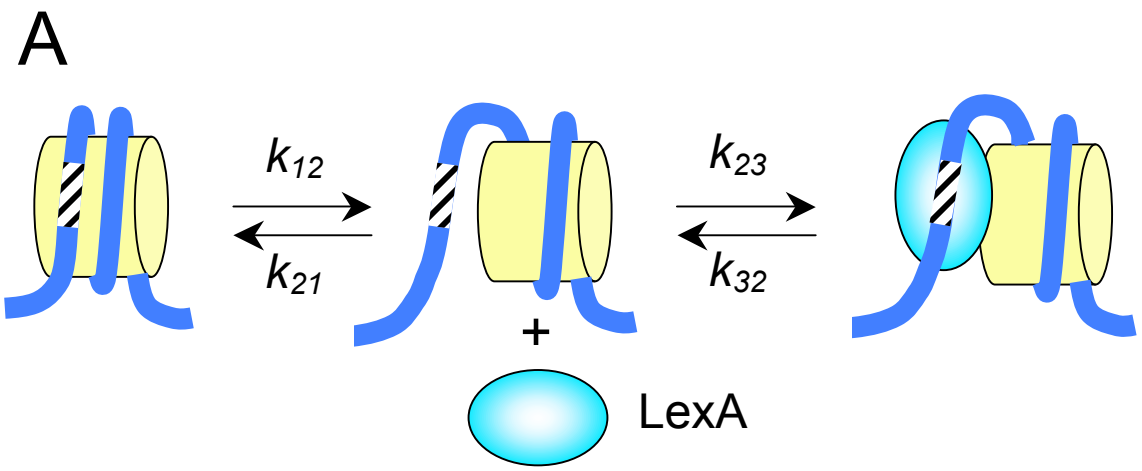

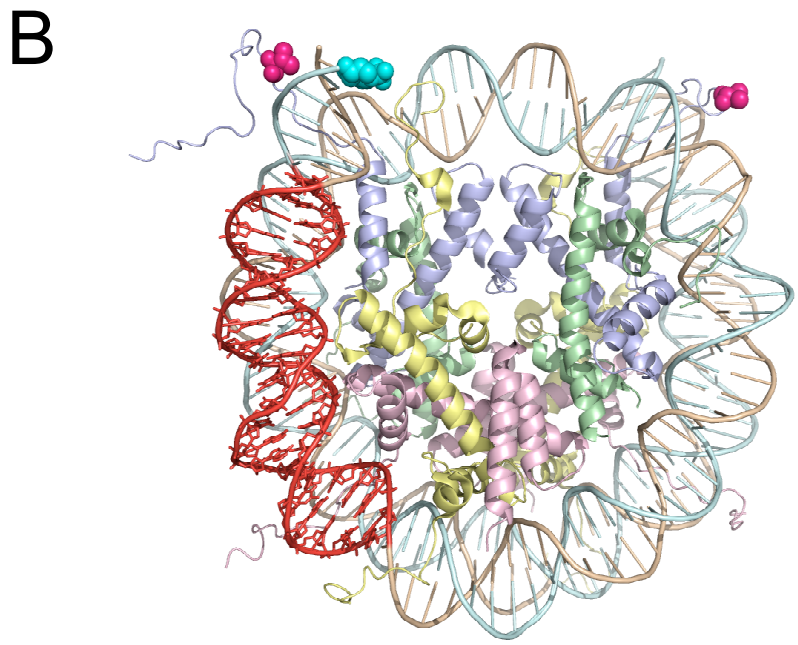

We choose locations for the FRET dyes such that the distance between D and A changes greatly when the DNA unwraps. One good choice, which we have used repeatedly, is between one end of the wrapped DNA and an adjacent region on the histone core, either histone H3 V35C or histone H2A K119C (Figure 1B).

Routine biotechnology allows dyes to be placed anywhere desired along a nucleic acid. The protein chemistry is more constrained, with only cysteine modification being both easily accomplished and adequately specific. Therefore it is necessary to have proteins in which any exposed free cysteines have been mutated away, and a single new one introduced at a desired location. Of course, having access to sequence alignments showing phylogenetically conserved residues, and to X-ray crystallographic structures, is enormously helpful.

One other important technical detail in experimental design bears mention. The histone octamer contains two molecules each of four different histone proteins, arranged in a complex with two-fold rotational symmetry (dyad symmetry). This means that there will be two engineered cysteines in the complex, not one. In such circumstances it may be beneficial to label the protein with the acceptor dye, and the DNA with the donor. This strategy will place one of the two A's nearby D, ensuring highly efficient FRET, while the other, (designated A' in Figure 1B) will be too far to exhibit any significant FRET. This strategy allows a full range of FRET efficiency, from 0–1, to be observed. Nanometer-scale increases in distance from D to the closer A will then be manifested as changes in FRET efficiency, while changes in distance to the further A will be invisible. In contrast, if one reversed the labeling (two D's on the protein, one A on the DNA), then the highest possible FRET efficiency is only 0.5, greatly compressing the dynamic range of the experiment.

FRET Dye Pair

We generally utilize acceptors that are also fluorophores, as this allows additional ways to quantify FRET [53]. The characteristic distance for energy transfer R_0 depends, among other things, on the degree of spectral overlap between the emission spectrum of D and the excitation spectrum of A. Many of the most commonly used dye pairs have R_0's of approximately ~5–6 nm. Because of the strong (sixth power) dependence of FRET efficiency on D–A separation distance (R) relative to R_0, such dye pairs yield large changes in FRET efficiency if R, changes from rather less than R_0 to rather greater (or vice versa). We therefore choose the locations of A on the histone octamer so as to place one of the two A's close to D when nucleosomes are in the native state, in the expectation that a large change in D–A distance will occur when the DNA unwraps to allow binding by LexA protein.

We use the especially popular pair Cy3 (as D) and Cy5 (A), which have R_0 of ~5–6 nm, because of their relatively great photostability. We attach a single Cy3 to the 5' end of DNA. We attach the Cy5 acceptor fluorophore via maleimide chemistry to a unique cysteine mutation introduced in the solvent exposed tail of histone H3 (V35C, C110A). The double mutation in histone H3 removes a cysteine that is naturally present, replacing it with a new unique cysteine at the desired location. Alanine is chosen as the replacement for the original C110, as this mutation is unlikely to be strongly destabilizing, moreover it occurs naturally in the otherwise nearly perfectly conserved sequence of histone H3 between *Xenopus* and yeast. We find empirically that labeling at these sites does not detectably affect the formation or stability of reconstituted nucleosomes. From the crystal structure of the nucleosome, these labeling sites on H3 are ~2 nm or ~7 nm away from D (Figure 1B), thus we expect ~100% efficient FRET to the near acceptor, and negligible FRET to the further dye.

Donor-labeled DNA construct

To ensure a high degree of homogeneity in the reconstituted nucleosomes, we assemble the nucleosomes on a derivative of the selected high affinity nonnatural nucleosome positioning sequence, "601" [56]. Using the 147 bp 601 nucleosome positioning sequence and separate stages of PCR amplification, we introduce a binding site for LexA covering nucleotides 8—27 (taking position 1 as the left hand end), and a Cy3 fluorophore at the 5' position of nucleotide 1. The orientation of DNA relative to histones is known from the crystal structure of the nucleosome, while the orientation of LexA bound on its target site is known from modeling and biochemical studies. The detailed location of the LexA site is chosen so that the face of DNA that will be occupied by LexA is oriented inward, wrapped against the histone protein core. Thus the LexA target site is inaccessible to LexA until the DNA unwraps. The LexA binding site does not significantly change the ability of 601 to position nucleosomes [57]. 5' Cy3 end labeled primers are purchased commercially, and are incorporated via PCR to fluorescently label the end of DNA nearest the LexA binding site (Figure 1).

Following PCR synthesis, the dye labeled full length DNAs are purified either by reverse-phase HPLC, or by extraction from an acrylamide gel. HLPC purification was done with a Zorbax column (Agilent), using a 10–15% (v/v) gradient of acetonitrille (ACN) in 0.1 M triethanolamine acetate (TEAA), pH 7.0, at a flow rate of 1ml/min over 20 minutes. We monitor absorbance at both 260 and 550 nm to detect DNA and Cy3 respectively. ACN was removed from pooled peak fractions using a SpeedVac (Savant), and the DNA exchanged into 0.1 x (v/v) TE buffer (TE is 10 mM Tris, pH 8.0, 1 mM EDTA) using Centricon 30 filters (Amicon). Gel extraction of DNA from acrylamide gels gives lower total yield of DNA, but is quick, easy, and yields DNA of high purity. Here DNA was run on a 5% acrylamide gel in 1/3x TBE, and full

length DNA was cut from the gel, and extracted by electroelution or crush and soak methods [58]. Concentrations of DNA and Cy3 are measured by UV-visible absorbance spectroscopy. We obtain DNAs with stoichiometries of 1 Cy3 per DNA, within (small) experimental error, implying complete labeling of the DNA.

Histones

Histones are expressed, purified, and refolded as described [59]. Histone octamers are refolded to a final concentration of 1mg/ml (~9 μM) in 0.5ml volume of 2 M NaCl, 20 mM HEPES, pH 7.3. Refolded histone octamers are reduced with 100-fold molar excess Bond-Breaker TCEP solution (Pierce) for 10 minutes at room temperature. Cy5 maleimide (Amersham Pharmacia Biotech) comes as aliquots to label 1mg of protein, and is dissolved in 50 μl dimethylformamide (DMF; Pierce) immediately before use as recommended. The maleimide dye is sensitive to photobleaching, so we take care to reduce light exposure by working in dimmed room light, and covering the tubes with aluminum foil. Additionally, maleimide dyes are minimally soluble in aqueous solutions, and are unstable in all solutions, and should be used within hours of dissolving in DMF. Half of the resulting dye stock solution is added slowly to the reduced histones, with mixing to reduce precipitation. The reaction is incubated for 2 hours at room temperature, then overnight at 4°C, with constant gentle mixing using a Labquake shaker. The reaction is quenched by addition of 100-fold molar excess 2-mercaptoethanol. Labeled histone octamer is stored in the quenched labeling reaction at 0°C until use. Excess unreacted dye is purified out of the octamer solution during the dialyses and sucrose gradient ultracentrifugation steps used in the nucleosome reconstitution and purification. In practice, we find ~70–95% labeling efficiency of maleimide dye. We have not succeeded in purifying

unlabeled histone H3 or histone octamer away from labeled.

LexA protein

LexA protein was prepared from expression plasmid pJWL228 (gift of J. Little, University of Arizona, Tucson) and purified to near-homogeneity as described [60].

Nucleosome Reconstitutions

Dye labeled 601 DNA is reconstituted into nucleosomes along with a 2.5-fold (w/w) excess of salmon sperm carrier DNA, at a total DNA to histone ratio of 2.2:1 (w/w), to increase the efficiency of nucleosome formation, similar to our previous work [8]. Reconstitution reactions are carried out in a final volume of 150 μl containing 43 μg salmon sperm carrier DNA, 17 μg specific Cy3-labeled DNA and 27 μg of Cy5-labeled histone octamer in TE, 2M NaCl, plus protease inhibitors (1 mM benzamidine hydrochloride, 0.5 mM phenylmethylsulfonyl fluoride (PMSF)). Donor-only constructs were prepared using unlabeled H3 V35C C110A histone octamer. All nucleosomes are reconstituted by double salt dialysis as described [57]. Any non-nucleosomal aggregates, and histones bound to the salmon sperm DNA, are purified away from FRET dye pair labeled nucleosomes through sucrose gradient ultracentrifugation as described [56]. Purified nucleosomes are stored in 0.5 x TE at 0 °C. Nucleosomes reconstituted on 601 DNA are indefinitely stable at 0 ˚C or room temperature.

Setting up the experiment

Equilibrium accessibility

In order to know how to set up the kinetic experiment, one must first understand the equilibrium (steady state) behavior of the system to verify the direction and magnitude of any FRET changes that are then to be monitored over time by stopped flow. For our case involving nucleosome unwrapping coupled to LexA binding, this means that we need to first characterize the FRET changes occurring during equilibrium titrations with increasing LexA in solution. Using the FRET double-labeled nucleosomes, we measure steady state fluorescence emission spectra as LexA is titrated into solution. We excite the samples at 515 nm, which directly excites Cy3, but gives little direct excitation of Cy5; we then switch the excitation wavelength to 610 nm to directly excite the Cy5 with no excitation of Cy3. (This second measurement allows for an absolute measurement of FRET efficiency even when the degree of labeling by acceptor is less than 100%.) The emitted light first passes through a 550 nm colored glass cut on filter to eliminate any scattered excitation light, and then into the emission monochrometer. We scan the emission monochrometer from 525 to 750 nm, or 625 to 750 nm, (for 515 and 610 nm excitation respectively). Figure 2B shows the results of a titration of 7 nM nucleosomes with 0 nM to 3 μM LexA. Figure 2A shows a control experiment in which the nucleosomes were labeled with donor only, to verify that LexA binding did not significantly alter the color or quantum yield of the Cy3 donor. The absolute FRET efficiency during the titration is plotted in Figure 2C. This representation of the data serves to define the isotherm for binding of LexA to nucleosomal DNA, while both this plot and the raw spectra themselves give the sign and magnitude of fluorescence changes to be expected upon LexA binding in the stopped-flow experiment.

In fact, in some of the systems we have analyzed, there do occur significant changes in donor quantum yield (quenching or enhancement) that are not attributable to FRET, and are even

Figure 2

Steady state fluorescence analysis of LexA binding titrations. A. Donor only nucleosomes were titrated from 0 to 3 μM LexA. A small LexA-dependent increase in fluorescence intensity is detected at the highest LexA concentrations. B. FRET labeled nucleosomes exhibit a LexA concentration dependent decrease in sensitized acceptor fluorescence, and concomitant increase (de-quenching) of donor fluorescence. C. FRET efficiency as determined by the ratio A method [11, 53].

Figure 2

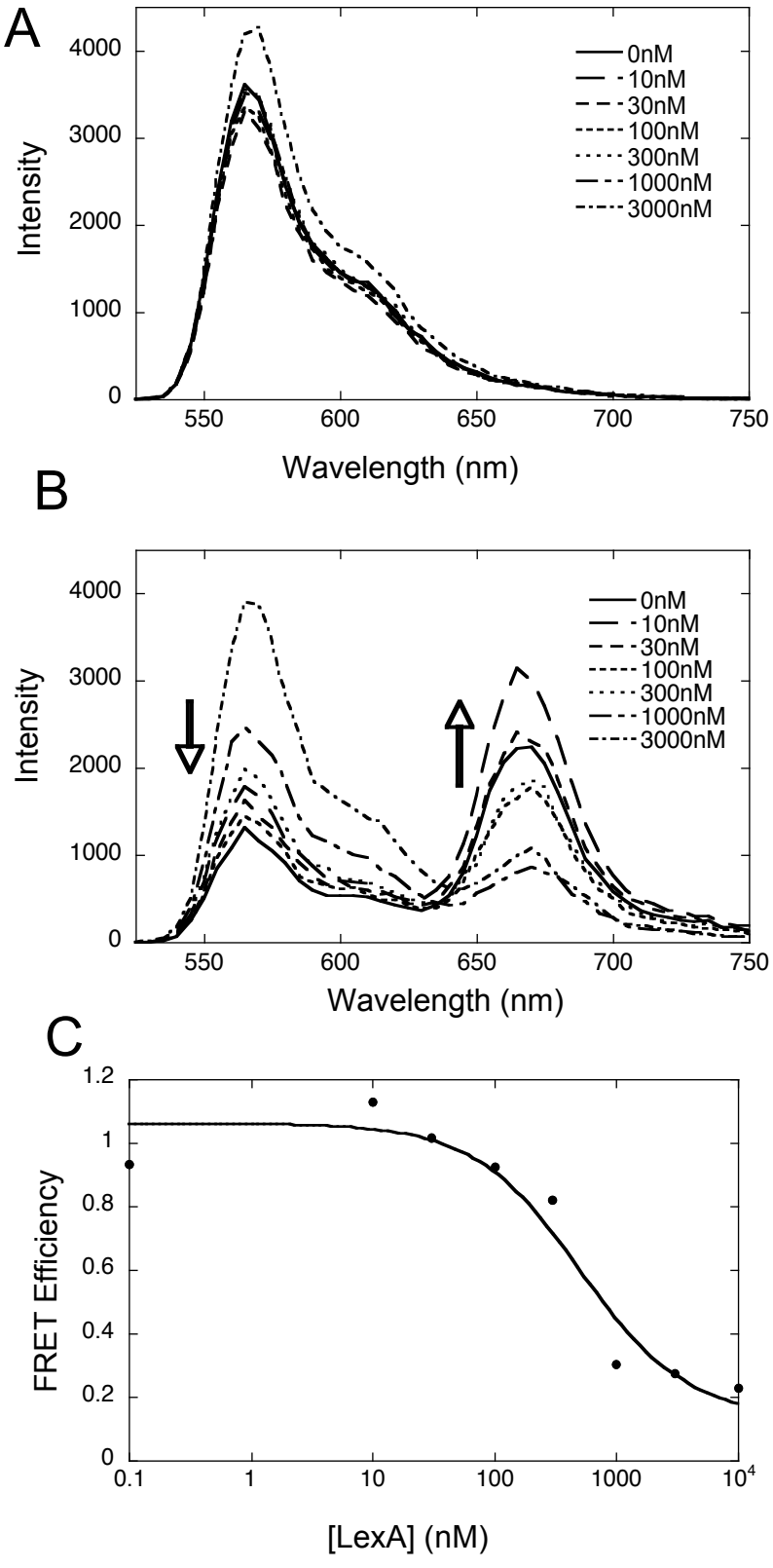
A
4000
3000
2000
1000
0
Intensity
550
600
650
700
750
Wavelength (nm)
0nM
10nM
30nM
100nM
300nM
1000nM
3000nM
B
4000
3000
2000
1000
0
Intensity
550
600
650
700
750
Wavelength (nm)
0nM
10nM
30nM
100nM
300nM
1000nM
3000nM
C
1.2
1
0.8
0.6
0.4
0.2
0
FRET Efficiency
0.1
1
10
100
1000
10^4
[LexA] (nM)

observed in samples labeled with donor only. For example, binding of a protein to a dye-labeled DNA can frequently lead to increases or decreases in fluorescence emission. In that case, depending on the exact question being asked, one may not need to go to the trouble of doing the real FRET experiment, but may be able to determine key kinetic parameters in a simpler stopped-flow fluorescence intensity experiment.

FRET calculations

FRET efficiency can be measured for samples in several ways. In our analysis we use absolute FRET efficiency calculations based on the ratio A method [11, 53]. We choose an excitation wavelength that gives efficient excitation of donor with minimal direct excitation of acceptor, and the fluorescence emission spectrum (from both donor and acceptor) is measured. Then the acceptor is directly excited by a longer wavelength light to collect the total possible acceptor fluorescence. FRET efficiency is calculated as the ratio of acceptor fluorescence from FRET to the total acceptor fluorescence from direct excitation. This gives the absolute FRET efficiency, and is useful when the acceptor can be directly excited independently of the donor.

If, as in our experiments, solvents or reagents added to solution alter the photophysics of the dyes, the proximity ratio is a useful alternative way to quantify FRET changes [61]. Proximity ratio is defined as the fluorescence from the acceptor divided by the total fluorescence from the system (donor and acceptor fluorescence together). We use the proximity ratio both for quantification of steady state LexA titrations, as well as stopped flow FRET changes.

Stopped-flow instrument

Our stopped-flow instrument is an Applied Photophysics model SX.18MV. The

instrument can be thermostatted, but for simplicity we use it at room temperature (~23 ºC). LexA binding to nucleosomes is monitored by the resulting changes in FRET, following the decrease in sensitized emission from Cy5, and the concomitant increase (de-quenching) of Cy3 emission. The instrument is configured to excite the samples with a xenon lamp and an excitation monochrometer centered at 500 nm. The Cy3 and Cy5 fluorescence emission signals are measured using appropriate filter combinations to isolate the light from Cy3 only or Cy5 only, which then impinges on two photomultiplier tubes (PMT's), one for each emission channel (Figure 3). In some cases the sensitivity may be further improved by replacing the excitation monochrometer with an appropriate bandpass filter.

Filters

It is necessary to choose filters that are capable of isolating the light emitted by the two fluorescent dyes from each other and from scattered and Raman-shifted excitation light. Otherwise, at the nM concentrations of many biochemical experiments, including ours on nucleosomes, scattered or Raman-shifted excitation light can completely overwhelm the fluorescence emission, leading to highly misleading apparent results. Scattered excitation light is centered at the same color as the excitation light itself. Unless a laser source is used, the excitation light will ordinarily have some significant spectral width, e.g., from an 8 or 16 nm bandpass in the excitation monochrometer, with significant spectral power extending out to many times this bandpass. In contrast, Raman-shifted excitation light is shifted toward the red by a constant amount of energy (the first vibrational level of the solvent), which equates to a variable number of nm shift depending on the excitation wavelength.

One must therefore choose the excitation wavelength and bandpass, and the emission

Figure 3

Schematic illustration of the stopped flow instrument, as set up for simultaneous recording of Cy3 and Cy5 fluorescence intensities in photomultiplier tube (PMT) 2 and 1, respectively.

Figure 3

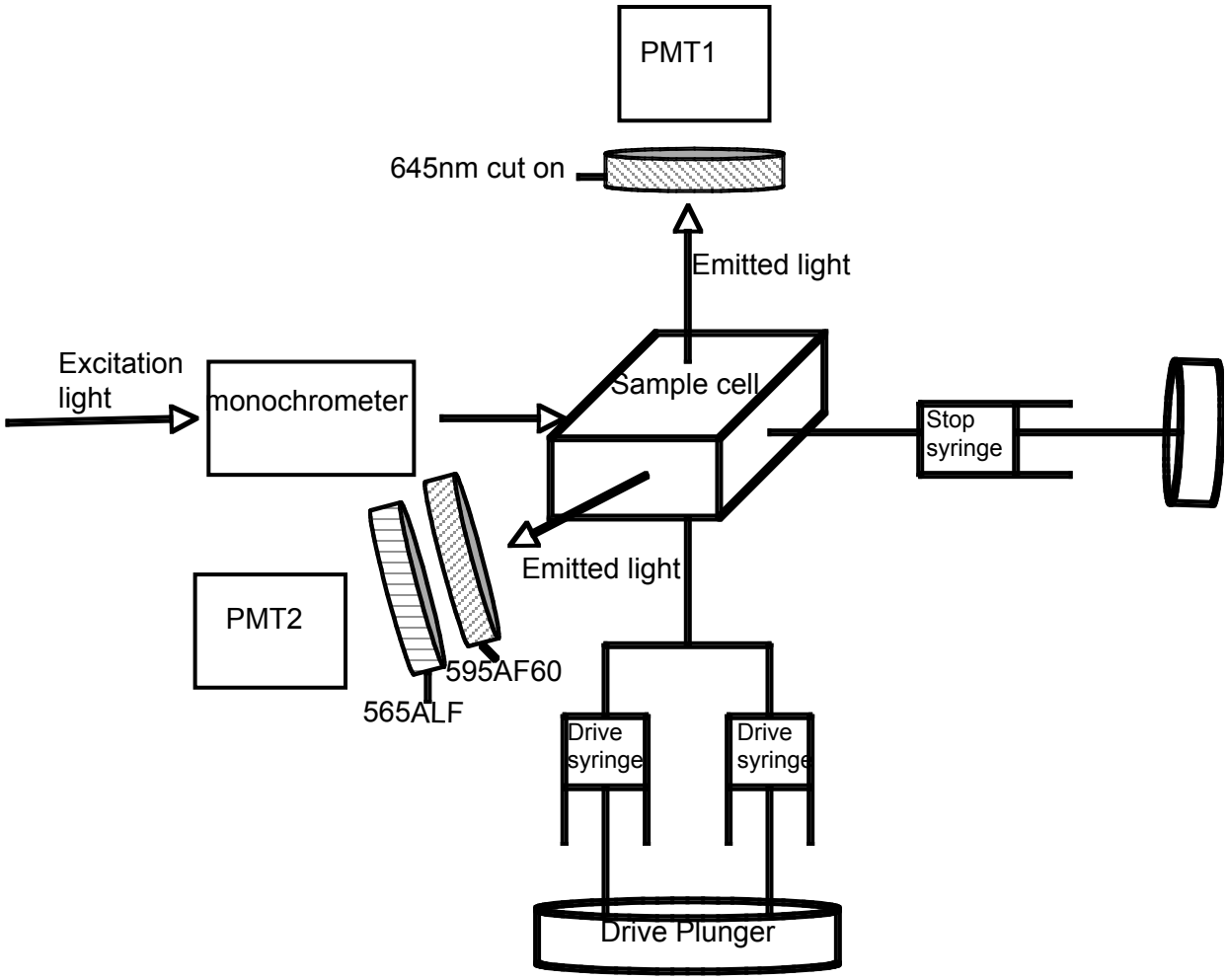
PMT1
645nm cut on
Emitted light
Excitation light
monochrometer
Sample cell
Stop syringe
Emitted light
PMT2
595AF60
565ALF
Drive syringe
Drive syringe
Drive Plunger

filter combinations, intentionally retaining as much of the emission intensity as possible, while adequately suppressing the signals from scattered and Raman-shifted light. To measure how well this has been accomplished, one need only measure the emission signals from buffer in the absence and presence of fluorescent sample.

In our previous stopped-flow FRET experiments we analyzed emission from Cy5 only. We excited the Cy3 donor using an excitation monochrometer set at 515 nm, and collected light emitted from the Cy5 acceptor, while eliminating most Cy3 emission, and scattered and Raman-shifted excitation light, using a 645 nm cut-on (long pass) colored glass filter [19]. This setup works well, but it would be desirable to detect changes in Cy3 fluorescence at the same time. This requires a second emission channel, with a bandpass filter set chosen to pass the majority of Cy3 fluorescence, while not overlapping with either the scattered or shifted excitation light, or with Cy5 emission. For this purpose we are at present using a combination of a colored glass 550nm cut on filter (Thor Labs), a 565ALP cut-on filter and a 595AF60 bandpass filter (Omega Optical) (Figure 3). The bandpass filter on its own effectively isolates Cy3 emission from Cy5, but allows too much scattered excitation light through. The additional cut-on filters help to reduce this otherwise problematic non-fluorescence background (Figure 4A). For an excitation wavelength of 500 nm, the peak of Raman-shifted light occurs at 610 nm. This falls within the bandpass region of our Cy3 emission filter, but accounts for less than 1% of the light that enters the PMT (Figure 4B).

Even with these precautions, we observe a substantial background of stray excitation light in the Cy3 channel. This (time-independent) background has to be subtracted off, which leaves the remaining (time-dependent) fluorescence signal quite noisy, at nM concentrations of Cy3-labeled molecules. We continue to use the colored glass 645 nm cut on filter for Cy5 light,

Figure 4

Transmission and emission spectra. A. Transmission spectra of the optical filters used for stopped-flow analysis of Cy3 and Cy5 fluorescence. Cy3 emission is isolated by a combination of 565AFL and 595AF60 filters, while Cy5 emission is isolated with a 645 nm cut-on filter. B. Steady state emission spectra recorded by a conventional fluorometer of TE buffer only, or of buffer + 7 nM Cy3 147 bp DNA, in the absence (no filter, NF) or presence (with filters, F) of the filters used in the stopped flow experiment. Note the increased emission intensity at the shortest wavelengths in the Cy3 147 bp DNA sample when filters are not used. This is the tail of the direct excitation light scattered by the sample, which degrades the signal to noise ratio, it is effectively eliminated by the filters used.

Figure 4

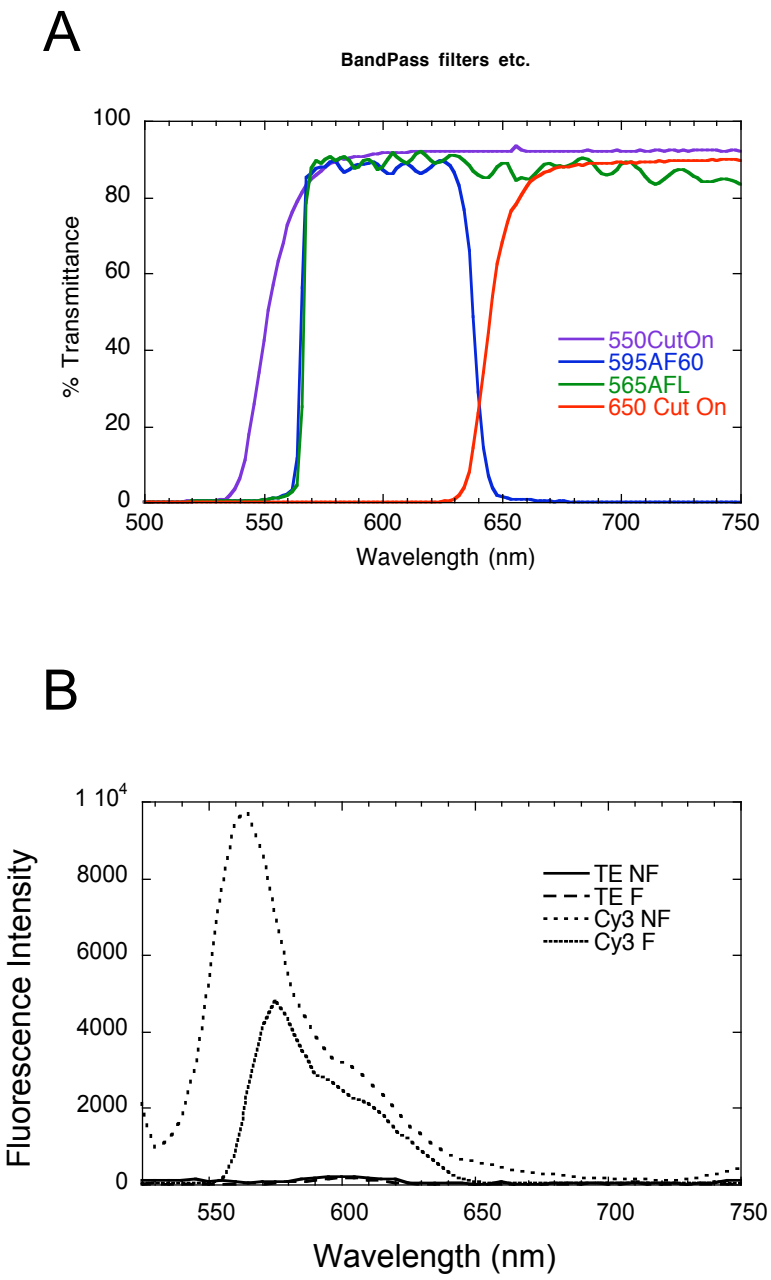
A
BandPass filters etc.
% Transmittance
Wavelength (nm)
550CutOn
595AF60
565AFL
650 Cut On
B
Fluorescence Intensity
Wavelength (nm)
TE NF
TE F
Cy3 NF
Cy3 F

which provides a high signal to noise ratio even at nM concentrations.

Software

There are several important considerations when setting the software parameters for the instrument. First, if the timescale for change is unknown prior to the experiment, one needs to sample over a wide range of time. Additionally, some samples may exhibit multiphasic changes in fluorescence, in which case data must be collected over distinct time scales simultaneously. Our instrument provides both a linear and a logarithmic timebase; the latter allows one to collect rapid time points at short times, capturing any rapid processes, while still allowing longer times to be appropriately sampled in the same run. If there is only one rate, or if two rates are not widely separate, it suffices and may be better to use linear time sampling. Once one knows the timescale of the most-rapid process in the system, the signal to noise ratio may be significantly enhanced by electronic integration prior to digitization. In our studies of nucleosomes, we find that the fastest timescale in the system is of order 250 msec; we therefore set an integration time of 20 msec, which negligibly distorts the measured kinetics while greatly enhancing the signal to noise ratio compared to a 1 msec integration time. In this way, it is possible to accurately measure both the long and short timescales of FRET change.

Sample concentrations and volumes

Modern instruments are extraordinarily sensitive. In our experiments we routinely use sample concentrations as low as 5 nM final concentration of nucleosomes. We set the instrument up to mix samples 1:1 (v/v) in the sample/detection chamber, thus we prepare 2x stock solutions of LexA and of nucleosomes. When one requires measurement of Cy5 only, even lower

concentrations suffice (M.G. Poirier and J.W., in preparation). We set the final LexA concentration so as to place us roughly in the middle of the binding titration (Figure 2C). Higher concentrations give larger FRET changes, and thus more robust signals, but also showed signs of causing aggregation [11], which we wish to avoid. The volume of the reaction chamber is 20 μl (10x2x1mm), and each successive mixing reaction requires at least 77 μl of sample. Use of larger "push volumes" (volumes used per reaction) shortens the dead time, and may be required for analysis of the fastest accessible reactions (i.e., for processes occurring on a ~1–10 msec timescale). Overall in our studies of nucleosomes (which do not require the fastest possible mix times), we expect to use ~1–2 ml of sample at the stock (2x) concentration for any one series of experiments (comprising typically 5–10 individual mixes) on one sample.

Data collection

Representative raw data from our recent studies on nucleosomes are shown in Figure 5A,B. Samples were rapidly mixed to a final concentration of 7 nM nucleosomes, with 0 nM, 200 nM, 400 nM, 1 μM, or 3 μM LexA in 0.5x TE buffer. We collected 1000 datapoints linearly spaced in time over 10 seconds, with a 20 msec integration time. Two channels were set to collect data simultaneously, one for Cy3 fluorescence, and the other for Cy5 fluorescence. With this setup, the Cy5 traces have very good signal to noise ratio despite the very low nucleosome concentrations. The Cy3 traces are usable but noisy with a 20msec sliding window binning, thus we further binned data to a final 100msec sliding window filter, which does not significantly change the fit parameters.

Figure 5

Raw stopped-flow FRET data. 7 nM FRET-labeled nucleosomes were rapidly mixed 1:1 (v/v) with buffer (0.5 x TE) only, or with 2 μM LexA protein (1 μM final concentration) in buffer, and fluorescence intensity in the Cy3 and Cy5 channels was monitored for 10 seconds with 1000 linearly spaced timepoints. **A.** Cy3 fluorescence data are noisy, and therefore were replaced by a moving average over 5 adjacent points to reduce the noise. Traces from rapid mixing with 0.5 x TE (▲) or 1 μM LexA (□) were fit to linear or double exponential curves respectively (solid line). **B.** Cy5 fluorescence measured simultaneously with the Cy3 channels of panel (A). Traces for the buffer only (▲) or 1 μM (final concentration) LexA (□) were fit to linear or double exponential curves (solid lines), respectively.

Figure 5

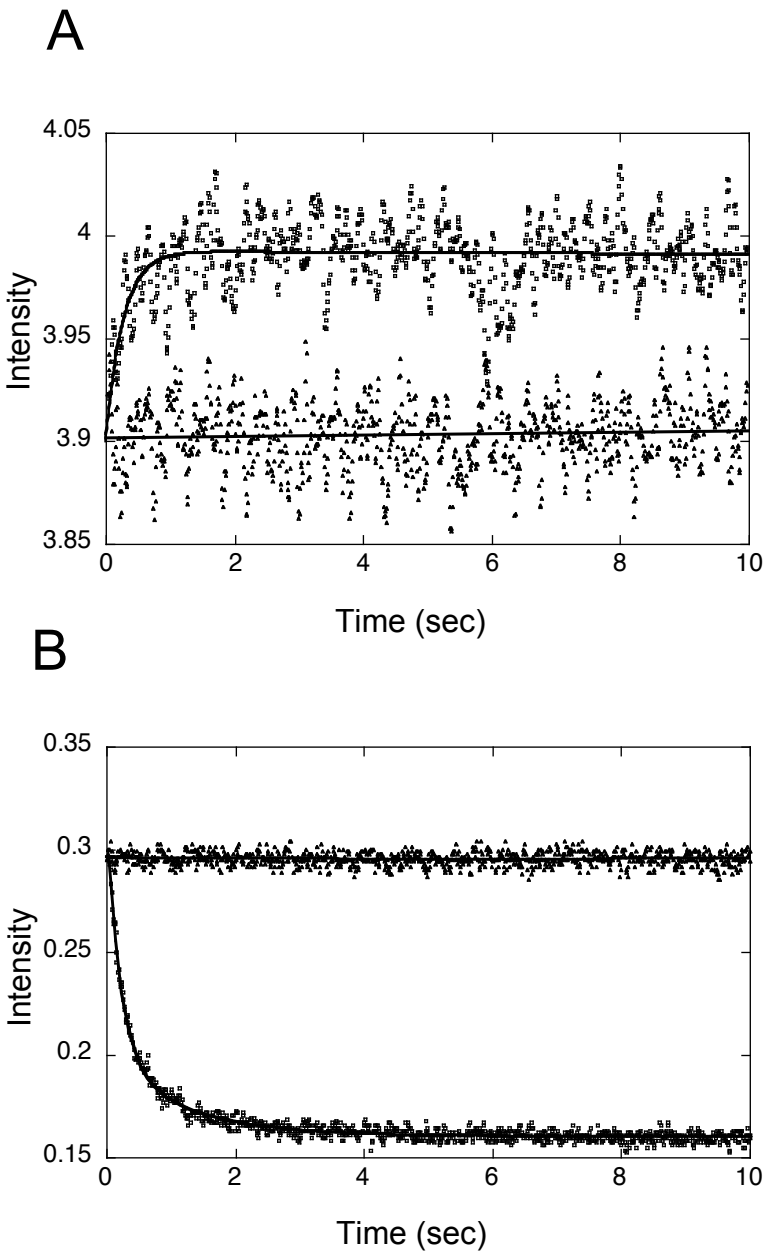
A
4.05
4
3.95
3.9
3.85
Intensity
0
2
4
6
8
10
Time (sec)
B
0.35
0.3
0.25
0.2
0.15
Intensity
0
2
4
6
8
10
Time (sec)

Data Analysis

The basic principles of data analysis from stopped-flow experiments are analogous to those of any other kinetic experiment. In our case the mechanism itself suggests that the kinetics should obey a single exponential. Behavior that is idiosyncratic to a particular system may complicate the real observed kinetics. For example, we find that for nucleosomes, site specific binding of a single LexA to a nucleosomal target site may be followed by additional cooperative nonspecific binding, seeded off the specific site, that occurs more slowly and is accompanied by an increased FRET change, perhaps due to concomitant increased DNA unwrapping [11]. Two exponentials, minimally, are required to describe such a system. We use KaleidaGraph software for single or multi-exponential fitting. Global analyses over many different conditions simultaneously using software such as Origin may yield more robust determinations of parameters when the kinetic mechanism is complex. These are specialized topics that are appropriately treated elsewhere [62].

One detail bears particular mention. A usual goal of stopped-flow experiments is to analyze kinetics over a range of timescales, including times that are as short as physically possible. Thus, it is of special interest to consider whether the kinetics that are recorded during a stopped-flow experiment have captured the entire kinetic history of a reaction, or whether it is possible that there occurred some additional process, on a far faster timescale, that is simply missed in the analysis because it has gone to completion by the first few milliseconds, which is the deadtime of the stopped-flow experiment.

This question can be answered by carrying out a second stopped-flow mixing experiment for a mock reaction instead of the real reaction. Thus, for example, for the case of nucleosomes we repeat the experiment except, instead of mixing in buffer plus LexA protein, we add buffer

only. The FRET signal from the real experiment includes any changes due to the kinetics, superimposed on changes due simply to dilution. The mock reaction measures the changes due only to dilution. Then, if (as in Figure 5) one finds that the processes measured in the real experiment, extrapolate back to zero time (with the fitted single or multi-exponential function), to the same numerical value as obtained in the pure dilution experiment, then this proves that there exists no additional process on any faster timescale contributing a significant FRET change.

Conclusions

The stopped-flow FRET experiment is a powerful and versatile tool with which to elucidate rates and detailed conformational changes as they occur in biological macromolecular complexes and machines. This approach is ideally suited for analysis of intrinsic properties of chromatin and of the machines that control chromatin assembly, disassembly, and function.

Chapter 3

Nucleosomal Heterodimer Exchange

Nucleosomal Heterodimer Exchange

Introduction

Genomic DNA in eukaryotes is organized into repeating arrays of nucleosomes, short stretches of DNA wrapped in ~1.6 helical turns around an octameric histone core. The histone core is composed of two copies each of four histone proteins, H3, H4, H2A, and H2B. The octamer is assembled *in vivo* by the chaperone directed deposition of an $H3_2H4_2$ tetramer onto the central DNA, to which two H2AH2B heterodimers are added to wrap an additional ~30 bp of DNA on either side, which allows the terminal bases to be contacted by the $H3_2H4_2$ tetramer, wrapping a total of 147 bp of DNA [1].

Histones carry many regulatory signals that are given as histone tail modifications or by specific replacement of the canonical histones with variants (see [63, 64] for a recent reviews). These histone signals are added or inserted by specialized exchange or enzymatic complexes, which are targeted and recruited in a DNA sequence specific manner [65]. A key question is once nucleosomes are marked in this way, whether the marked histones stay put, or are in free exchange. The expectation from other multi-protein complexes is that subunits have finite affinity, and therefore exchange freely. However if histones are in free exchange this creates a problem for maintaining the epigenetic information content of genes [3-5]. Localized maintenance of this information carried by histones could be accomplished by constant monitoring of the modified state of histones in a region. Additionally, the nucleosome, by maintaining the set of specifically marked histones until it is specifically remodeled, could contribute to maintenance of signals with defined DNA regions.

After decades of research there remains conflicting data and unknowns about the structure, dynamics, and function of chromatin, nucleosomes, and the histones. Of interest here is the stability of the histone octamer when it is wrapped into nucleosomes that, in vivo, are often disrupted, moved, or disassembled for normal cellular functions. Many labs have shown that nucleosomes, when serially diluted, dissociate, but as you re-concentrate the solution they can reassemble nucleosomes (for example [16]). This suggests that nucleosomes follow the law of mass action, where components are in dynamic equilibrium with solution and association is driven by concentration [16]. On the other hand, there is a large body of evidence, including direct tests, showing that individual nucleosomes maintain a stable histone octamer for very long periods of time [66, 67]. In balance, we conclude that in vivo unperturbed nucleosomes are stably associated with their histone components, which are not in free exchange with solution.

However this leaves open the question of what happens to nucleosomes when they are perturbed by DNA binding proteins, polymerases, or remodelers that require long stretches of DNA to be unwrapped from the histone core in order to access their target DNA [6, 8]. The crystal structure of the nucleosome suggests that the wrapped DNA acts as a cage holding the histones in place [1]. Making it plausible that as DNA is unwrapped from the histone core, the octamer is destabilized and exposed to solution, which may facilitate histone dissociation and exchange with histones from neighboring nucleosomes (Figure 1).

The real affinities and lifetimes of the histone components are difficult to measure, and thus are not yet known and cannot be used to calculate the expected dynamic state of the histone components [16, 68]. Studies of a DNA binding protein Amt1 binding to its nucleosomal target site near the dyad have shown stable association of the histones when the protein is bound [55, 69, 70]. However Amt1 binding does not require unwrapping of DNA from the histones, and

Figure 1

Histone Exchange Model shows DNA in gray as a cage wrapped in two turns around the histone octamer with H2A yellow, H2B red, H3 green, and H4 blue as in [1]. The fully wrapped nucleosomes cages the histones in place with DNA wrapping, but when it is unwrapped, the heterodimer–DNA interface is exposed to solution making it feasible that histones are free to dissociate and exchange with neighboring nucleosomes.

Figure 1

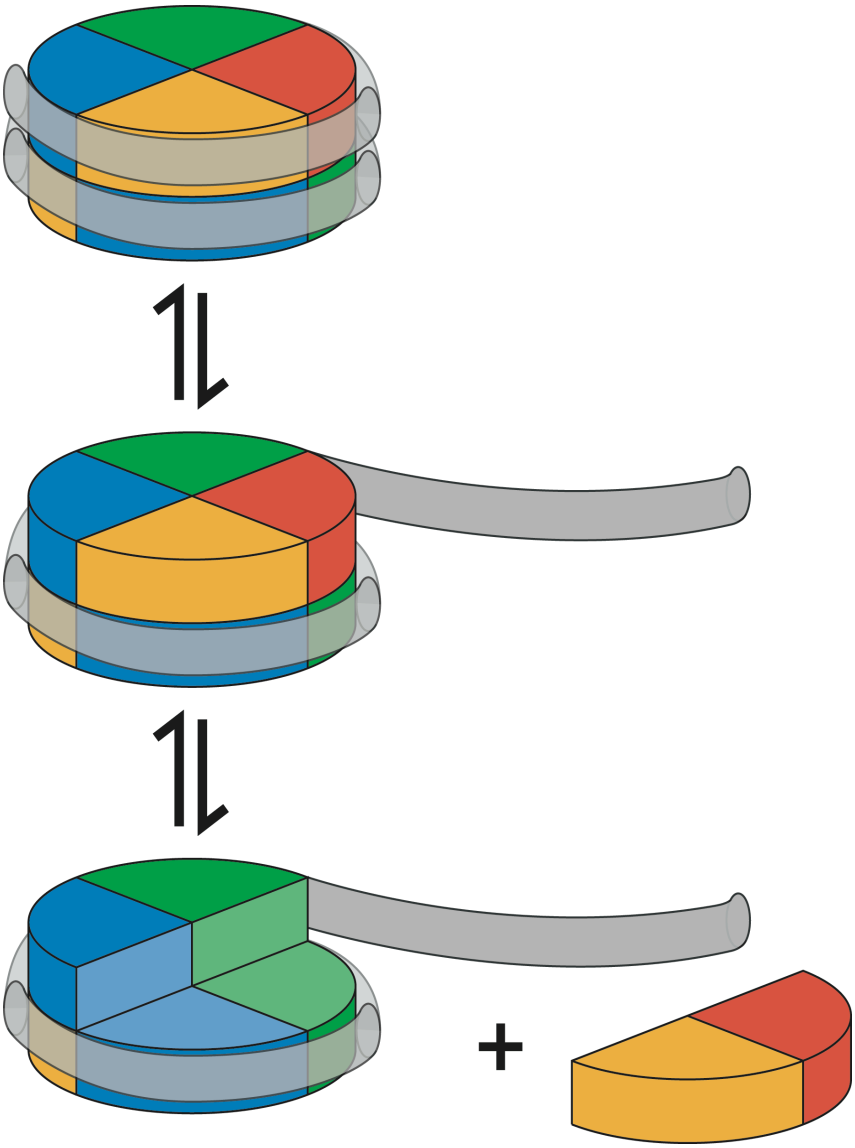

thus does not directly address stability of the histones when they are uncaged [55]. Evidence for exchange coupled to DNA unwrapping has been shown in vivo and in vitro with RNA Pol II (see [71, 72] for review, also [15, 73]). For smaller phage polymerases, data show nucleosomes are destabilized by transcription, but exchange has not been observed [74, 75]. We set out to test histone stability in uncaged conditions directly using FRET dye labeled histones.

Methods

DNA

Nucleosomal DNAs were derived from the 601 high affinity nucleosome positioning sequence [56]. For native and LexA binding experiments, we used 601 with a LexA binding site 7bp in from one end as described in [11]. For transcription assays with T7RNAP, we used the 216bp DNA described in Portacio and Widom 1996 [76] that contains the 147-601 positioning sequence with an additional T7RNAP promoter and a stall site outside of the positioned nucleosome. DNAs were amplified with PCR and purified by HPLC as described (Chapter 2).

Histones and LexA

Histones were expressed and purified as described [59, 77]. Histones H3V35C, C110A and H2AK119C were mutated, expressed and purified as described [11]. These mutant histones, along with purified H2A, H2B, H3C110A, and H4 were used to refold histone octamers. Octamers were refolded either with unique cysteine at H3V35C, which were labeled with a Cy3, or unique cysteine at H2AK119C, which were labeled with Cy5. Dyes were maleimide reactive as described in Chapter 2. LexA was expressed and purified as described in J. Little 1994 [60].

Reconstitutions

Reconstitutions contained 1μM DNA, 0.8μM labeled histone octamer, 2MNaCl, 0.5mM PMSF, 1mM BZA in 0.5x TE. Reconstitutions were dialyzed stepwise from 2MNaCl to no salt at 4°C. Nucleosomes were purified as described on sucrose gradients. Free dye is purified away from reconstituted nucleosomes during sucrose gradient purification.

Mixing experiments

For solution mixing reactions with NaCl or LexA, we used a stabilizing buffer containing 0.5mg/ml BSA, 0.1% NP40, and 10% glycerol, 0.1-0.5x TE to prevent adhesion of nucleosomes to the sides of tubes during long experiments. Dye labeled nucleosomes were mixed 1:1 to a final concentration of 15nM. Steady state fluorescence was monitored as described in Chapter 2.

LexA binding assay

LexA binding to nucleosomal constructs was tested on nucleosome constructs with the same DNA sequence labeled at the 5' end with Cy3 donor. Nucleosomes were reconstituted as described in Chapter 2 with the Cy5 acceptor on H3V35C and fluorescence changes were monitored as LexA was titrated into solution. FRET efficiency was quantified by the ratio A method, and a binding curve shows saturated binding by 1μM LexA.

Polymerase solutions/conditions

Transcription assays were done as described in [76]. Briefly, polymerase was bound to the template nucleosomes and transcripts were allowed to initiate and proceed to the stall site by

adding solutions devoid of dUTP. Full length transcripts were produced once the fourth nucleotide was added to solution, and transcription was allowed to reinitiate and transcribe many times. RNA transcripts were visualized by internal labeling with α^{32}P-ATP and run on high percentage denaturing acrylamide gels. Nucleosomes binding was monitored on agarose gels for gel shifting of bound complexes which show that nucleosomes fall apart, and transcript accumulates.

Results and Discussion

To test the stability of the heterodimer association with the histone octamer we developed a FRET system that would be sensitive to histone exchange between nucleosomes, or to net loss of histones from nucleosomes. For the exchange and loss assays we separately labeled two pools of histone octamers, one with the donor dye Cy3 on the $H3_2H4_2$ tetramer at H3V35C, the other with the acceptor dye Cy5 on the H2AH2B heterodimer at H2AK119C. Because there are two copies each of the four core histones, these dye labeled residues are 20 or 60 Å apart on the crystal structure of the nucleosome, so we expect to see FRET between the molecules if labeled histones coexist in one nucleosome (Figure 2). Nucleosomes were reconstituted with fluorescently labeled histones onto DNAs with a 601 nucleosome positioning sequence. In all exchange assays pools of donor and acceptor labeled nucleosomes were mixed 1:1 to a final nucleosome concentration of 15 nM. In these experiments, an increase in FRET would indicate exchange, while no change in FRET implies stable histones or loss of histones from nucleosomes without subsequent reassociation. To test for histone loss, nucleosomes were reconstituted with histone octamers labeled with both donor and acceptor fluorophores. With double-labeled

Figure 2

FRET system for analysis of exchange or loss of histones from nucleosomes. A) Schematic illustration of dye positions on the nucleosome. Three populations of nucleosomes were reconstituted, 1) nucleosomes with the donor on H3V35C, shown in the upper right, with H3 in blue, the labeled residue in cyan shown in spacefill. 2) Nucleosomes with the acceptor on H2AK119C, in the upper left, H2A is orange and the labeled residue shown in magenta as spacefill. 3) Nucleosomes with Cy3 on H3 and Cy5 on H2A, in the lower panel, with H3 in blue and H2A in orange. In NaCl or LexA binding experiments the DNA contained a LexA binding site is shown in teal as sticks representation from 8-28bp in from one end. T7 RNAP transcription experiments contained DNAs with the same histone arrangement, but with no binding site inside the nucleosome positioning sequence. B) Emission spectra from nucleosomes excited at 515nm for donor excitation with minimal direct excitation of the acceptor. Fluorescence from a mixed population of donor and acceptor nucleosomes in 500mM NaCl for an hour show no increase in FRET from initial mixing. Nucleosomes with donor and acceptor labeled histones show FRET.

Figure 2

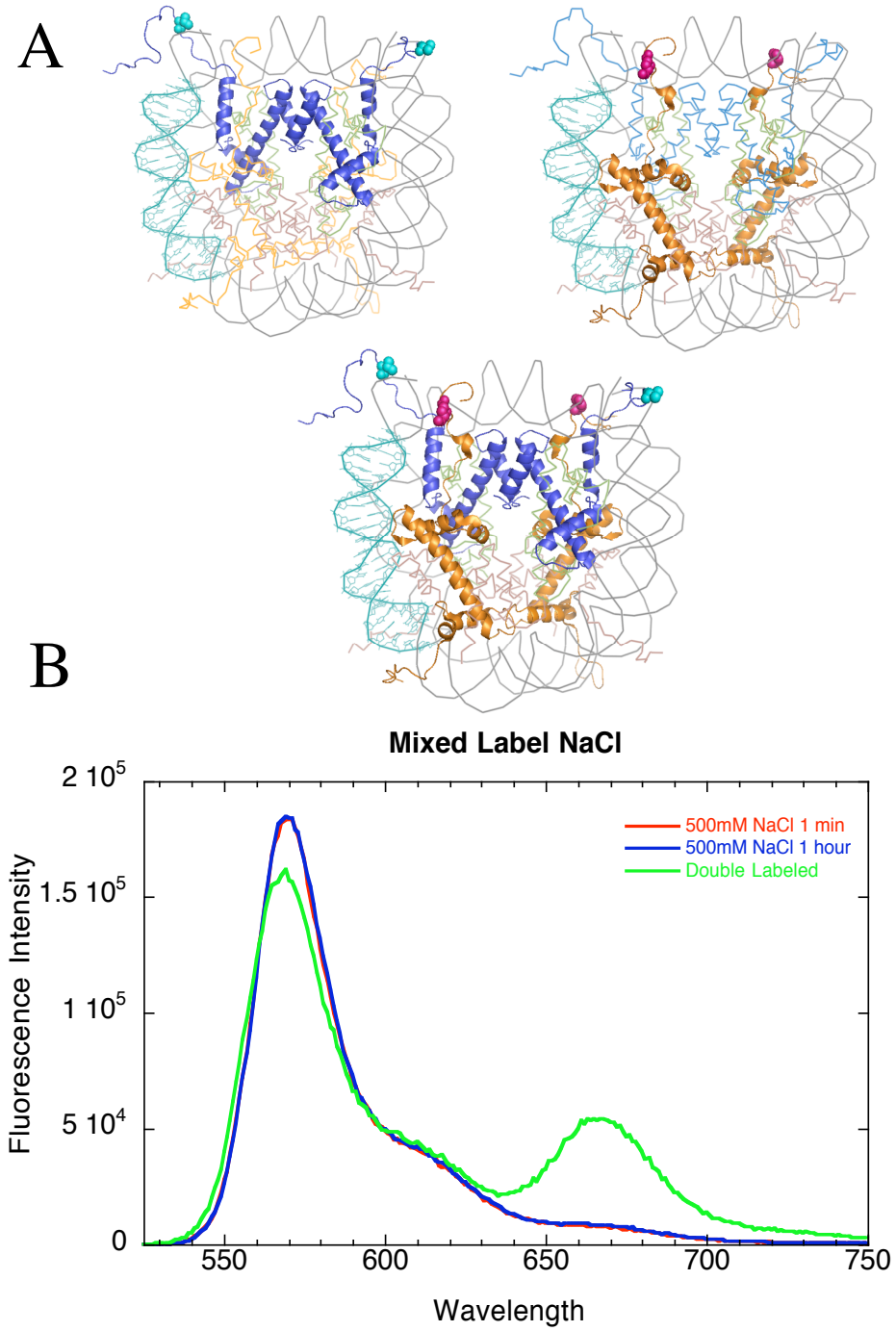
A
B
Mixed Label NaCl
2 10^5
1.5 10^5
1 10^5
5 10^4
0
Fluorescence Intensity
550
600
650
700
750
Wavelength
500mM NaCl 1 min
500mM NaCl 1 hour
Double Labeled

nucleosomes we can test for loss of histones indicated by a decrease in FRET, while exchange would not change the fluorescence of the system.

To confirm previous experiments, we first looked at nucleosomes under conditions of 90-99% of nucleosomes fully wrapped where we expect stable association of histones with one nucleosome [11]. We mixed nucleosomes in low salt solutions, and monitored fluorescence over an hour mixing at room temperature; fluorescence due to FRET was unchanged. Looking at histone loss under the same conditions, we again saw no change (data not shown). This supports previous findings that the nucleosomes are stable when in a fully wrapped state.

Previous experiments in the lab [11] have shown that when NaCl concentration is increased above physiological levels, the nucleosomes sample unwrapped conformations a larger fraction of the time. Thus we wanted to look at histone behavior when the nucleosome was encouraged to explore unwrapped conformations. Here we monitored exchange or loss of histones in solutions with 500 mM NaCl, which has been shown to facilitate partial DNA unwrapping from the nucleosome, but slightly lower than the concentration at which heterodimers completely dissociate from the nucleosome. Watching FRET for an hour at room temperature with these constructs again shows that there is neither loss nor exchange of histones (Figure 2B).

These experiments agree with previous data showing stable association of histones with individual nucleosomes. Not until slightly higher salt concentrations did Luger et al see FRET changes between labeled histones in the nucleosome with canonical H2A or with H2A.Z [66]. This new work watches histone exchange when DNA is unwrapped from the nucleosome core to expose the whole binding surface of the heterodimers, and to transiently expose all histone DNA binding surfaces.

To watch histone exchange when the DNA has been significantly unwrapped from the core histones we added LexA protein, which binds its target site with high affinity but is significantly excluded from binding sites wrapped in nucleosomes. Nucleosomes were reconstituted with DNAs containing a LexA binding sequence positioned at base pairs 8-28 from one end of the DNA (Figure 2A in teal sticks). We engineered the binding site to face the histone core, thus DNA must unwrap past the target sequence in order for LexA to bind (Figure 3A). This uncages the heterodimer-DNA interface and exposes it to solution. Under these conditions we monitored histone exchange or loss with subsaturating or saturating concentrations of LexA, 400nM or 1μM respectively (Figure 4) [11]. We know from LexA titrations of similar nucleosomes that most LexA binding sites are occupied at this concentration of LexA (Figure 3), yet we see no change in FRET due to exchange or loss of histones (Figure 4A, B for 400nM, 1μM LexA data not shown). We conclude that histone association in the nucleosome is robust against DNA unwrapping to expose a significant histone interface to solution without loss or exchange of components.

LexA binding to nucleosomal DNA exposes the heterodimer surface, but we wanted to look at histone stability when the whole histone DNA binding interface is disrupted. Previous studies have shown that when phage (or other small) polymerases transcribe through nucleosomes the histone octamer steps around the proceeding polymerase with minimal nucleosome loss [73, 74, 78]. For this reason we wanted to monitor histone stability when DNA was disrupted by T7RNA polymerase transcribing mRNA from nucleosomal DNA templates. Transcription through nucleosomes requires the unwrapping of all DNA from the core, and indeed, heterodimer exchange has been shown in regions of moderate transcription with a larger polymerase, RNA Pol II [15, 71]. We chose to use T7RNAP because it can transcribe through

Figure 3

LexA titration to binding a site inside the nucleosome. LexA binding to the target sequence inside nucleosomes was measured by a decrease in FRET between the donor Cy3 on the 5'end of the DNA, and the acceptor Cy5 on H3V35C as in Gu Li [11]. A) Model of LexA binding to the target site occluded in the nucleosome with histones colored as in Figure 1. The system is in dynamic equilibrium between the three states. As DNA is unwrapped LexA binds with high affinity and holds the DNA in an unwrapped conformation, exposing the heterodimer binding surface. B) LexA was titrated into solution with 5nM nucleosomes. Increasing [LexA] drives nucleosomes to a partially unwrapped state as LexA occupies the binding site inside the nucleosome. C) FRET efficiency at each [LexA] was calculated by the ratio A method and is proportional to the fraction of nucleosomes bound by LexA. Binding is saturated by 1000nM LexA, and significantly occupied by 400nM LexA.

Figure 3

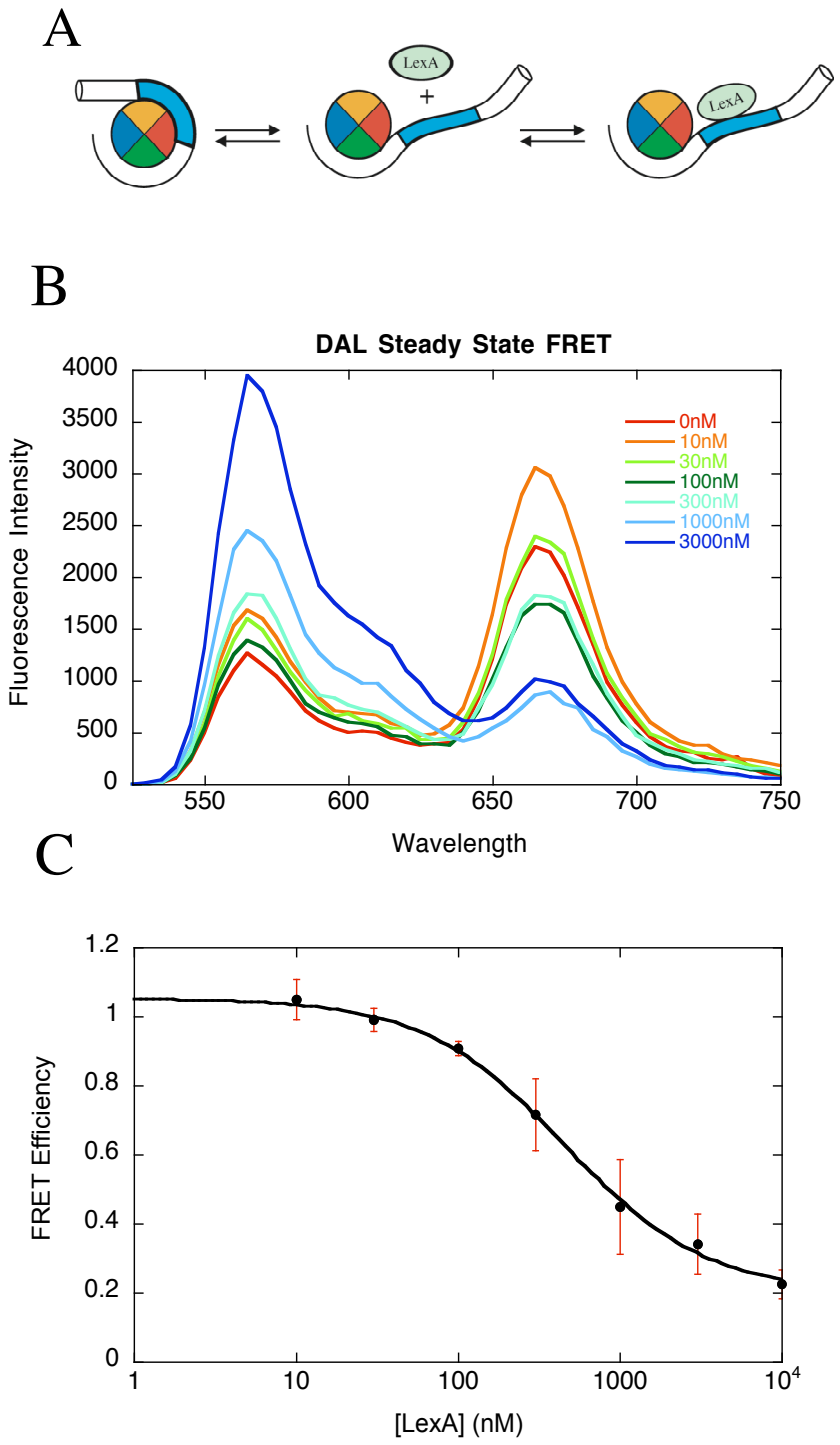
A
LexA
+
LexA
B
DAL Steady State FRET
Fluorescence Intensity
4000
3500
3000
2500
2000
1500
1000
500
0
550
600
650
700
750
Wavelength
0nM
10nM
30nM
100nM
300nM
1000nM
3000nM
C
FRET Efficiency
1.2
1
0.8
0.6
0.4
0.2
0
1
10
100
1000
10^4
[LexA] (nM)

Figure 4

LexA binding inside the nucleosome does not facilitate exchange. A) In the exchange assay, fluorescence from FRET is not changed above initial levels after a hour incubation with LexA. In blue and pink, the donor or acceptor only fluorescence scans, in black initial mixing and a hour incubation at room temperature shows no FRET changes. B) In the histone loss assay, we see no change in FRET indicative of histone dissociation from the nucleosome. In green, double labeled nucleosomes, in black the time points of incubation.

Figure 4

A

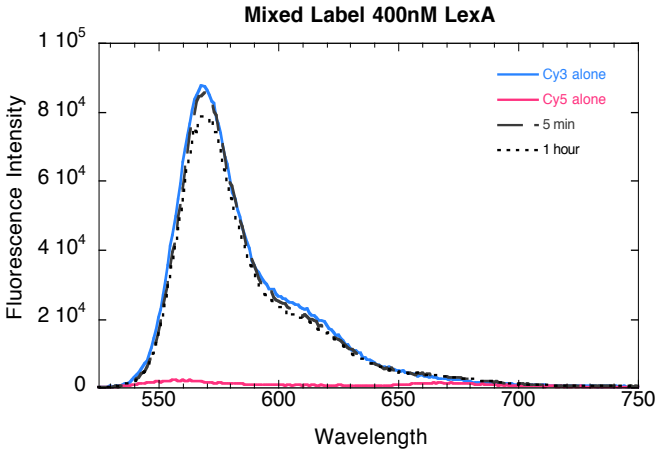
Mixed Label 400nM LexA
Fluorescence Intensity
1 10^5
8 10^4
6 10^4
4 10^4
2 10^4
0
550
600
650
700
750
Wavelength
Cy3 alone
Cy5 alone
5 min
1 hour

B

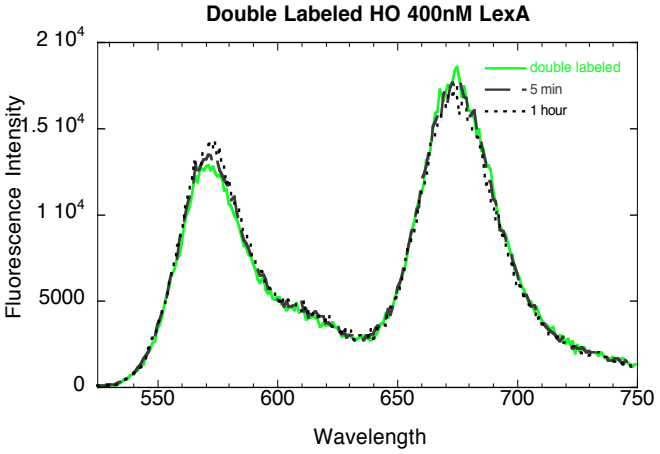
Double Labeled HO 400nM LexA
Fluorescence Intensity
2 10^4
1.5 10^4
1 10^4
5000
0
550
600
650
700
750
Wavelength
double labeled
5 min
1 hour

nucleosomes without additional remodeling proteins, and has been shown to replace nucleosomes along the DNA after passing by without disrupting location or components.

DNAs used for nucleosome reconstitutions contained a T7RNAP promoter along with a short minus U cassette that would stall the polymerase outside of the 601 nucleosome positioning sequence, with the dye labeled histones (Figure 5A). We show that all DNAs with an initiated transcript chase to full length upon addition of the fourth nucleotide, indicating all bound nucleosomal DNAs are transcribed (Figure 5B) [76]. These nucleosomes were mixed and we monitored exchange and loss when the polymerase bound and stalled outside of the nucleosome seeing no exchange as the nucleosome wasn't yet disrupted (Figure 5C, D). Then we monitored fluorescence changes when the polymerase was allowed to proceed through the nucleosome, reinitiate, and transcribe many times (Figure 5C, D). Fluorescence changes due to FRET were small, but significant in the exchange assay (Figure 5C). On the timescale of our experiment, when transcription is allowed to proceed to full-length product, the polymerase is allowed to retranscribe many times. T7RNAP transcription through nucleosomal templates occurs on the seconds timescale [79, 80], which means that in our experiments each nucleosome has been transcribed many times before exchange is detected. We show in Figure 6B that transcript does accumulate significantly over 20 minutes of transcription, and that many more transcripts are made than the first initial RNA. We also show that all nucleosomes are gel shifted to slower migrating species when polymerase is added (Figure 6C), previous experiments showed that bound DNAs were initiated by the polymerase and transcribed to full length [76]. The small increase in FRET that we see could be due to aggregation of nucleosomes that fall apart after many rounds of transcription. We show in Figure 6C that nucleosomes are destabilized by many rounds of transcription, and naked DNA accumulates over time in transcription assays. We do

Figure 5

Transcription by T7RNAP does not cause significant exchange or loss of histones. A) DNA construct for T7RNAP experiments as in Portacio [76]. Nucleosomes were positioned with the 147-601 sequence. A T7 promoter followed by a minus U cassette and spacer are positioned prior to the nucleosome on nucleosome free DNA. With this construct, polymerases are free to bind their promoter and initiate transcription, at which point they are stalled just outside of the nucleosome until all dNTPs are added to solution. B) Exchange was monitored as before. In blue and pink, are the fluorescence spectra from the donor only and acceptor only nucleosomes. In black, fluorescence from mixed nucleosomes was monitored after stalling the polymerase and after several rounds of transcription. The stalled complex does not show increased FRET due to exchange, but there is a small increase in FRET after 5 min transcription due to histone exchange or nucleosome/histone aggregation. C) There is no significant histone loss in either the stalled complex or after several rounds of transcription as seen by the curves in black versus the green curve for double labeled nucleosomes.

Figure 5

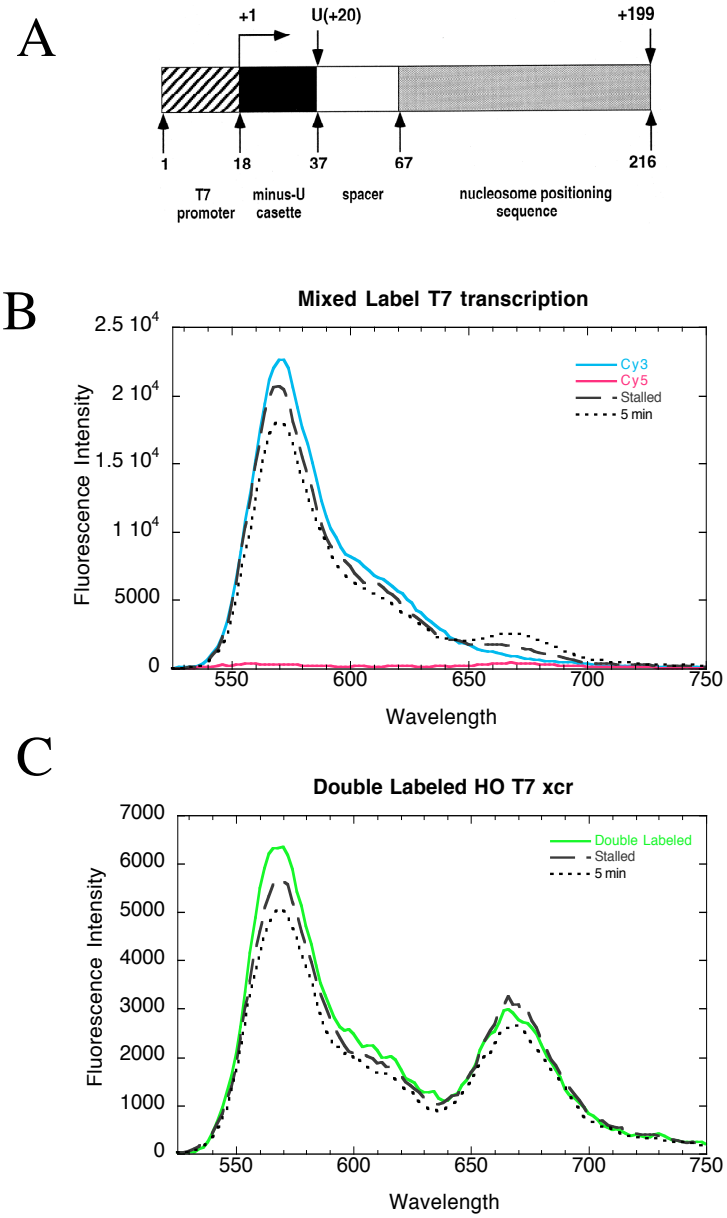
A
+1
U(+20)
+199
1
18
37
67
216
T7 promoter
minus-U casette
spacer
nucleosome positioning sequence
B
Mixed Label T7 transcription
Fluorescence Intensity
Wavelength
Cy3
Cy5
Stalled
5 min
C
Double Labeled HO T7 xcr
Fluorescence Intensity
Wavelength
Double Labeled
Stalled
5 min

Figure 6

T7RNA polymerase transcribes through nucleosomes, transcript accumulates, and all nucleosomes are bound. A) All initiated and stalled transcripts chase to full-length transcript as monitored by watching production of RNA via incorporation of αdCTP. Transcription was tested on several constructs. In lanes 1-2, naked DNA, 3-4 Cy3 nuc, 5-6 Cy5 nuc, 7-8 double labeled nuc. In all cases the initiated and stalled transcripts (odds) chase to full length transcript upon addition of dUTP (evens). See note in Protacio for presence of two stalled complexes [76]. B) Transcript accumulates over time as the polymerase is allowed to rebind and transcribe many times. In lane 1 the stalled complexes are below threshold, lanes 2-5 are increasing time of transcription, initial, 5 min, 10 min, and 20 min transcription. C) All nucleosomes and DNA are bound by polymerase as seen in the gel shift assay in a native agarose gel. Lane 1 shows nucleosomes, and free DNA, which in lanes 2 and 3 are shifted with addition of polymerase or stalled complex. In lanes 4-7 transcription proceeds to full length for 30 sec, 5 min, 10 min and 20 min respectively. There is accumulation of free DNA, RNA transcript running just slower than DNA, and shifted bound complexes.

Figure 6

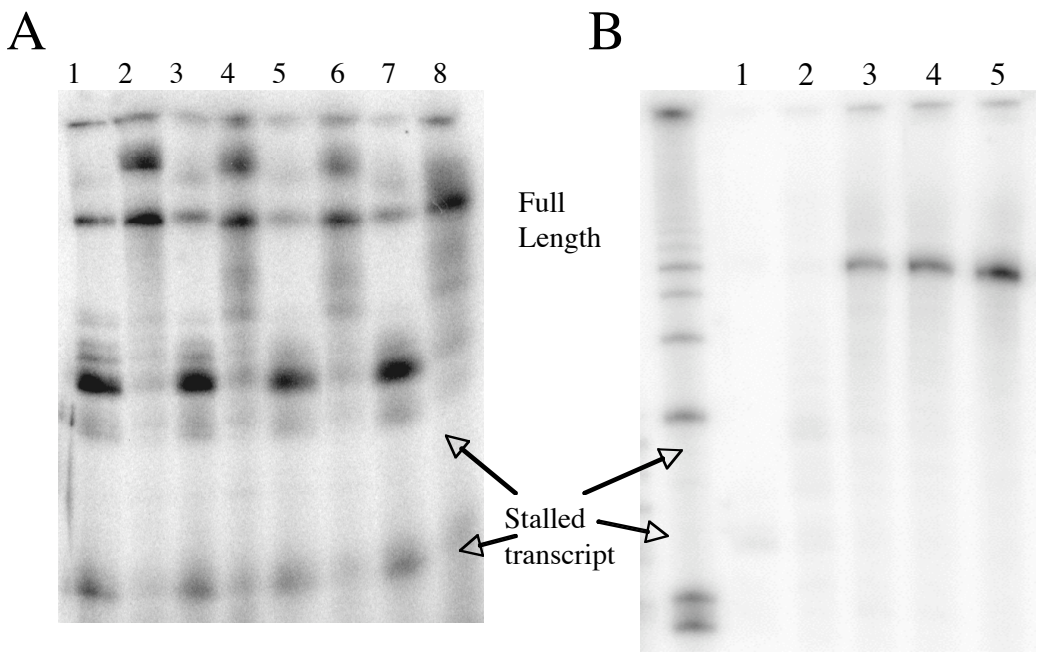
A
1 2 3 4 5 6 7 8
Full
Length
Stalled
transcript
B
1 2 3 4 5

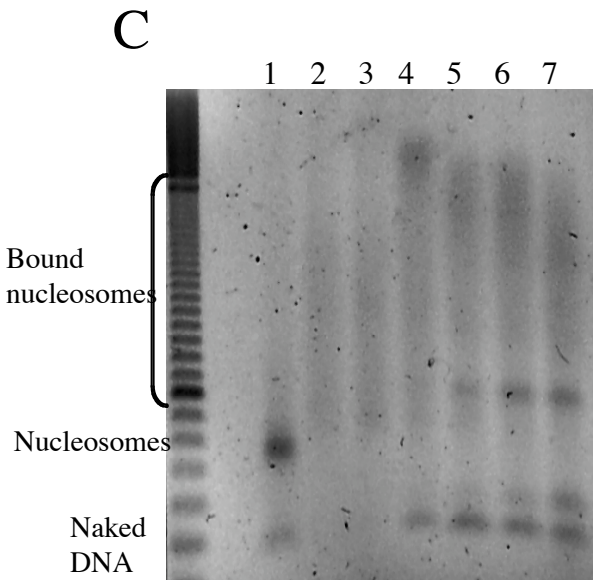
C
1 2 3 4 5 6 7
Bound
nucleosomes
Nucleosomes
Naked
DNA

not detect histone loss from nucleosomes after many rounds of transcription (Figure 5D). This amazing tenacity of the nucleosomes for their specific histone components survives after complete disruption of the histone DNA contacts due to many rounds of T7RNAP transcription.

Chromatin as a molecular assembly is constantly being compacted, relaxed, moved, transcribed, remodeled, and reassembled during cell life. The nucleosome is also in dynamic equilibrium between fully wrapped and partially unwrapped DNA, it is remodeled and moved by ATPases, invaded by DNA binding proteins and polymerases, and histones are exchanged and modified to affect chromatin packaging and gene regulation [8, 10, 15]. However we show that the histone octamer is a stable molecular assembly with its assigned DNA, and is not in free exchange with histones from neighboring nucleosomes, even when significant DNA is unwrapped by protein binding or by passage of RNA polymerase. This stability of the octamer with a particular DNA sequence may facilitate segregation and stability of epigenetic marks on the histone tails, which define active and silenced DNA regions. This work does not address the role of chromatin modifying enzymes in initiating and spreading silencing signals, but proposes an additional mechanism by which epigenetic marks on histones are actively maintained to regulate gene expression.

Acknowledgements

Special thanks to the Keck Biophysics Facility for use of instruments, and to Daniel P. Grilley for help with figures.

Chapter 4

Rate of Unwrapping Buried Nucleosomal DNA

Rate of Unwrapping buried nucleosomal DNA

Introduction

Genomic DNA in vivo is packaged by histones and organized into nucleosomes that are further packaged and compacted by higher order folding into chromatin [2]. This packaging of the DNA occludes binding proteins from their target sites by steric hindrance [1, 7]. Nucleosome formation and location are influenced by DNA sequence, nucleosome assembly factors, chromatin remodelers, and by the presence of other competing DNA binding proteins present on the DNA. However, too simple a view of the architecture of organized chromatin at promoters is often painted by studies of nucleosome positioning. Important regulatory protein binding sites are depicted at internucleosomal regions, so that target sites are accessible for binding and there is efficient activation at all promoters. But the reality is more complicated, as even at well organized promoters there is diversity in the detected nucleosome location among the many cells in a population [81]. Some target sites in a population are in internucleosomal regions, thus are freely bound, and the gene activated, while other sites are buried in nucleosomes, and the proteins cannot bind their targets, affecting gene activation.

Recent studies on genome wide nucleosome positioning shows non-zero occupancy of nucleosomes in the 'valleys' between well studied positioned nucleosomes [82, 83]. For example, studies on the global genomic positioning of the histone variant H2A.Z show high probabilities of nucleosome occupancy at particular locations on the genome, but also significant occupancy of nucleosomes over the linker DNA regions which on average are nucleosome free [82]. At the much-studied Pho5 promoter, regions usually depicted as devoid of nucleosomes

show significant nucleosome occupancy and corresponding protection from restriction enzyme digestion, while predicted nucleosome locations are sometimes easily accessible [81]. These experiments prove that many cells in a population place nucleosomes directly over critical regulatory protein binding sites, yet these cells can still respond to stimuli. This raises a question of how proteins find their target sites when the target sites are buried inside of nucleosomes. To make buried sites accessible, chromatin remodeling proteins must either be specifically directed to move nucleosomes, or must act ubiquitously at promoter regions. Alternatively, target sites might be spontaneously transiently accessible for binding proteins [6, 8].

Chromatin remodeling complexes are specifically recruited to promoters by DNA site specific DNA binding proteins (for review [84]). These recruitment proteins bind target sites at promoters that are in need of reorganization, and signal remodeling complexes that modify the chromatin architecture to increase the accessibility of potentially buried target sites [85]. However this view raises a chicken and egg problem: if the recruitment factor's DNA binding site is itself potentially buried in a nucleosome, DNA sequence information will not always be available to allow for recruitment of the chromatin remodeling machinery. This, then, cannot be the only mechanism cells use to access buried DNA.

Although remodelers are specifically recruited to promoters, it is also possible that remodeling complexes act ubiquitously at all promoters or over all chromatin, effectively making nucleosomes transparent, and binding sites readily available. Such a ubiquitous activity has not been shown, and the available data do not support this as an explanation for accessibility to buried DNA. In fact, recent studies of accessibility in yeast show that the rate of access to some nucleosomal DNA exceeds the rate of chromatin remodeling complex activity [9].

Work in our lab has shown that nucleosomes facilitate their own invasion by spontaneous partial unwrapping of DNA away from the histone core to allow proteins access to buried binding sites [8, 11]. Indirect tests of nucleosome unwrapping using restriction enzyme digest assays show that this spontaneous unwrapping facilitates access to the entire length of nucleosomal DNA, with decreasing probability as sites are moved further inside the nucleosome [7, 8]. This spontaneous unwrapping is progressive, starting from one edge of the nucleosome and proceeding inward, and is independent of ATP dependent remodeling factors [8]. These indirect restriction enzyme digest assays, and additional direct studies of accessibility using FRET dye pairs probing nucleosome structural changes at nucleosome edges, agree that DNA near the nucleosome ends is readily accessible. FRET based assays of accessibility probe nucleosome structural fluctuations by monitoring changes in fluorescence, as DNA is partially unwrapped from the nucleosome core [11, 19]. By placing FRET dye pairs at the nucleosome edges it was shown that partial unwrapping of DNA at the ends of nucleosomes is rapid (faster than seconds) and allows access to binding sites near nucleosome edges, in vivo and in vitro, on a biologically relevant timescale [9, 19].

However, studies using restriction enzymes to assay accessibility of nucleosomal DNA reveal that binding to sites further inside the nucleosome occurs with a probability that is reduced relative to binding at the nucleosome ends by as much as several orders of magnitude, raising the possibility that the rate of accessibility might be comparably reduced [7]. If the rate of unwrapping DNA to expose target sites buried deep within the nucleosomes is significantly slowed, nucleosome positioning might result in a time delay for gene activation. To overcome such a delay, remodeling enzymes could act to make buried targets available more rapidly by moving nucleosomes, or proteins could bind cooperatively within a nucleosome to increase

accessibility. We extend direct studies of nucleosomal DNA with FRET assays to study the nature of the structural changes that make buried sites accessible. There are limited data available from previous direct assays of the accessibility of buried nucleosomal DNA [86], this work is controversial, and its validity has been challenged by several groups (J. van Voort and M. Levitus personal communications). In this work we measure the rates of accessibility to buried nucleosomal DNA using FRET dye pairs that probe structural changes in the nucleosome interior, together with protein binding sites located far inside the nucleosome.

Several terms need to be defined. The unwrapping event can be characterized by several parameters: the lifetime in the closed state with a corresponding rate of unwrapping (opening), and the lifetime of the unwrapped state with a corresponding rate of re-wrapping (closing) [8]. The lifetime of the closed state represents an average amount of time the molecule spends fully wrapped in between unwrapping events (in seconds), and the rate of unwrapping is defined as the number of unwrapping events per time (k_{12} in sec^{-1}) from a wrapped state. Similarly, the lifetime of the open state represents the time the molecule spends unwrapped before returning to a fully wrapped state (in seconds), and the rate of unwrapping is number of re-wrapping events per time (k_{21} in sec^{-1}), given that the system is in an unwrapped conformation (Figure 4). From these definitions, the equilibrium wrapped state of the nucleosome could be decreased either by decreasing the rate of unwrapping, or decreasing the lifetime of the unwrapped state, or both.

Materials and methods

DNA, Histones and LexA

DNAs for nucleosome reconstitutions were prepared by PCR. 147 basepair DNA from the 601 nucleosome positioning sequence [56] was mutated by PCR to contain a 20 bp LexA binding site [11] starting 7, 17, or 27 bp from one end. Using a second round of PCR and commercially available Cy3 labeled oligos (IDT), the DNA was 5' end labeled with Cy3 fluorescent dye on the end closest to the LexA binding site, and purified as described (chapter 2). Using DNA with a LexA biding site 7 bp from one end, we made two additional constructs with Cy3 dye attached internally on the DNA at nucleotide 35 or 57 from the end (Cy3-35 and Cy3-57). Fluorophores were attached by amide linkers to oligos that contained an amide reactive linker group off base 35 or 57. Full length DNAs were made from the labeled oligos by PCR, and DNAs were purified as before. An additional DNA was constructed with the Cy3 dye 69bp in from one end. We ordered long DNA oligos (IDT) with a Cy3 dye attached off the 3' end of a 69 bp oligo, and together with oligos that were 78bp long, 99bp and 48bp long, we assembled a 147bp DNA with the 601 nucleosome positioning sequence. These long oligos were annealed in a 1:1.1:1.1:1.1 ratio by slowly reducing the temperature from 95°C to 23°C. We used slightly less Cy3-69 DNA so that it would be fully incorporated into full length DNA, purified as before. Recombinant histones and LexA were expressed, purified, and labeled with Cy5 as defined elsewhere, with the addition of H4L22C, and H2BT112C histone mutants, made as described [11, 87] and Chapter 2.

Nucleosomes

Several nucleosome constructs were assembled from these DNAs and histones. Donor-acceptor (DA) nucleosomes were reconstituted as follows: DNA Cy3-1 was reconstituted with Cy5-H3C110A,V35C, Cy3-35 was reconstituted with Cy5-H2BT112C, Cy3-57 was reconstituted with Cy5-H4 L22C, and Cy3-69 was reconstituted with Cy5-H3C110A,V35C. LexA-7, 17 and 27 DNAs were end labeled with Cy3, and reconstituted with Cy5-H3C110A,V35C. We also reconstituted donor-only (DO) nucleosomes from Cy3 labeled DNAs, with unlabeled histone octamers. All reconstitutions were done with excess long salmon sperm DNA to facilitate reconstitutions in a double dialysis bucket system [57]. Nucleosomes were purified away from free DNA, Salmon Sperm DNA, aggregates and free dye in sucrose gradients and the concentration of nucleosomes was analyzed by Cy3 absorbance.

Fluorescence Measurements

Steady state and stopped flow fluorescence measurements were done as described in Chapter 2. Specifically, nucleosomes were used at a 5nM concentration, and stopped flow kinetic experiments were done with 400nM or 1μM LexA. Stopped flow fluorescence changes were measured simultaneously from two channels for 10 to 1000 seconds, and FRET changes were quantified by calculating the proximity ratio. Data from the fluorescence reads were smoothed (so as not to loose kinetic information) and then proximity ratio was calculated by acceptor fluorescence/ total fluorescence (donor plus acceptor).

Fluorescence Correlation Spectroscopy measurements

Free solution FCS experiments were done in 0.5xTE with 20 mM DTT (to decrease photobleaching) exciting with the 488nm laser, light was collected through filters 530-610nm and 655-710nm band pass filters respectively to isolate fluorescence from Cy3 and Cy5. We used 1mm coverslips and cover well strips (cat. no. PC8R-0.5 Research Products Inc.). Each well holds about 20-30μl of solution, from which we saw no evaporation or photobleaching at relatively high laser power. To slow diffusion of nucleosomes to catch slower kinetics from the molecules, nucleosomes were restricted in acrylamide as suggested (Marcia Levitus personal communication). We ran a 5% native acrylamide gel in Tris Borate EDTA (1/3xTBE), cut the nucleosome band from the gel, and soaked it in 200μL 0.5x TE with 100mM DTT for 1.5 hours on ice. Gel slices were covered with cover well slips, and additional buffer added to keep them hydrated. Correlations were measured for fluorescence fluctuations from DO and DA nucleosome constructs Cy3-1 and Cy3-35.

Correlation curves from FCS experiments are dominated by diffusion of the molecules through the confocal volume, but are complicated by detector specific afterpulsing and triplet state of the dyes [88-90]. We directly determined the afterpulsing for each detector by correlating the random scattering from a buffer only solution. These data, sensitive only to the electronic correlations of each detector decay by 10^{-6} seconds. Therefore, data were arbitrarily truncated at short times at 10^{-6} seconds. Reigler and Mets have an equation that describes diffusion of molecules through FCS, with fitting for triplet state (eqn. 5 [88]). Using this we found good fits to our data, and found that the triplet contribution is done by 100μsec, thus we looked at the curves on timescales longer than 100μsec, which does not interfere with the kinetic contributions. Kinetic contributions to the correlation curves were isolated by dividing the donor

autocorrelation (DD) by donor acceptor cross correlation (DA), the acceptor autocorrelation (AA) by DA, and DD by AA as described [91].

Results

Steady State Accessibility of Nucleosomal DNA

DNA inside the nucleosome is mostly wrapped at low salt concentrations

Similarly to our earlier experiments in which FRET dye pairs were attached at the nucleosomal DNA ends, we set up a direct assay of DNA fluctuations further inside the nucleosome. We labeled the DNA with Cy3 donor, and the histone with Cy5 acceptor dye. Dye pair locations were chosen so that the distance between the donor and one or both of the acceptor dyes would be well within the Förster radius for Cy3 and Cy5. DNAs were end labeled with Cy3 or internally labeled off the base at position 35, 57 or 69 from the end (referred to as Cy3-1, Cy3-35, Cy3-57, or Cy3-69 respectively). Nucleosomes were reconstituted with these DNAs and histones labeled with Cy5 on H3C110A-V35C, H2BT112C, H4L22C, or H3C110A-V35C respectively (Figure 1). These nucleosomes all have robust FRET in low salt solutions that stabilize the fully wrapped state.

Nucleosome solutions were titrated with increasing concentrations of NaCl to measure the equilibrium DNA unwrapping at physiological or higher salt concentrations. Here there are two ways to interpret fluorescence changes in the system. First we can think of a decrease in FRET occurring from a continuous salt dependent release of DNA from the histone core, where FRET decreases as DNA is unwrapped incrementally by increasing salt. However, in keeping with what is known about systems in equilibrium, we interpret the data as dynamic equilibrium

Figure 1

Schematic of nucleosome constructs with FRET dye pairs inside, coordinates taken from the crystal structure of the nucleosome ([1] pdb 1EQZ). Fluorophore attachment sites are shown in spacefill with Cyan for Cy3 location on the DNA, and Magenta for Cy5 attachment sites on the histones. LexA binding site (where applicable) is shown in red with sticks representation. Nucleosome models are shown with titrations of DO and DA nucleosomes with NaCl. A) Cy3-1 Nucleosomes with the FRET dye pairs near the nucleosome ends, DNA labeled off the 5' end of the 1st nucleotide, histones labeled on H3C110A,V35C. B) DO titration, C) DA titration. D) Cy3-35 nucleosome with FRET dye pairs inside, Cy3 off basepair 35, and Cy5 on H2BT112C, E and F) DO and DA titrations. G) Cy3-57 nucleosome with Cy3 off base pair 57, histone labeled with Cy5 at H4L22C, H and I) DO and DA titrations. J) Cy3-69 with DNA labeled off the 3' end at base pair 69, histone labeled with Cy5 at H3C110A,V35C, K and L) DO and DA titrations. All nucleosome titrations of 5nM samples with NaCl from 0 to 2M were excited at 515nm and fluorescence measured from 525nm to 750nm.

Figure 1 A-F

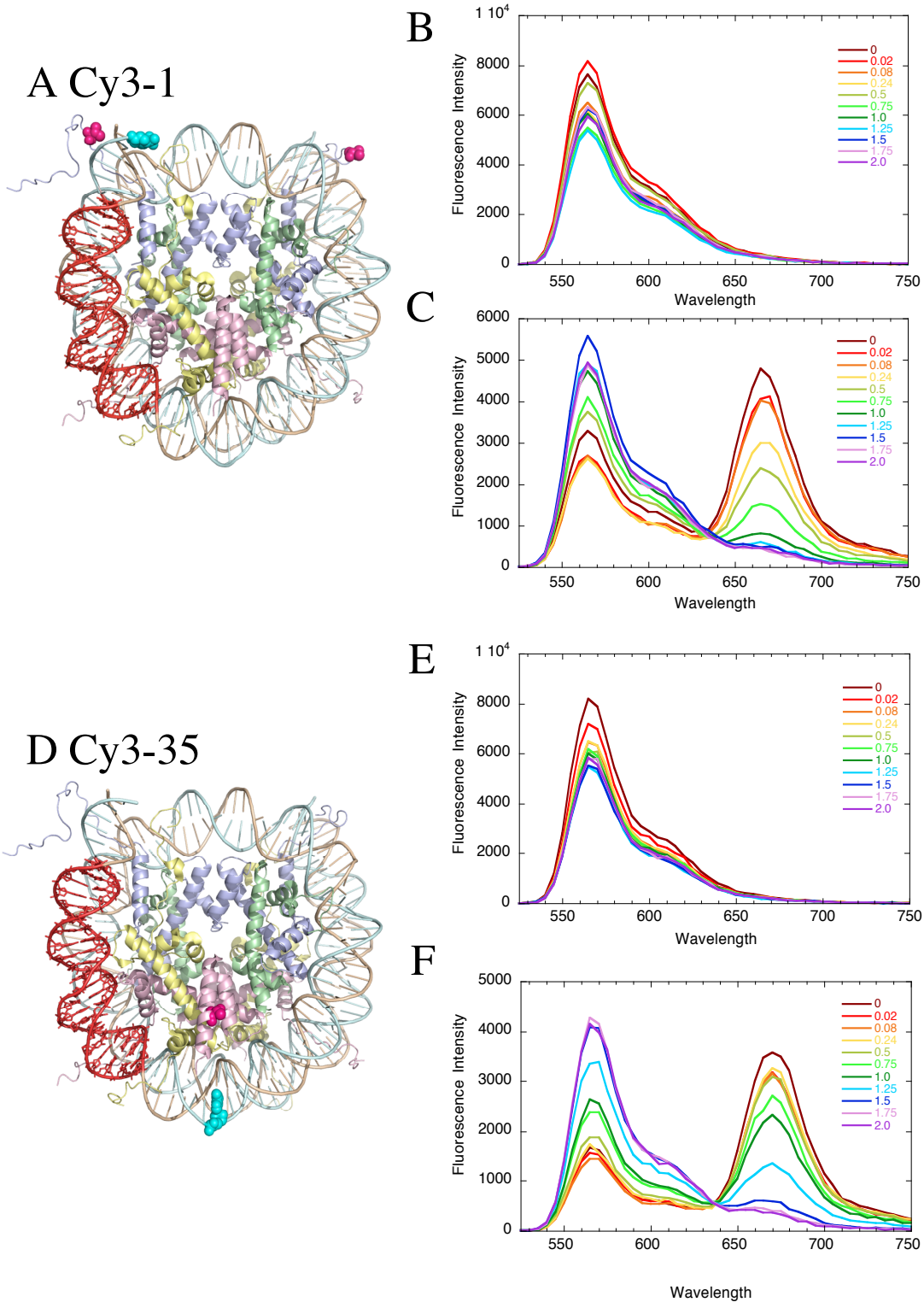
A Cy3-1
B
C
D Cy3-35
E
F
Fluorescence Intensity
Wavelength
0
0.02
0.08
0.24
0.5
0.75
1.0
1.25
1.5
1.75
2.0

Figure 1 G-L

G Cy3-57

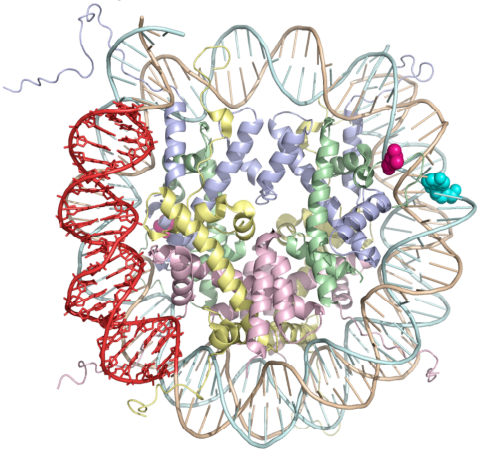

H

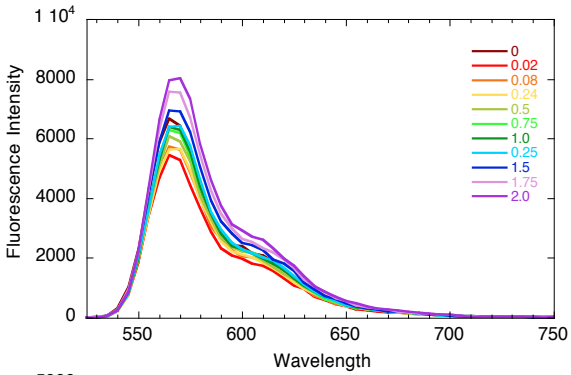

I

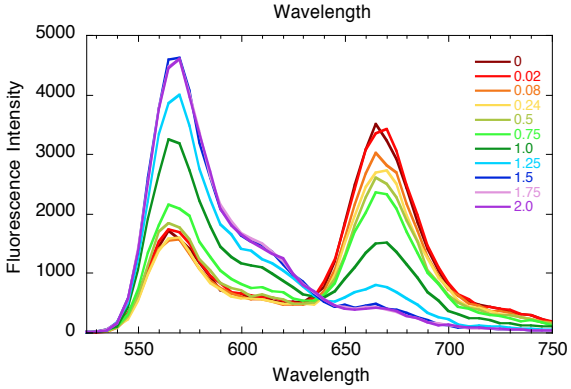

K

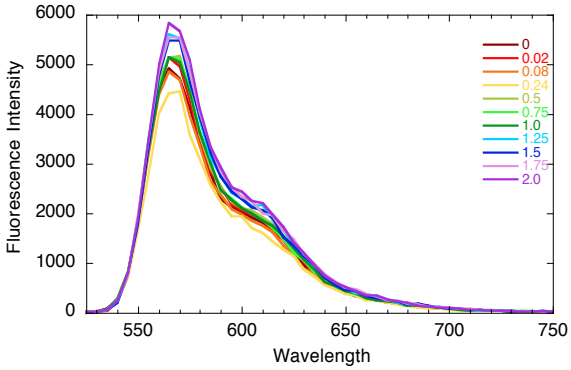

J Cy3-69

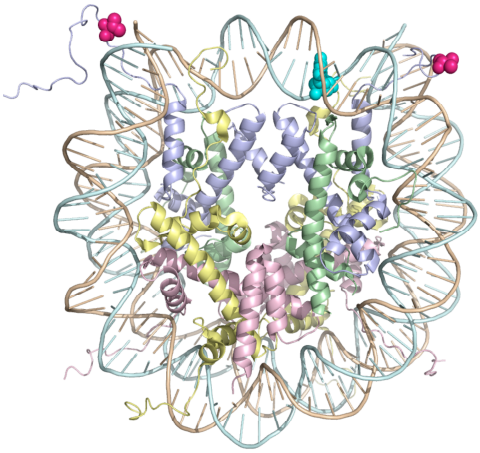

L

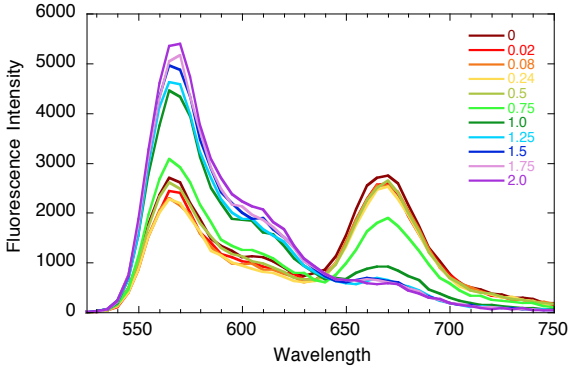

between two extreme states. In one state DNA is fully wrapped, and there is 100% FRET transfer, in the other state DNA is substantially unwrapped, and there is no FRET. As the concentration of salt in solution increases, the DNA spends a larger fraction of its time in an unwrapped conformation, thus we observe a decrease in FRET from the system. FRET efficiency was calculated at each titration point using the ratio A method [11, 92]. At salt concentrations of ~0.75M and above, FRET changes are in part or largely due to loss of histones, and are not simply interpretable as partial DNA unwrapping events.

We find that DNA inside the nucleosome is fully wrapped near physiologic ionic conditions (~0.2M) more than 99% of the time, while DNA at the ends is unwrapped 2-10% of the time (Figure 2) [11]. These data are consistent with and confirm results from earlier indirect studies using restriction enzymes that show DNA buried inside the nucleosome occupies unwrapped conformations that expose interior DNA a small, but significant, fraction of the time, much less than DNA at the nucleosome edges [7]. Lower equilibrium opening may reflect shorter lifetime in an open state, or a much slower rate for unwrapping in the first place. If this decreased accessibility is due to a shorter lifetime, solution proteins will not have time to find the buried targets before they are rewrapped. If the second, than this begs the question how long do you have to wait to access target sites buried in the nucleosome by spontaneous fluctuations?

LexA binding slightly destabilizes DNA further inside from the target site

Cooperative binding of target proteins to nucleosomal DNA has been shown previously in vivo, as the facilitated access to buried DNA binding sites by occupancy of first one, then another buried target site by a DNA binding protein [12, 22]. To test cooperativity we designed nucleosomes with internal FRET dye pairs at 35 and 57bp from the DNA end to contain the

Figure 2

A) Absolute FRET efficiency was calculated from the NaCl titration spectra by ratio A method [11]. Calculations from three individual titrations were averaged for Cy3-1, Cy3-35 and Cy3-57. Four individual titrations were averaged for Cy3-69. Error bars represent standard deviation from the mean, and a line is added to guide the eye. High FRET from internal dye locations represents a fully wrapped nucleosome state up to moderate NaCl concentrations. Cy3-1 shows a decrease in FRET from partial DNA unwrapping, as evidenced by a decrease in FRET, at significantly lower salt concentrations than the internal label sites. All salt concentrations are written as [NaCl] above the additional monovalent cations provided by buffer (0.5x TE) B) FRET efficiency is normalized to scale between 1 and 0 since the fully wrapped state represents 100% FRET efficiency, but variations in absolute FRET efficiency originate from incomplete labeling of histones with acceptor dyes. C) Equilibrium constants (k_{eq}) from data in B. Values for equilibrium below 0.001 are not shown, as FRET efficiency of 1 or greater indicates fully wrapped nucleosomes. At concentrations near physiological DNA buried inside the nucleosome is fully wrapped almost all of the time.

Figure 2

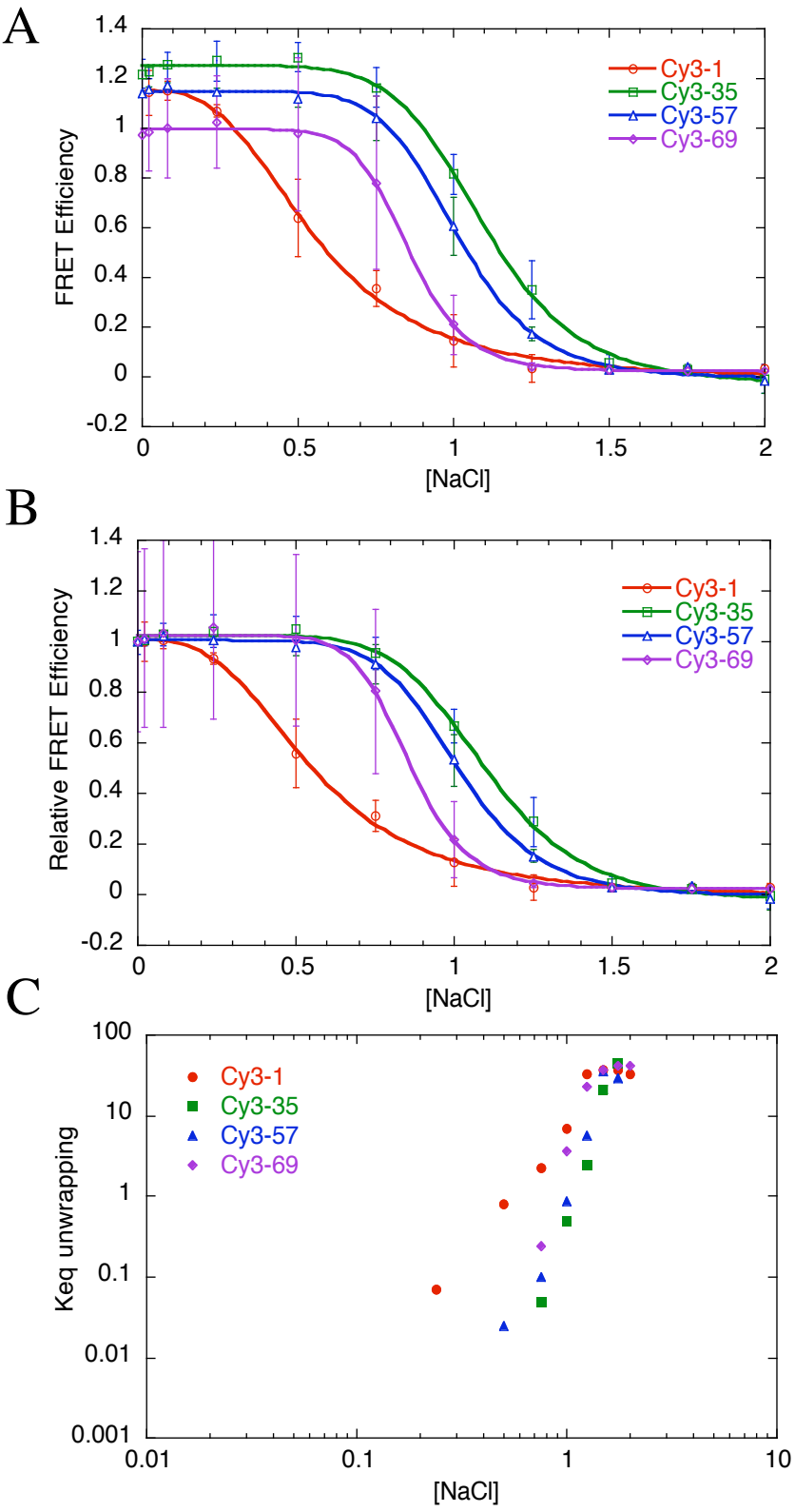
A
FRET Efficiency
[NaCl]
Cy3-1
Cy3-35
Cy3-57
Cy3-69
B
Relative FRET Efficiency
[NaCl]
Cy3-1
Cy3-35
Cy3-57
Cy3-69
C
Keq unwrapping
[NaCl]
Cy3-1
Cy3-35
Cy3-57
Cy3-69

LexA-7 binding site occupying bases 8-28 of the 601-147 sequence. The LexA target site is 20 base pairs long to which LexA binds on one face as a homodimer. We have positioned the target binding surface to face in toward the histone octamer so that DNA must unwrap for LexA to occupy the site (Figure 4B). Our assay monitored FRET from the internal dye locations as LexA was titrated into 5nM nucleosome solutions in 0.5xTE.

We see moderate FRET changes as LexA is titrated into the system (Figure 3C). LexA binding to nucleosomal DNA causes a bulk increase in quantum yield from Cy3, which affects the calculations of FRET efficiency. We chose to use the proximity ratio to monitor changes in FRET, since this takes into account changes in the general shape of the curve, as seen by the scaled fluorescence curves (Figure 3C and D). This allows us to take into account the increased quantum yield from Cy3 for the FRET calculations. These titrations show that when LexA binds its target site, and drives occupancy, the buried DNA wrapped further inside the nucleosome is destabilized (Figure 3E).

Experiments in the previous section prove that unwrapping occurs only a small fraction of the time for DNA buried inside the nucleosome. One way the equilibrium constant can be increased is through nucleosome dependent cooperative binding, which we refer to as collaborative competition [22]. These results extend our earlier biochemical analyses by showing direct effects of protein binding on the stability of remaining unwrapped DNA. Initial work on collaborative competition show that occupancy of one DNA binding protein within a nucleosome increases the probability of binding a second protein in vitro and in vivo. Here we use distance sensitive probes to directly prove the structural changes that were conferred by this earlier work, which supports cooperative binding as a mechanism for accessing DNA buried inside the nucleosome.

Figure 3

DNA inside the nucleosome is slightly destabilized by LexA binding. A) Model nucleosomes show FRET dye pairs (in spacefill representation) located further inside the nucleosome than the LexA binding site (shown in sticks, red). Cy3-35 and Cy3-57 nucleosomes were titrated with LexA, and fluorescence monitored from B) DO and C) DA nucleosomes. Because LexA binding causes a bulk increase in fluorescence of Cy3 and Cy5, D) Spectra were scaled to a constant area under the curve to show that FRET decreases upon LexA binding to DNA near the nucleosome ends. This agrees with data on cooperative binding of factors within a nucleosome. E) The proximity ratio calculated at each LexA concentration shows a small decrease in FRET due to LexA binding and destabilizing buried DNA.

Figure 3

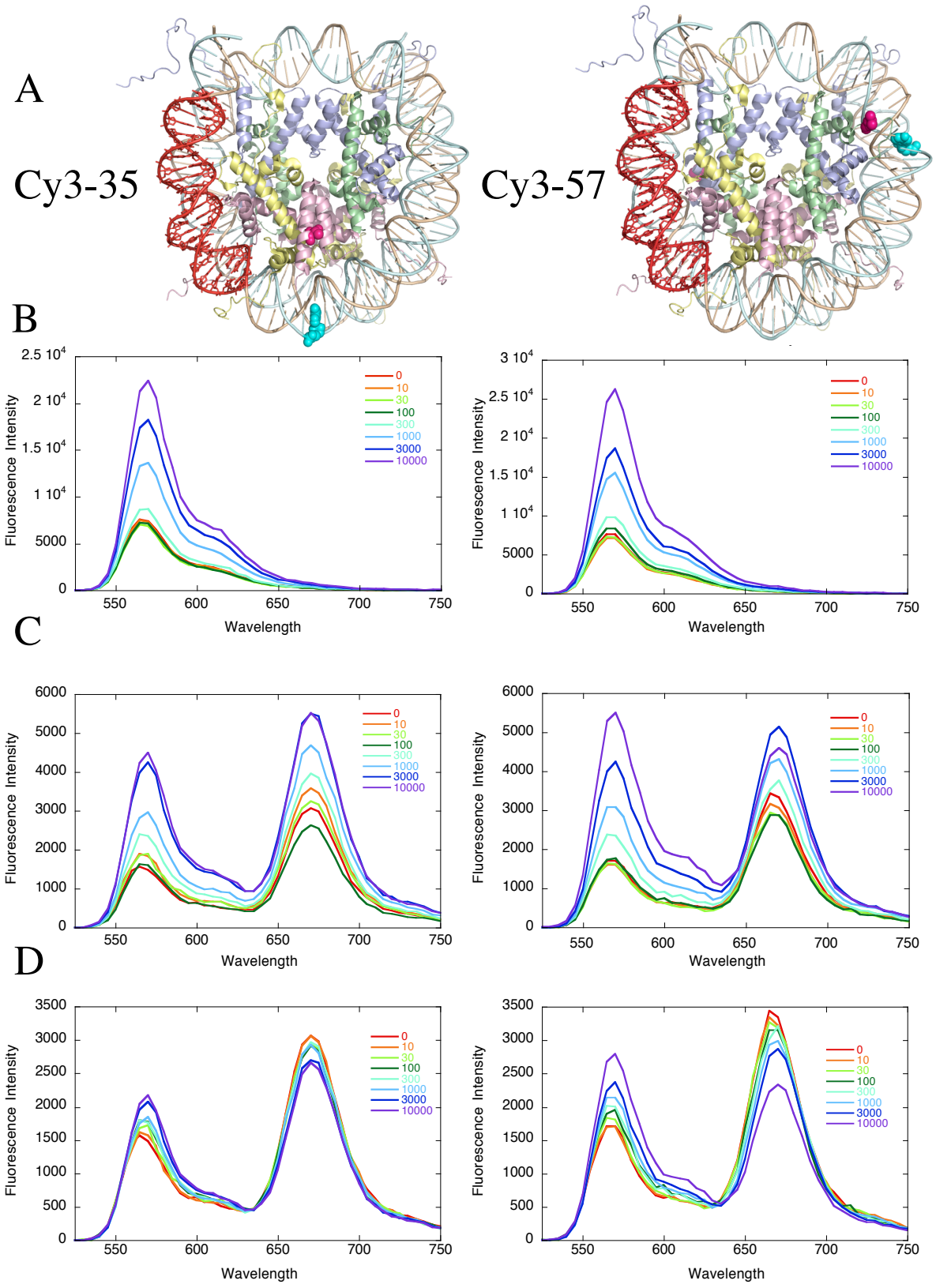
A
Cy3-35
Cy3-57
B
C
D
Fluorescence Intensity
Wavelength
0
10
30
100
300
1000
3000
10000

Figure 3 E

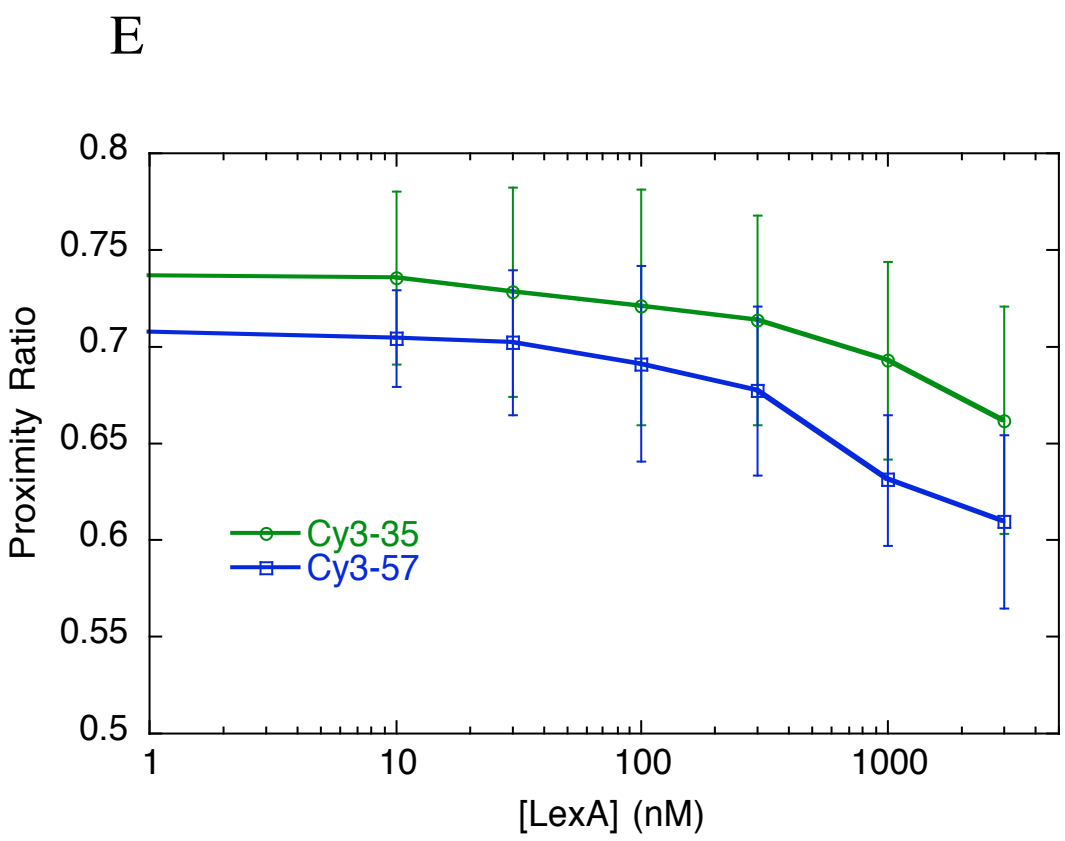
E
0.8
0.75
0.7
0.65
0.6
0.55
0.5
Proximity Ratio
Cy3-35
Cy3-57
1
10
100
1000
[LexA] (nM)

Figure 4

Schematic of nucleosomes with LexA target sites moved further interior from the end. A) FRET dye pairs are labeled with Cy3 at the 5' end of the DNA, and Cy5 on H3V35C shown in spacefill. LexA target sites are shown in red LexA-7, green LexA-17, and blue LexA-27. B) Model of LexA binding to a buried target site, DNA must unwrap from the nucleosome to allow LexA binding to the target sequence [11]. As the target is moved further inside, more and more DNA is required to unwrap before LexA can access the buried site.

Figure 4

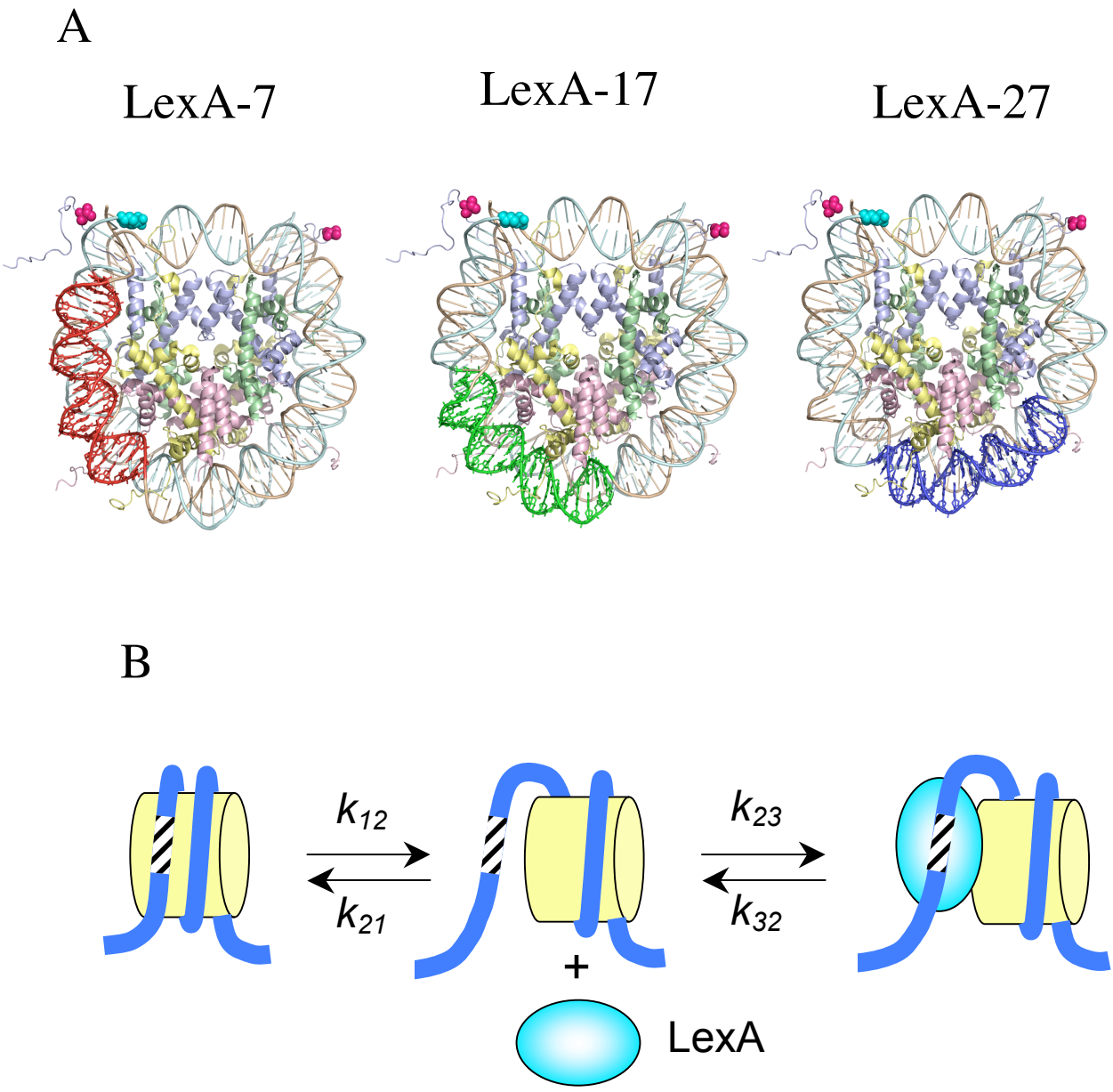

LexA is significantly occluded from binding target sites inside the nucleosome

We next looked directly at equilibrium binding of proteins to target sites buried deep within the nucleosome. While DNA inside the nucleosome is mostly wrapped at low salt concentrations, we know from previous experiments with restriction enzymes, that this DNA can be bound. We used a combined protein binding and FRET assay to look at DNA target site occupancy and accessibility as the target sites are moved further inside the nucleosome. Using DNAs labeled with Cy3 off the 5' end, and histone octamers labeled with Cy5 on H3C110A-V35C, we moved the LexA target site further inside the nucleosome in 10 base pair increments. DNA constructs were named LexA-7, LexA-17, or LexA-27 for the distance of the beginning of the LexA binding sequence from the nucleosome end (Figure 4). By moving the target site in 10 basepair increments, we maintain the orientation of the binding surface towards the histone octamer, requiring unwrapping of DNA from the nucleosome for binding. With the LexA nucleosome constructs we titrated LexA into 5nM nucleosome solutions and measured steady state fluorescence. Donor only nucleosomes made for control titrations show that there is a strong affect on Cy3 fluorescence from non-specific LexA effects independent of nucleosome unwrapping requiring that we look again at the proximity ratio for these constructs (Figure 6A-C, Figure 7).

We find that LexA can bind with relatively high affinity (k_d ~300nM) to the target site near the nucleosome edge, but LexA is significantly occluded from target sites 17 or 27 base pairs from the end of the nucleosome (K_d > 10μM). However, gel shift experiments show that LexA can bind with high affinity (K_d ~ 3nM) to the naked DNA from all three constructs (Figure 5). Additionally, we know from restriction enzyme studies that all nucleosomal DNA can be accessed, but occupancy of binding sites cannot be saturated inside the nucleosome, even at

Figure 5

Gel shift assay of LexA binding the target sequence. A) From the top down is LexA-7, 17, 27 gel shift of naked DNA. LexA concentrations are 0, 1, 3, 10, 30, 100, 300, 1000, 3000nM LexA, with low concentration DNA. All DNAs show equivalent gel shifts with K_d of 1-3nM. Naked DNA is lowest band, which shifts to one defined band with one LexA homodimer binding, and higher molecular weight species with non-specific LexA binding on the DNA. B) From the top down is LexA-7, 17, 27 gel shift of nucleosomes. LexA concentrations are 0, 10, 30, 100, 300, 1000, 3000, 9000nM LexA, with low concentration nucleosomes. All nucleosomes show equivalent gel shifts showing K_d values of ~300nM-1μM LexA, which proves that nucleosome gel shifts with LexA are not sensitive to specific protein binding site occupancy, but to non-specific interactions which shift nucleosomes. Here all nucleosomes are supershifted by LexA binding by 3-9μM LexA.

Figure 5 A

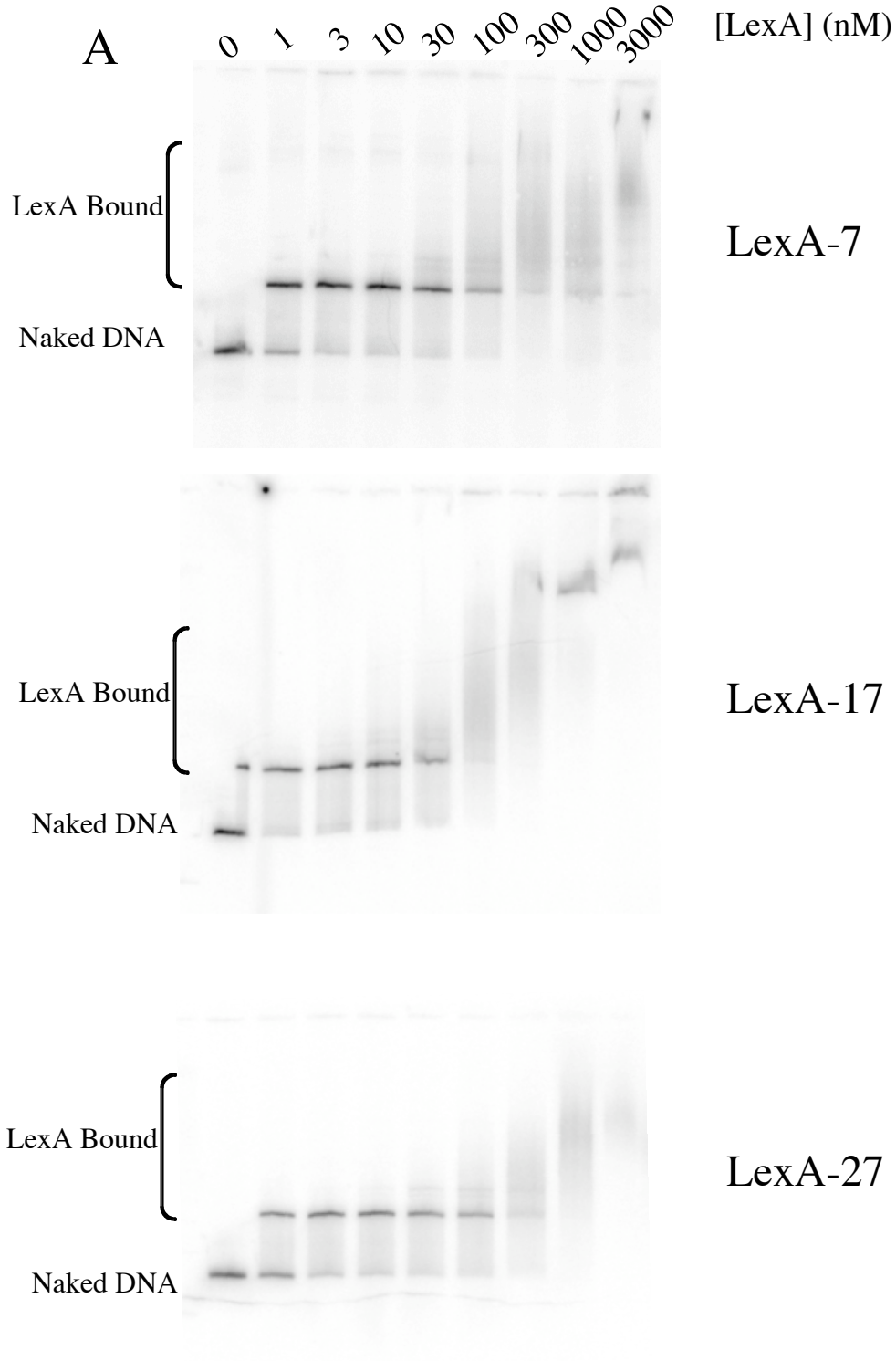
A
0
1
3
10
30
100
300
1000
3000
[LexA] (nM)
LexA Bound
Naked DNA
LexA-7
LexA Bound
Naked DNA
LexA-17
LexA Bound
Naked DNA
LexA-27

Figure 5 B

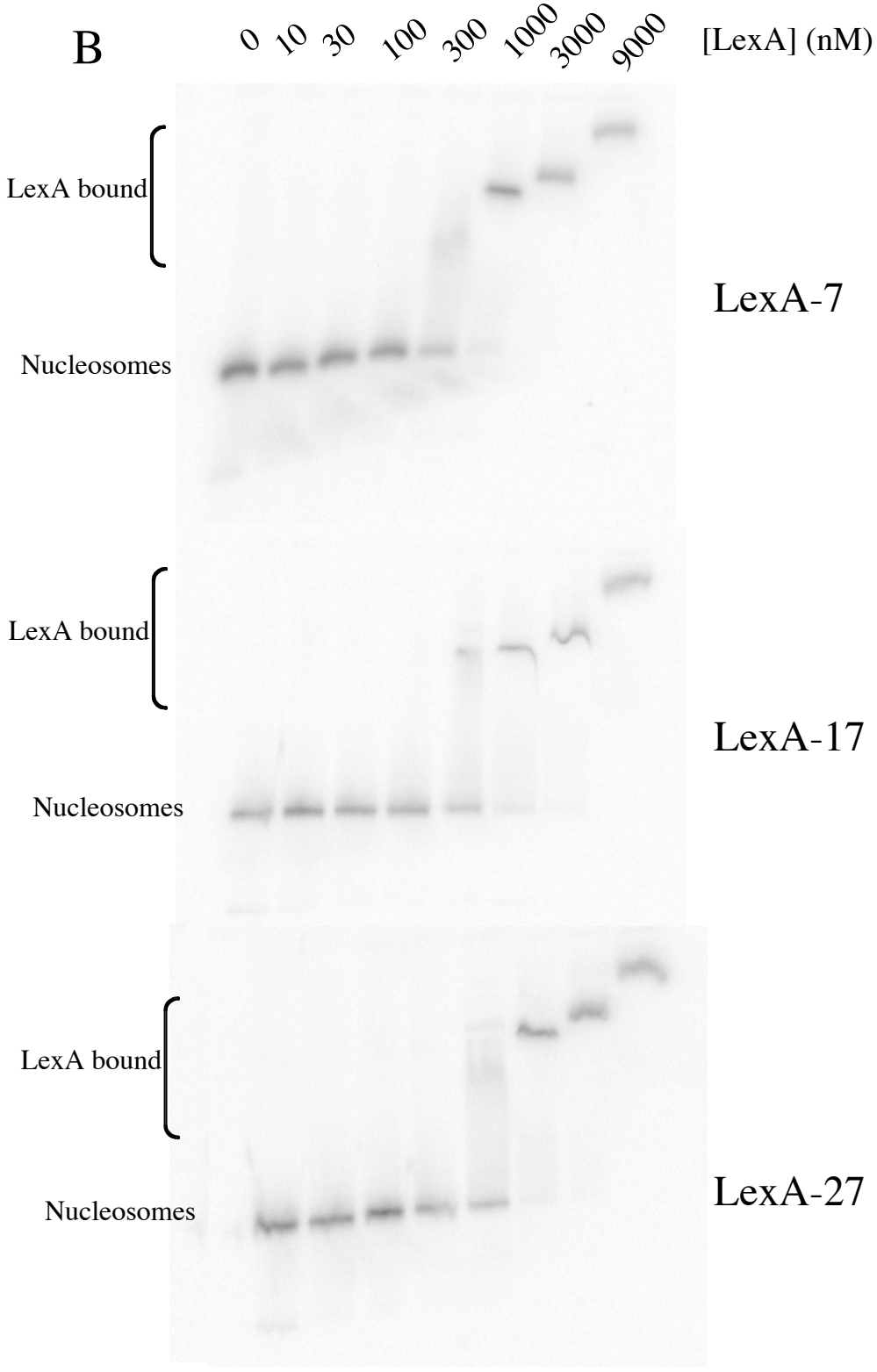
B
0
10
30
100
300
1000
3000
9000
[LexA] (nM)
LexA bound
Nucleosomes
LexA-7
LexA bound
Nucleosomes
LexA-17
LexA bound
Nucleosomes
LexA-27

Figure 6

Fluorescence assay of LexA binding to nucleosome constructs. LexA was titrated into 5nM solutions of DO or DA nucleosomes. A) LexA-7, B) LexA-17, C) LexA-27, in each the top panel DO titrations show a nonspecific increase in Cy3 fluorescence with high concentrations of LexA. Middle panel, DA nucleosomes show significant FRET changes due to LexA binding for LexA-7, while fluorescence changes are minimal for LexA-17 and 27 until high concentrations of LexA. Bottom panel, DA spectra were scaled to constant area under the curves to correct for non-specific affects of LexA on Cy3 fluorescence.

Figure 6 A

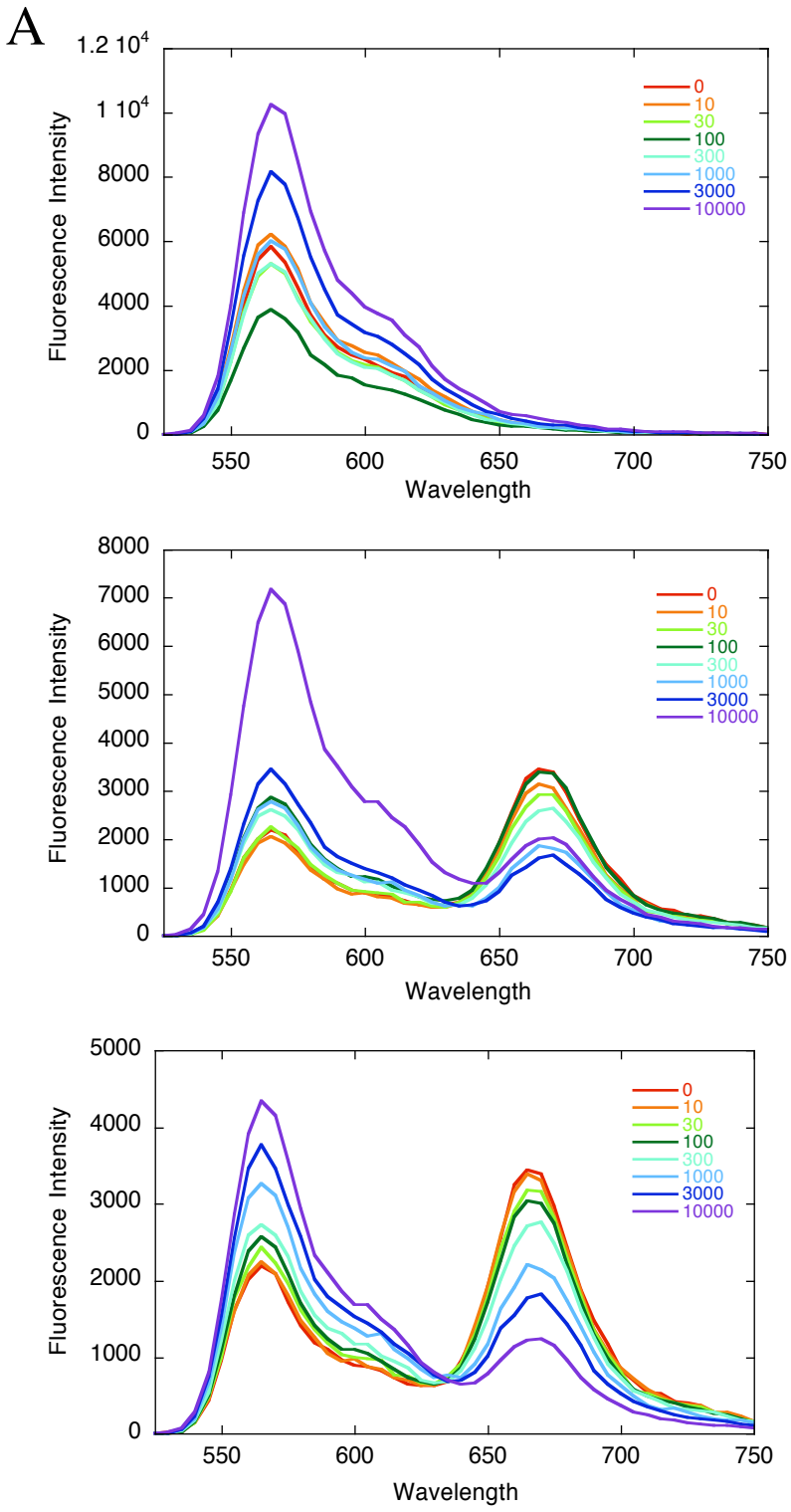
A
1.2 10^4
1 10^4
8000
6000
4000
2000
0
Fluorescence Intensity
550
600
650
700
750
Wavelength
0
10
30
100
300
1000
3000
10000
8000
7000
6000
5000
4000
3000
2000
1000
0
Fluorescence Intensity
550
600
650
700
750
Wavelength
0
10
30
100
300
1000
3000
10000
5000
4000
3000
2000
1000
0
Fluorescence Intensity
550
600
650
700
750
Wavelength
0
10
30
100
300
1000
3000
10000

Figure 6 B

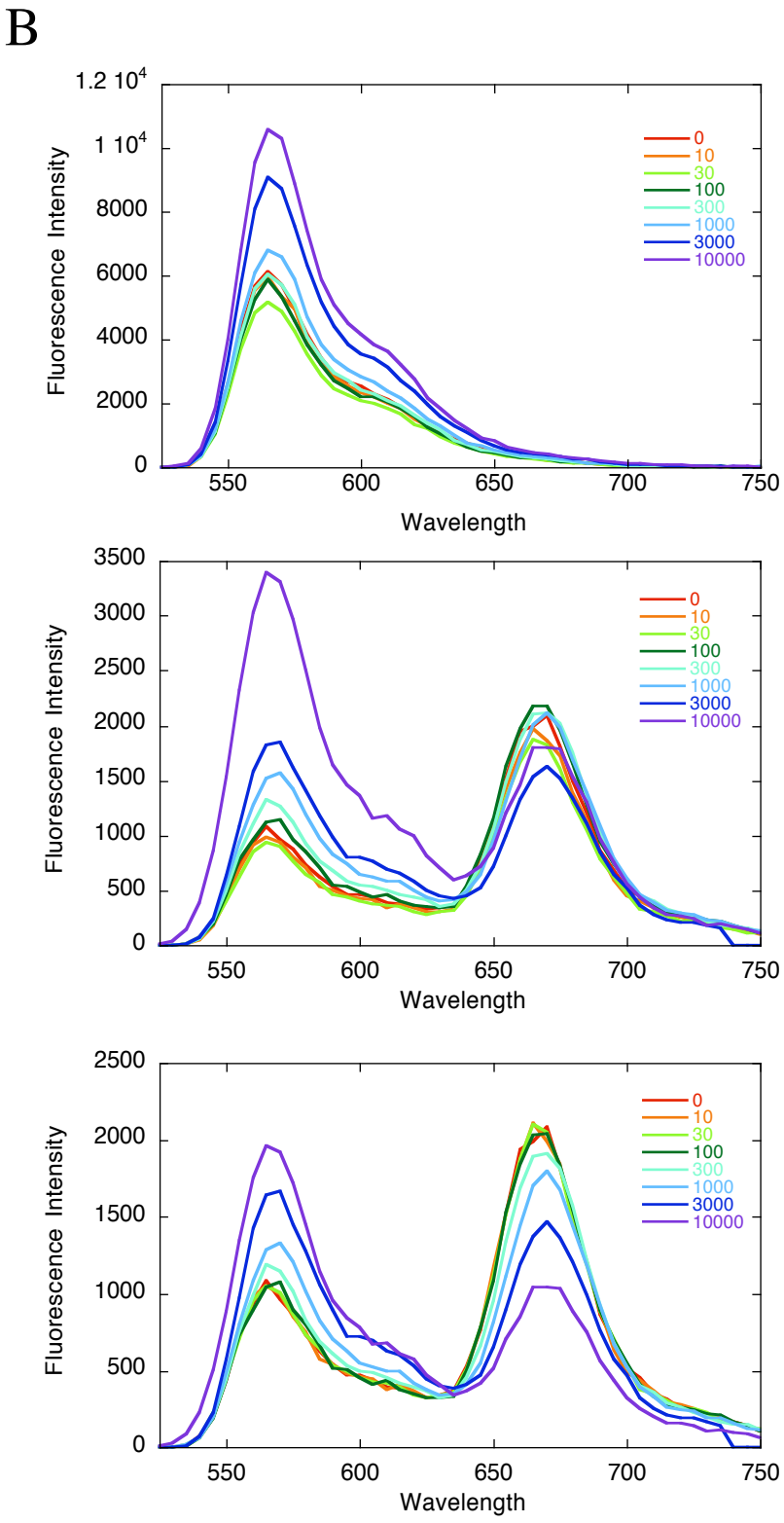
B
1.2 10^4
1 10^4
8000
6000
4000
2000
0
Fluorescence Intensity
550
600
650
700
750
Wavelength
0
10
30
100
300
1000
3000
10000
3500
3000
2500
2000
1500
1000
500
0
Fluorescence Intensity
550
600
650
700
750
Wavelength
0
10
30
100
300
1000
3000
10000
2500
2000
1500
1000
500
0
Fluorescence Intensity
550
600
650
700
750
Wavelength
0
10
30
100
300
1000
3000
10000

Figure 6 C

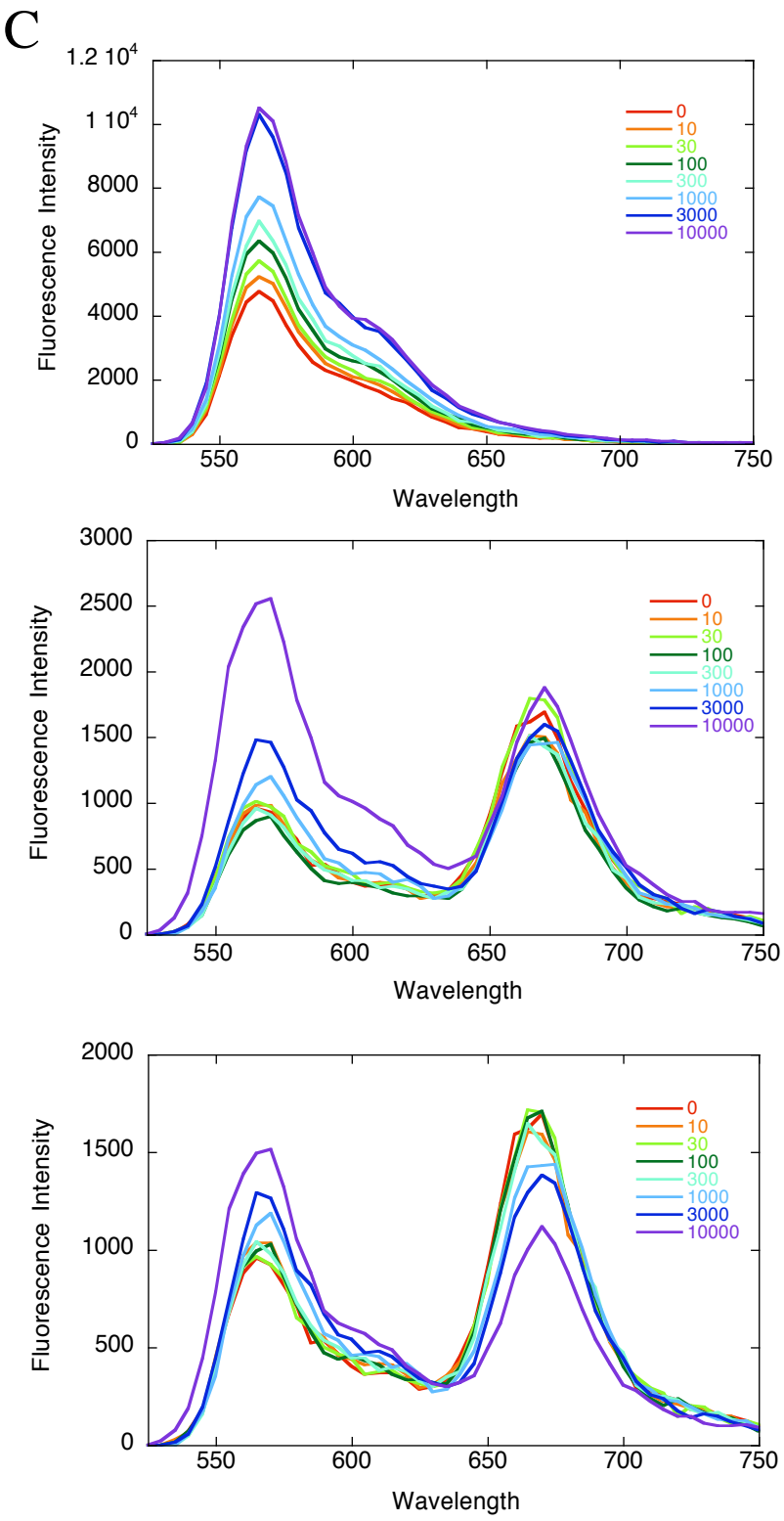
C
1.2 10^4
1 10^4
8000
6000
4000
2000
0
Fluorescence Intensity
550
600
650
700
750
Wavelength
0
10
30
100
300
1000
3000
10000
3000
2500
2000
1500
1000
500
0
Fluorescence Intensity
550
600
650
700
750
Wavelength
0
10
30
100
300
1000
3000
10000
2000
1500
1000
500
0
Fluorescence Intensity
550
600
650
700
750
Wavelength
0
10
30
100
300
1000
3000
10000

Figure 7

LexA binding curve is shown from quantification of FRET changes by proximity ratio. Data points are an average of 3 independent titrations, with error bars representing the standard deviation from the mean. Curves are colored as before, LexA-7 red, LexA-17 green, LexA-27 blue, and fit to a simple binding curve. This analysis shows that LexA occupancy is not saturating at any concentration, and the fraction of nucleosomes bound by LexA decreases as the target site is moved further inside.

Figure 7

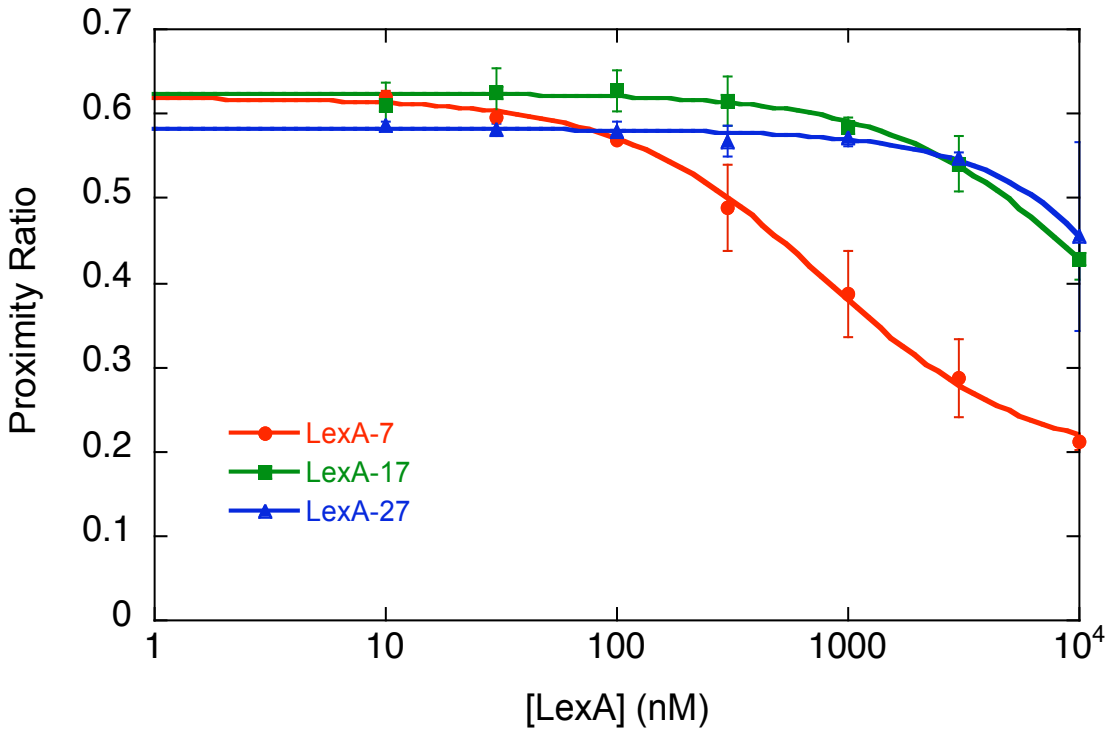
0.7
0.6
0.5
0.4
0.3
0.2
0.1
0
Proximity Ratio
LexA-7
LexA-17
LexA-27
1
10
100
1000
10^4
[LexA] (nM)

LexA concentrations above physiological levels (1μM) [93]. We find that while DNA inside the nucleosome must be occasionally accessible the free energy of LexA binding sites far inside the nucleosome, for reasonable concentrations of LexA, is less than the energetic cost of keeping DNA unwound from the nucleosome core.

Kinetics of Unwrapping nucleosomal DNA

Kinetics of unwrapping DNA inside the nucleosome are slower than diffusion

DNA inside the nucleosome is mostly wrapped at low salt concentrations, and the accessibility of DNA sites buried inside the nucleosome is significantly reduced. However, we also know that DNA inside the nucleosome does transiently unwrap to expose nucleosomal DNA to solution and DNA binding proteins. DNA near the ends of nucleosomes unwraps quickly, 2-5 times per second, which is a biologically relevant timescale of accessibility [9, 19]. The rate of access to DNA buried further inside the nucleosome is not known, but we prove that the equilibrium unwrapping is very low. From our definition of rates and lifetimes, this means that either the rate of unwrapping is decreased, or the lifetime of the unwrapped state is reduced, and the re-wrapping rate is increased.

We use nucleosomes with FRET dye pairs inside the nucleosome and FCS to look at fluorescence fluctuations due to structural changes on the short timescale. Fluorescence correlation spectroscopy is a useful method for monitoring fluorescence fluctuations, but the time scale is bounded by the rate of diffusion (in free solution ~300msec for nucleosomes) and the time resolution of the instrument (10^{-7} seconds). Initial experiments with Cy3-35 nucleosome solutions in 0.5xTE with 20mM DTT show no kinetic fluctuations faster than the diffusion time of the molecules through the confocal volume (data not shown). This means that the timescale of

fluctuations inside the nucleosome is slower than at the ends, since previous free solution experiments were used to determine the rate of wrapping and unwrapping at the DNA ends [19]. To extend the time resolution of the experiment, and improve the readable extent of our data, diffusion of the molecules through the confocal volume must be slowed. We applied a technique recently used by M. Levitus (personal communication) to slow diffusion so that kinetics could be measured from our nucleosome constructs with dye pairs inside. Here we restricted diffusion of the molecules in a polyacrylamide gel, before monitoring correlations from the sample. We were able to slow diffusion of the nucleosomes to ~1300msec, which increases the time resolution of the correlation (Figure 8).

Isolating the kinetic component of the curve as described [91], we see that the kinetics of FRET fluctuations inside the nucleosome are slowed, as expected, for DNA buried inside the nucleosome (Figure 8). This slowed kinetics is shown as a failure of the kinetic component to clearly begin to turn over for FRET dye pairs 35 bp from the end, while FRET dye pairs at the ends, turn over earlier.

DNA unwrapping to reveal sites buried deep inside the nucleosome slows as sites are moved further interior

To monitor spontaneous unwrapping of DNA to reveal sites deep inside the nucleosome we used LexA to capture DNA partially unwrapped from the histone core. We make use of LexA-7, 17 and 27 binding sites and FRET dye pairs at the nucleosome end to watch bulk solution changes in fluorescence as LexA binds its target site inside the nucleosome. Monitoring changes on the short timescales with the Applied Photo Systems (APS) stopped flow instrument allows us to determine the rate of unwrapping DNA from the nucleosome to reveal the buried

Figure 8

FCS experiments show that there is no faster timescale of unwrapping buried DNA than can be detected with the Stopped-flow instrument A) Correlation curves from Cy3-1 and Cy3-35 DA nucleosomes. Cy3 autocorrelation green, Cy5 autocorrelation red, Cy3-Cy5 cross-correlation blue. Data fit well to a diffusion plus triplet curve above 10^{-6} seconds [88]. B) Kinetic contributions to the curves were isolated by dividing the correlation curves from donor autocorrelation (DD) by the cross correlation (DA) (red), the acceptor autocorrelation (AA) by DA (green) and DD by AA (blue). This results in the diffusion component of the curves dropping out, leaving only the kinetic contributions, which can then be fit according to the method discussed [91]. In this case, the data were too noisy to fit at long times, but show clearly that there are no faster fluctuations for Cy3-35 than Cy3-1.

Figure 8

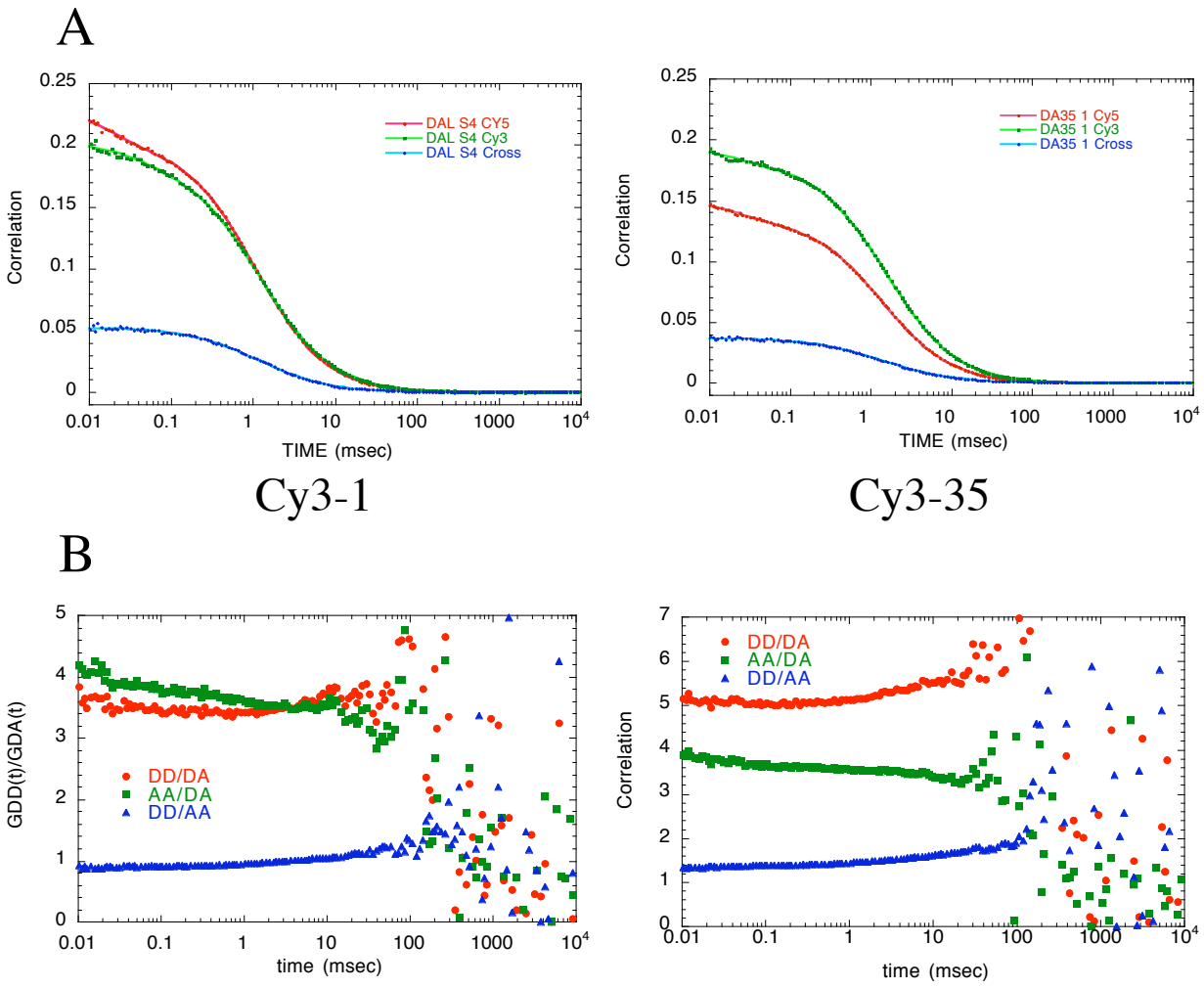
A
DAL S4 CY5
DAL S4 Cy3
DAL S4 Cross
Correlation
TIME (msec)
Cy3-1
DA35 1 Cy5
DA35 1 Cy3
DA35 1 Cross
Correlation
TIME (msec)
Cy3-35
B
DD/DA
AA/DA
DD/AA
GDD(t)/GDA(t)
time (msec)
DD/DA
AA/DA
DD/AA
Correlation
time (msec)

target. Using the stopped-flow instrument we were able to simultaneously follow changes in fluorescence from the donor and acceptor dyes on the sub-second to minutes timescale as nucleosomes are mixed with LexA (Chapter 2).

Nucleosomes were mixed 1:1 (v/v) with LexA solution or a mock buffer mix to final concentrations of 5nM nucleosomes and 400nM or 1μM LexA in 0.5xTE. Changes in fluorescence intensity were counted until the signal stabilized using linearly spaced timepoints for 10 to 1000 seconds. Control experiments consisted of both donor only labeled nucleosomes, and a mock buffer only dilution of the nucleosomes. We detected no fluorescence changes in the mock buffer only reactions (Figure 9), but did see small fluorescence changes from donor-only constructs (data not shown), consistent with steady state experiments showing a non-specific LexA effect on Cy3 fluorescence. In steady state experiments with LexA titrations, we see a bulk increase in fluorescence from both Cy3 and Cy5 upon addition of LexA above 400nM (Figure 7 A-C). Consistent with this observation, the kinetic traces from these constructs show a bulk increase in fluorescence from both channels upon addition of LexA (compare Figure 9 with top panel of Figures 10, 11 and 12). This rapid increase is faster than the time resolution of the instrument, and is followed by a slow decay of fluorescence as DNA unwraps and LexA binds its target site inside the nucleosome. We interpret these changes in fluorescence signal as a rapid interaction of LexA with the dye, non-specifically modifying the quantum yield of Cy3, which is seen both in donor only and donor-acceptor experiments, and results in a bulk increase in fluorescence from donor and acceptor channels. This fast increase is followed by fluorescence changes due to LexA binding its target site inside the nucleosome, which requires DNA to unwrap from the histone, and corresponds to the decrease in acceptor fluorescence, and increase in donor fluorescence. Our data agree well with the steady state fluorescence measurements of

Figure 9

Mock mixing reactions of LexA-7, 17 and 27 (from top down) in 0.5xTE show no fluorescence change over the same times measured in LexA binding experiments. Raw data from Cy3 fluorescence, and intensity units are shown in cyan, Cy5 is shown in magenta.

Figure 9

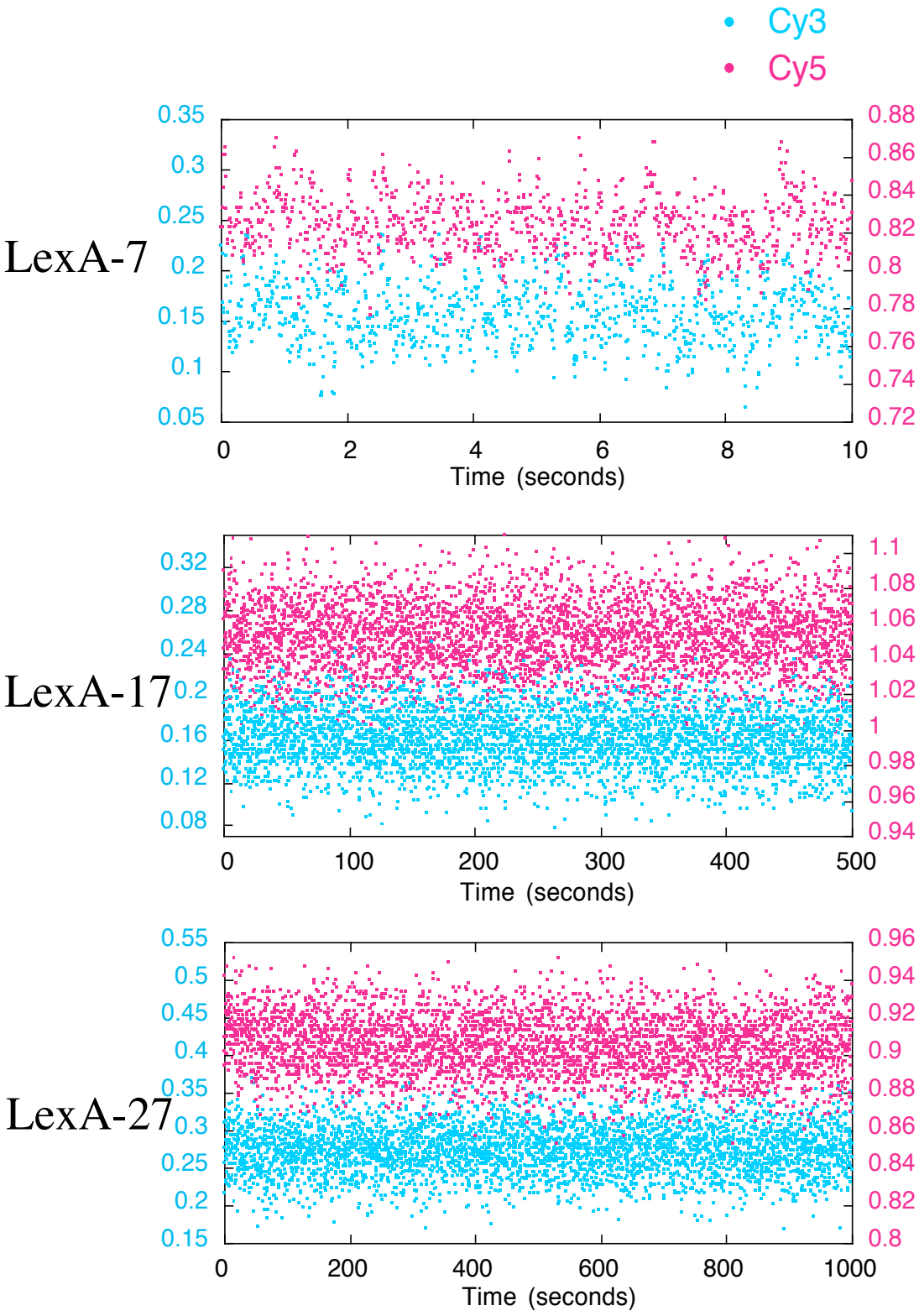
Cy3
Cy5
LexA-7
0.35
0.3
0.25
0.2
0.15
0.1
0.05
0.88
0.86
0.84
0.82
0.8
0.78
0.76
0.74
0.72
0
2
4
6
8
10
Time (seconds)
LexA-17
0.32
0.28
0.24
0.2
0.16
0.12
0.08
1.1
1.08
1.06
1.04
1.02
1
0.98
0.96
0.94
0
100
200
300
400
500
Time (seconds)
LexA-27
0.55
0.5
0.45
0.4
0.35
0.3
0.25
0.2
0.15
0.96
0.94
0.92
0.9
0.88
0.86
0.84
0.82
0.8
0
200
400
600
800
1000
Time (seconds)

Figure 10

Data for kinetics of 1μM LexA binding to LexA-7. Top, raw data (averaged from 5 runs) for Cy3 (cyan) and Cy5 (magenta) fluorescence changes on the 10 second timescale. Raw data was further averaged and smoothed and the proximity ratio calculated for each timepoint. Data was fit to a single exponential curve (middle panel, residuals shown in lower panel). Kinetics of unwrapping are $k_{12} = 4.1\ sec^{-1}$, which agrees well with calculations from the same construct by Gu Li [19].

Figure 10

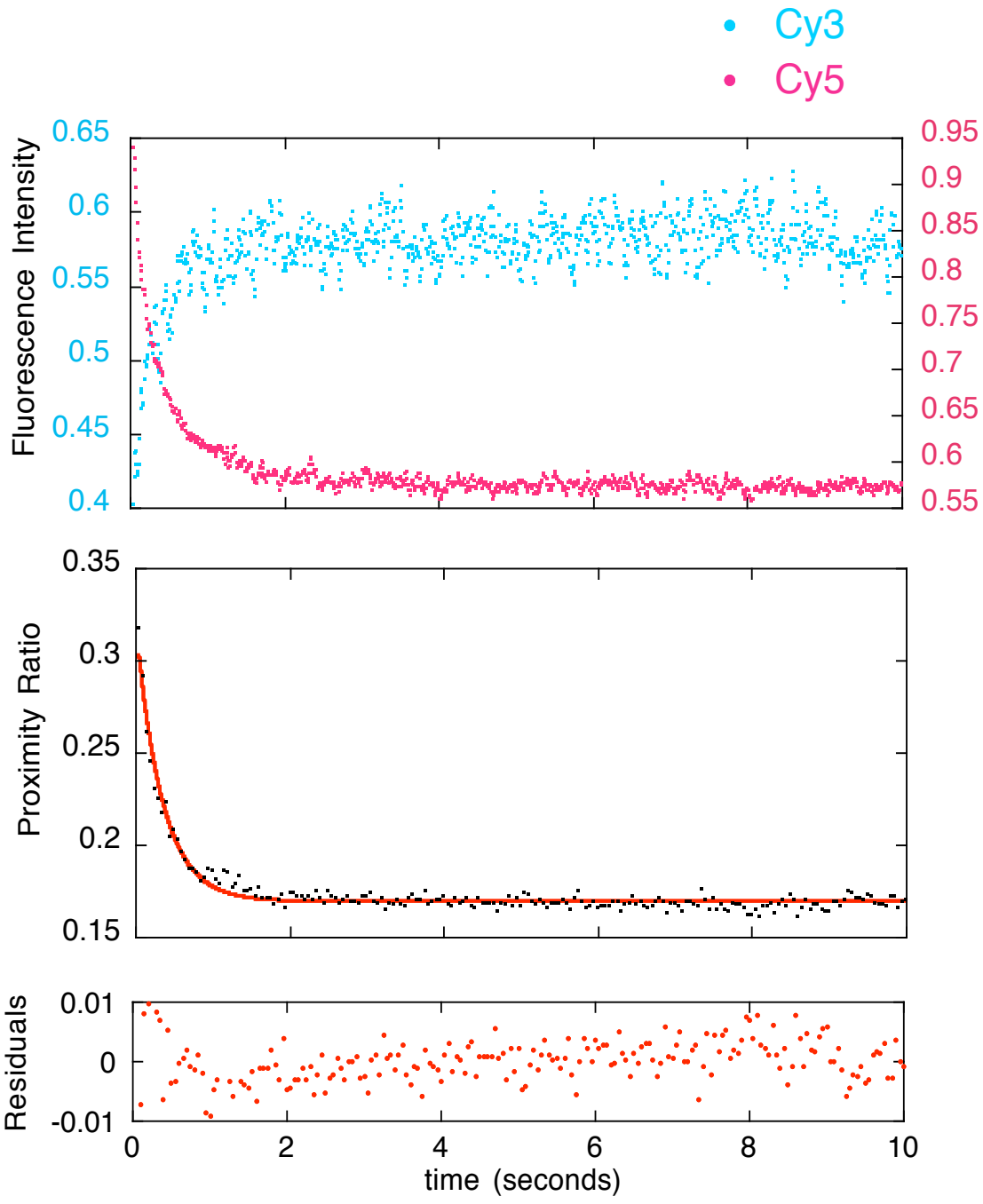
Cy3
Cy5
Fluorescence Intensity
0.65
0.6
0.55
0.5
0.45
0.4
0.95
0.9
0.85
0.8
0.75
0.7
0.65
0.6
0.55
Proximity Ratio
0.35
0.3
0.25
0.2
0.15
Residuals
0.01
0
-0.01
0
2
4
6
8
10
time (seconds)

Figure 11

Data for kinetics of 1μM LexA binding to LexA-17. As above, top panel is raw data averaged from two runs, middle panel, proximity ratio calculated from averaged and smoothed data fit to a single exponential fit, with residuals lower panel. Fit data show kinetics of unwrapping are k_{12} = 0.016 sec^{-1}, which is one unwrapping event in 2-5 minutes.

Figure 11

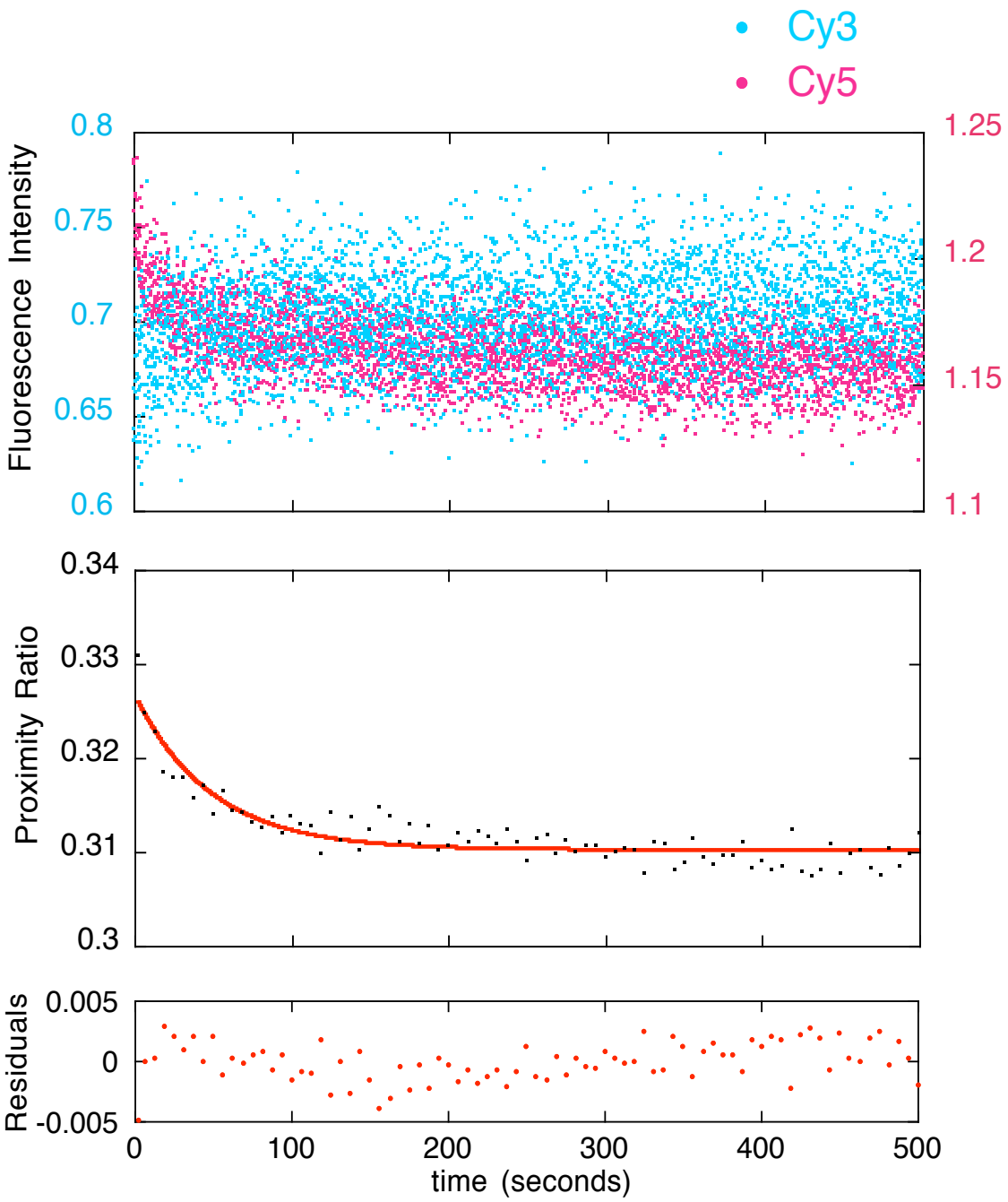
Cy3
Cy5
Fluorescence Intensity
0.8
0.75
0.7
0.65
0.6
1.25
1.2
1.15
1.1
Proximity Ratio
0.34
0.33
0.32
0.31
0.3
Residuals
0.005
0
-0.005
0
100
200
300
400
500
time (seconds)

Figure 12

Data for kinetics of 1μM LexA binding to LexA-27. As above, top is raw data averaged from two runs, and smoothed to one second bins (0-500seconds) or simply binned to one second increments (500-1000sec). Middle panel is smoothed and fit proximity ratio with residuals in the lower panel. LexA binding to DA27 is very slow k_1~0.0017 sec^{-1} or once in 15-20 minutes. This is an upper limit on the kinetics since the decay trace does not reach an equilibrium after 1000seconds, which is the time limit of the instrument.

Figure 12

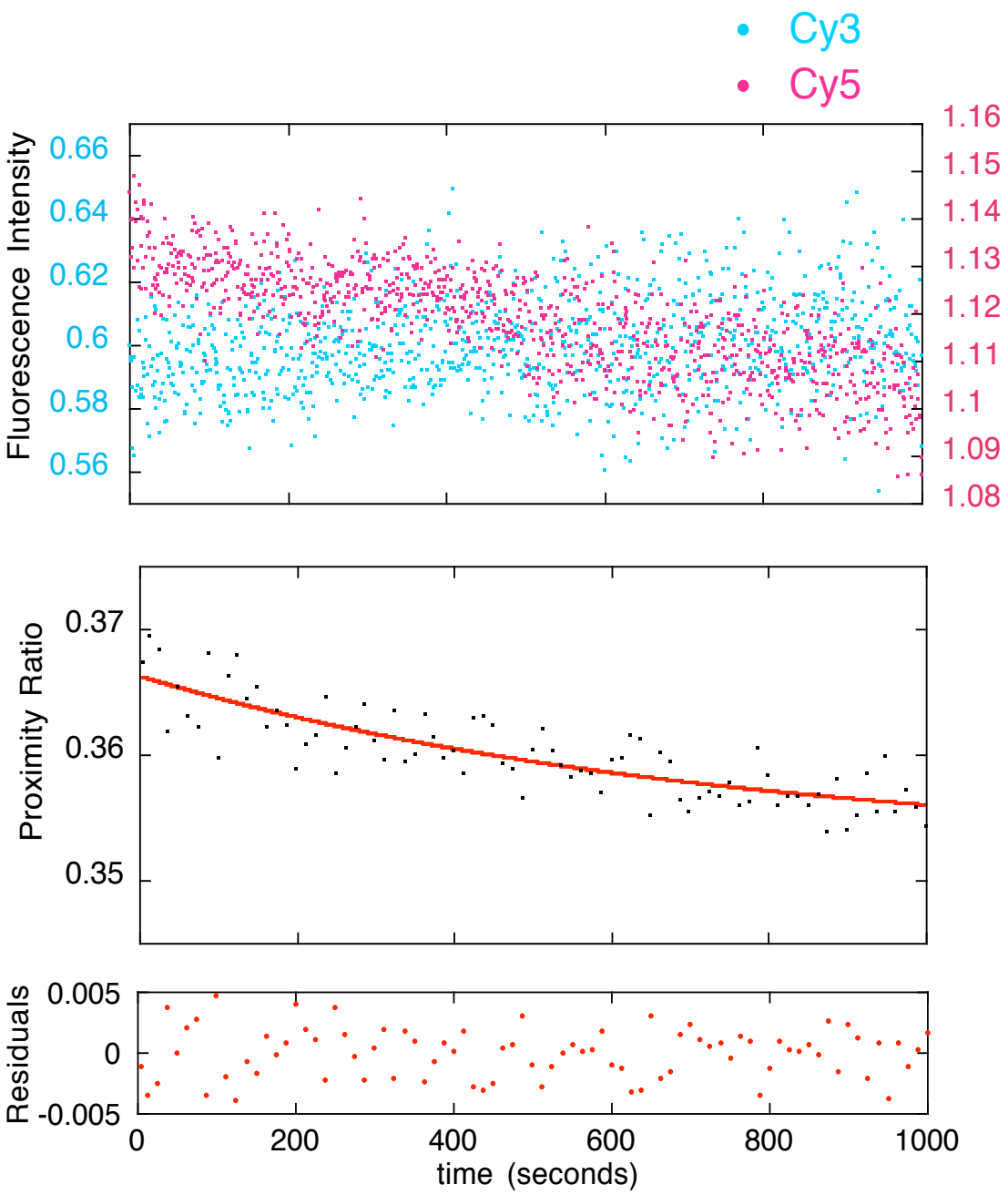
Cy3
Cy5
Fluorescence Intensity
0.66
0.64
0.62
0.6
0.58
0.56
1.16
1.15
1.14
1.13
1.12
1.11
1.1
1.09
1.08
Proximity Ratio
0.37
0.36
0.35
Residuals
0.005
0
-0.005
0
200
400
600
800
1000
time (seconds)

the bulk increase in fluorescence, and the difference in the amplitude of fluorescence changes for the three constructs.

The raw data was averaged for several experimental runs (Figure 10, 11, 12 top panel) and smoothed with a running average to decrease noise (care was taken that the running average did not skew kinetic data). FRET efficiency for these constructs was calculated from the averaged and smoothed data using the proximity ratio. For our calculations we scaled the fluorescence signal to the mock buffer mixed reaction, and divided the Cy5 fluorescence signal by the combined fluorescence from Cy3 and Cy5 at each timepoint to give us the proximity ratio (Figures 10, 11, and 12 middle panel). These data curves were fit with single exponential decay curves to quantify the rate of unwrapping DNA from the nucleosomes for LexA binding (Figure 13). Data were also fit with double exponential decay curves, but this does not improve the error of the curves to the data, thus we conclude that the single exponential fit captures the essence of kinetic changes from the system (Figure 14).

We find that the rate of unwrapping DNA from the nucleosome decreases by orders of magnitude as binding sites are moved further inside the nucleosome. Fitting the data show that as the LexA binding site is moved interior in steps of 10bp, the rate of unwrapping decreases in proportion to the decrease in accessibility of the DNA. Our data agree with kinetics of unwrapping for the LexA binding site near the nucleosome edges, which is in rapid equilibrium between wrapped and unwrapped conformations, allowing easy access of binding proteins on the sub-seconds timescale. For LexA-17 binding site, 10 bases further interior, the rate of unwrapping (k_{12}) is slowed from k_{12} ~4second^{-1} for LexA-7 to k_{12} ~0.016second^{-1}. Binding to LexA-27 is slowed even further to k_{12} ~0.0017second^{-1}, only once in 15-20 minutes! (Figure 10, 11, 12, 13, 14) This very slow rate of accessibility to buried nucleosomal DNA could be a

Figure 13

Kinetics of unwrapping for internal target sites is slowed by orders of magnitude for each 10bp increment moved further inside. Here we show k_{12}, the unwrapping rate for the constructs taken from the proximity ratio plots fitted to a single exponential curve. Error bars are generated by KaleidaGraph, and come from the error in the single exponential fit to the data points.

Figure 13

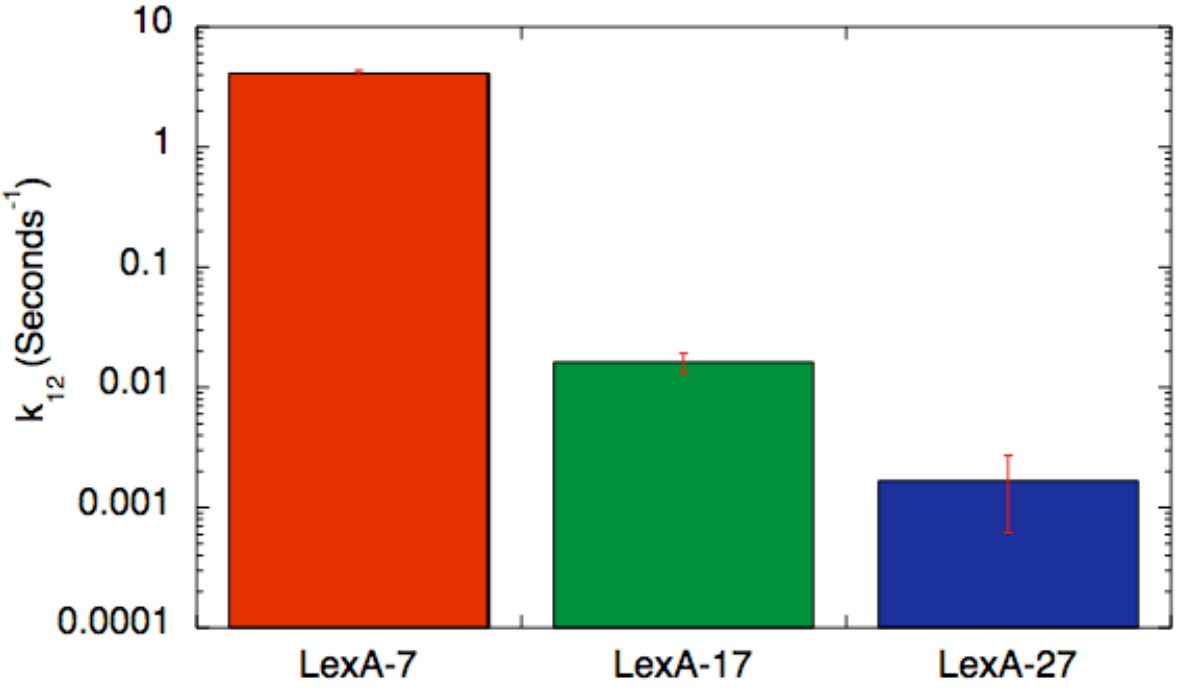

Figure 14

Data for the single and double exponential curve fits to the LexA binding kinetic traces. Although single exponential decay curves fit the data well, and account for the fluorescence changes in the system, double exponential decay curves can give additional information on rates of unwrapping. A) Single exponential curve fits for k_{12} are given with the error of the fit and the amplitude of change. B and C) Double exponential curve fits for k_1 and k_2, along with error and the amplitude of change for each.

Figure 14

A

Single Exponential Fit	k_{12}	Error	Amp	Error
LexA-7	4.1	0.2	0.16	0.007
LexA-17	0.016	0.003	0.014	0.001
LexA-27	0.0017	0.001	0.013	0.005

B

Double Exponential Fit	k_1	Error	Amp	Error
LexA-7	8.7	1.4	0.16	0.014
LexA-17	0.18	0.05	0.015	0.002
LexA-27	0.12	0.21	0.0049	0.005

C

Double Exponential Fit	k_2	Error	Amp	Error
LexA-7	1.3	0.3	0.47	0.01
LexA-17	0.0077	0.002	0.012	0.0007
LexA-27	0.0009	0.0013	0.021	0.05

significant contributor to the strong repression of binding sites inside the nucleosome, implying that the timescale of gene activation is strongly dependent on nucleosome location at promoters.

A caveat worth mentioning is that all nucleosomes used in these experiments use DNAs based on the 601 nucleosome positioning sequence, which may artificially decrease the accessibility of DNA measured here below that of typical stretches of genomic DNA. However, the affinity of 601 DNA for the nucleosome is similar to (only a few-fold greater than) that of some genomic regions [94], so these studies using 601 are relevant to the accessibility of natural genomic DNA in nucleosomes.

Discussion

Chromatin organization is affected by DNA sequence, chromatin remodeling and positioning complexes, histone modifications, DNA binding proteins, and polymerase traffic, which vary for each individual cell and cell type. This complex set of factors influence the location of nucleosomes along DNA, causing variation in positioning from one cell to the next, even in genetically identical cells. This varied location of nucleosomes creates problems when binding sites near promoters are targeted by activators, but the sites are buried deep within nucleosomes. Here we discuss the implications of reduced accessibility of nucleosomal binding sites and various methods that may be used to make target sites accessible.

Earlier biochemical and FRET based assays prove that DNA spontaneously unwraps from the histone core to expose buried targets to solution. These studies show that there is decreased accessibility to DNA buried inside the nucleosome, but that this DNA is accessible a small fraction of the time. We have extended these data to show how DNA is unwrapped to

reveal buried sites. Site exposure hypothesizes that DNA is progressively unwrapped from one end, and that DNA must be unwrapped for proteins to occupy their target sites. Other recent studies with FRET dyes at the DNA ends show that unwrapping is not necessary for protein binding, but in this case the binding site faces out towards solution so that accessibility is reduced only by a factor of three, although the site is located at the nucleosome dyad [55]. We show that, for target sites that face in towards the histone core, occupancy is possible only when DNA is unwrapped. We find that proteins can gain access to targets buried in the nucleosome, but with significantly lower occupancy and slower rate.

We determined the rate of accessibility to buried nucleosomal DNA showing that the decreased accessibility to buried DNA is due to a decrease in the rate of unwrapping (k_{12}). These data for nucleosome accessibility paint a picture of spontaneous DNA unwrapping events (Figure 15 A). Near the nucleosome edges, DNA is in rapid equilibrium between a fully wrapped and partially unwrapped state, this allows easy and fast access to targets. As you move progressively further inside the nucleosome, it becomes less likely that a spontaneous unwrapping event will extend far enough to expose the target site. This increases the lifetime of the closed state for buried target sites, and decreases the rate of accessibility. FCS analysis shows that the rates of opening and closing for DNA partially unwrapped from the nucleosome are slow inside the nucleosome. Stopped-flow measurements have revealed the rate of unwrapping DNA to be drastically decreased as targets are moved further inside the nucleosome. The rate of unwrapping/opening (k_{12}) decreases by an order of magnitude or more for each 10bp a target site is moved further in from the nucleosome ends. Which means that while DNA at the edges of nucleosomes are available many times per second, DNA buried farther inside is only available after many minutes (Figure 15 A).

Figure 15

A) Cartoon of chromatin organization near a promoter. As DNA in vivo is packaged into nucleosomes that occlude DNA from other binding proteins, target sites have reduced accessibility and occupancy at buried sites. Nucleosomes (shown as ellipses) occlude proteins from binding their target sites, which may cause slowed activation of gene expression. Target sites in internucleosomal regions are freely accessible (green), and targets at the edges of nucleosomes are easily bound (yellow), while targets buried deep in a nucleosome are largely inaccessible at all times (red). Slowed accessibility to buried targets at promoters may contribute to the noise in response time to signals seen on the single cell level. B) Cartoon showing methods of proteins accessing buried DNA target sites. Target sites are shown colored in red or blue on the DNA (in black). Spontaneous unwrapping of DNA from the nucleosome allows rapid accessibility to sites near nucleosome edges, but limited and slow access to sites buried deep inside the nucleosome. Collaborative competition of binding proteins to buried DNA occurs by progressive invasion of a nucleosome by binding first one, and then subsequent proteins to increase occupancy, and potentially rate of access to buried targets. Remodeling complex activity to move nucleosome location along DNA is another mechanism to increase access to buried targets. Remodeling complexes increase accessibility of target sites by moving nucleosomes along DNA. Remodelers are recruited to promoters to remodel nucleosomes specifically, but may also act ubiquitously to make all DNA more accessible.

Figure 15

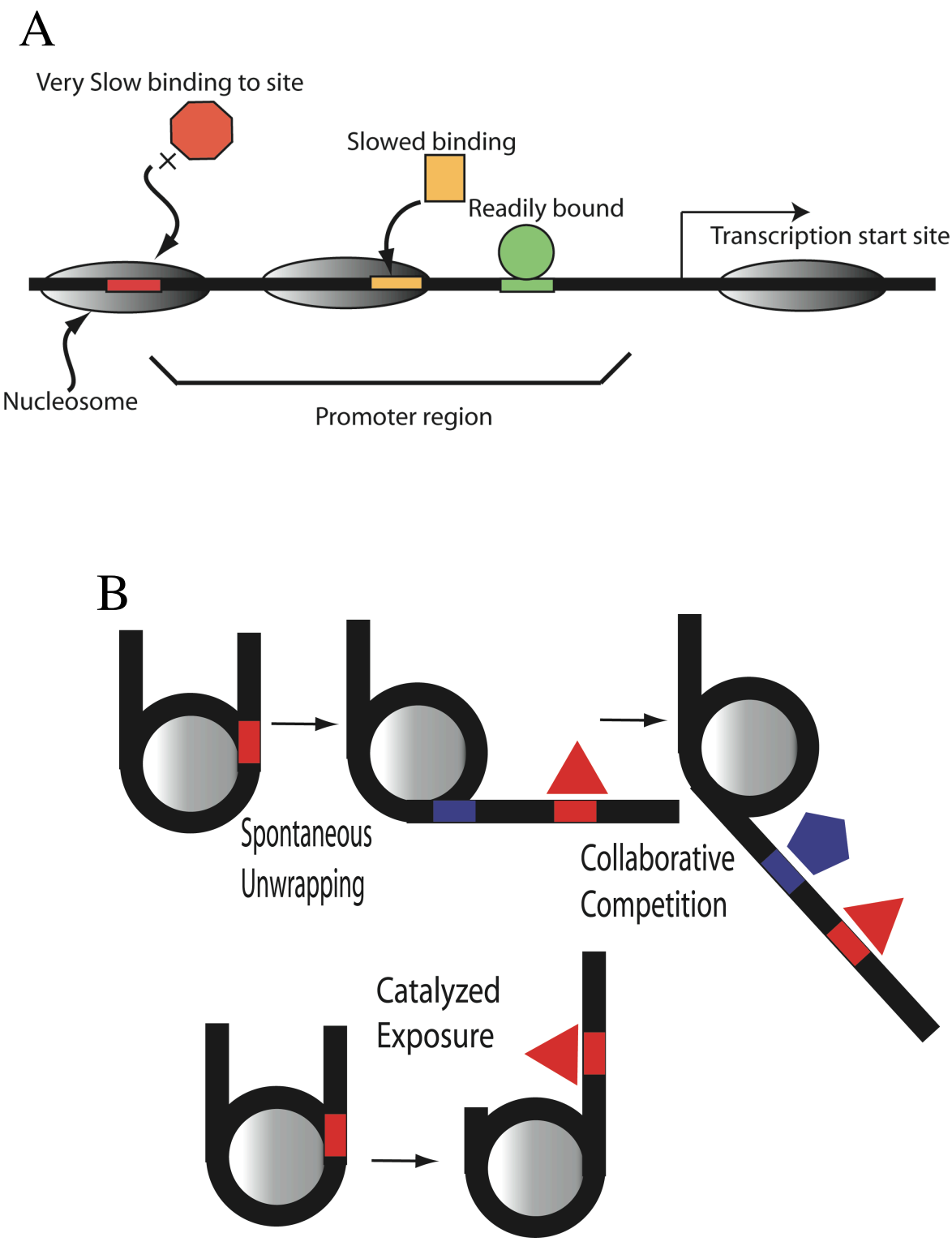
A
Very Slow binding to site
Slowed binding
Readily bound
Transcription start site
Nucleosome
Promoter region
B
Spontaneous
Unwrapping
Collaborative
Competition
Catalyzed
Exposure

These data show that target site location within a nucleosome can be a source of variability in the response time of a particular cell to signaling. Indeed, recent studies on gene activation at the single cell level show that there is significant diversity in the time of response to a signal. This delay in response time is also on the many minutes timescale, showing that nucleosome positioning could be the single source for this delay. Slowed accessibility also indicates that if cells want to ensure a timely response to a signal, they must increase accessibility (and potentially rate of unwrapping) through cooperative binding of proteins, or by recruiting remodeling complexes to rearrange nucleosomes, thus making DNA accessible (Figure 15 B).

We present data supporting collaborative competition of proteins to nucleosomal DNA. Here biochemical studies prove that in vitro and in vivo, occupancy of one DNA binding protein in a nucleosome increases occupancy of a second binding protein. We show directly with FRET assays what was conferred from these biochemical data that target sites near nucleosome edges destabilizes DNA wrapped further inside. This may be a mechanism that cells use to access buried target sites, as often at promoters important regulatory protein binding sites occur in multiples. This increases accessibility of buried sites even if all of the targets are partially covered by a nucleosome, as binding one nucleosomal site increases occupancy of sites buried further inside (Figure 15 B).

Significantly slowed unwrapping of DNA to expose buried targets points to the need for additional chromatin remodeling complexes to increase access to nucleosomal DNA. Chromatin remodeling enzymes act to increase accessibility by catalytically moving nucleosomes from one location to another. It is easily imagined that these remodelers act ubiquitously at all promoters,

and over all DNA, however, there is no data to support this, while there is evidence to support recruitment of remodelers to specific sequences. These remodeling complexes can increase accessibility of DNA by moving nucleosomes to expose buried targets, or they can repress binding sites by moving nucleosome to bury previously exposed target sites. Thus we find that nucleosome location has a strong affect on gene regulation, and that variant nucleosome positioning can lead to misregulation of genes.

Acknowledgements

Thanks to Michael Poirer for help with data analysis of steady state fluorescence experiments. Dan Grilley and Georgette Moyle for help with data analysis of FCS data.

Chapter 5

Method for Mapping Nucleosome Dyad Position with Basepair Resolution

Method for Mapping Nucleosome Dyad Position with Basepair Resolution

Introduction

Mapping the exact translational position of nucleosomes in the genome would allow better resolution of internucleosomal distance, better algorithms for nucleosome alignment, and the ability to monitor changes in nucleosome location resulting from polymerases, chromatin remodelers, heat or other stimuli. Here we adapted a method to map the position of nucleosomes with base pair resolution *in vitro* and, potentially, *in vivo*. Current methods take advantage of enzymes that cut unprotected DNA, or are time and chemistry intensive. Enzymes present several issues for exact nucleosome measurements. First, thermal fluctuations in which DNA lifts away from the histone core allow the enzymes to cut inside the nucleosome [6, 8], or the enzymes can stop before they reach the edge of the nucleosome, by happenstance or because of steric hindrance from other chromatin structures. Additionally these enzymes have sequence or base preference. For these reasons, nucleosome positions mapped using enzyme digestion approaches can give skewed results, which are a close approximation to, but not an exact map of, true nucleosome positions. In contrast, the method presented here is highly specific (base pair resolution), has no known sequence preference, and the experiment is fast, easy, and inexpensive. It is adapted from related procedures developed by Flaus & Richmond [95-97] and Reid Johnson [98], and Thomas Sigman [99], but we use a different chemistry, which allows the use of commercially available reagents, greatly facilitating the work and providing highly reproducible results.

For the mapping method, we use histones with the H4S47C mutation. This residue is positioned very close to the DNA backbone, ~3-4 bases from the nucleosome dyad. We attach 1-10 phenanthroline (OP) with an iodoacetamide sulfhydryl reactive functional group to the cysteine in H4S47C. The OP chelates a Cu2+ ion, which reacts with reducing agents and peroxide to produce free radicals. The OP is thus a highly localized source of OH• free radicals tethered to H4S47C, which itself is in close proximity to the DNA backbone. The free radicals cause backbone cleavage of DNA near the nucleosome dyad through the Fenton reaction [97]. After the mapping is quenched, solutions are enriched for nucleosomes, and cut DNA fragments are resolved on 8% denaturing gels for basepair resolution of DNA fragment lengths. This reaction results in one major cutting site for each OP labeled H4 (on each DNA strand), and a few lower probability cut sites on either side of the major site. These cut sites define the location of the OP and, together with equivalent reactions using the other labeled DNA strand, define the nucleosome dyad location with basepair resolution.

Method

DNA

For our experiments we used the 601 high affinity nucleosome positioning sequence with and without additional flanking DNA for final lengths of 147 or 278bp. DNAs were individually end labeled on the Watson or Crick strand (or preferably both, separately) by radioactively phospho-labeling the left or right primer individually before amplification. PCR was done with one ^{32}P labeled primer, the other primer cold, and 5-10ng template DNA, 0.5uM primers, 200μM dNTPs, ThermoTaq buffer (NEB) and Taq polymerase (NEB). After amplification we gel

purified the full length DNA on 5% polyacrylamide gels with crush and soak [100]. Crush and soak solution contains 0.5 M NaOAc, 0.1 mM EDTA, and 0.1% SDS. Gel slices were frozen at –80°C and crushed in an eppendorf tube with the melted p1000 tip. Crushed acrylamide gel was resuspended in 500µl - 1mL crush and soak solution, and incubated overnight at 37°C. Acrylamide gel pieces were pelleted from solution by centrifugation at high speed for 15 min, and the extracted DNA (in the supernatant) was ethanol precipitated, and washed into 0.5x TE for use in reconstitutions.

Labeling Histones

Histone octamers were refolded from recombinant histones expressed and purified *in vitro*. We used histone H3C110A, H2A, H2B, and H4S47C. H4S47C is a histone mutant with a cysteine near the nucleosome dyad, and is used as the attachment site for the mapping agent (Figure 1). Histones were expressed and purified as described elsewhere in detail (chapter 2), , excepting that the final buffer change contains no reducing agent that can quench the labeling reaction. OP is a light sensitive compound, and all experiments from this point until the reaction was quenched were done in reduced ambient light, and stored covered in foil to reduce exposure to light. Additionally, OP chelates Cu to initiate the mapping reaction, so contaminating heavy metals could cause the reaction to activate inappropriately. In practice, we find that it is safe to not worry about removing trace metal contaminants from solution, as there is very little cutting from the reaction if Cu is bound, but not activated by addition of MPA and H_2O_2 (A reaction was accidentally run with the addition of $CuCl_2$, but not MPA or H_2O_2. When the reaction was run on a sequencing gel, there were no cut bands in any lanes.)

Figure 1

Model of OP labeled nucleosome. H4S47C OP attachment residues are shown in blue and spacefill. In the top down view of the nucleosome, you can see the close proximity of the OP labeling sites to the DNA backbone on either side of the dyad.

Figure 1

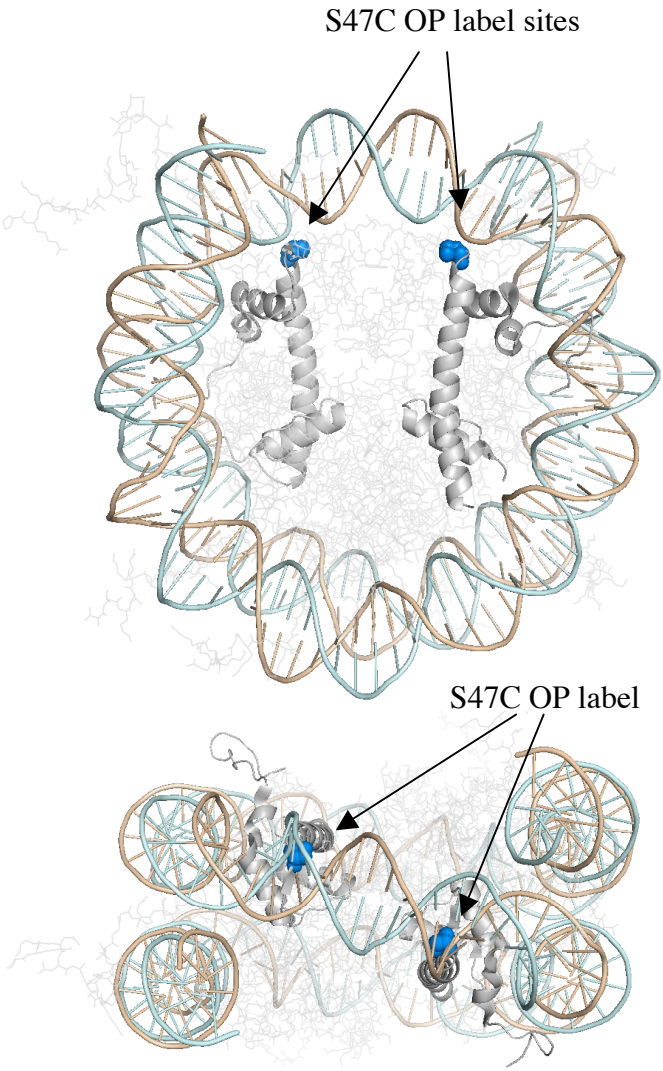

Histone octamers were labeled with N-(1,10-phenanthrolin-5-yl)iodoacetamide (OP, Invitrogen) on H4S47C as follows. Refolded octamers stored in solution (40mM Tris pH 7.5, 1mM EDTA, 2M NaCl, No βME) were reduced with 10 fold molar excess BondBreaker TCEP solution (Pierce) for 10 minutes at room temperature. While the octamer is being reduced fresh OP is dissolved in high quality dimethylsulfoxide (DMSO, Sigma). We used 10-20x molar excess of OP to octamer for labeling solutions. Histone octamers are typically refolded and stored at 1mg/ml ~ 9μM concentrations, so we used ~200μM OP solutions. OP was added dropwise to reduced octamer solutions with mixing to increase solubility. Labeling reactions were incubated at room temperature for 2 hours with mixing, and overnight at 4°C with mixing (Labquake shaker). Labeling reactions were quenched by addition of excess 2-Mercaptoethanol (βME Sigma, we typically use ~200-300μM final concentration of βME). Excess unreacted OP was removed, and octamers were exchanged into storage buffer by running the octamers through Micro Bio-Spin 30 chromatography columns (BioRad). Microspin columns were exchanged into storage buffer containing 10mM Tris pH 7.5, 1mM EDTA, 2M NaCl by washing 3x as described in the protocol before OP octamers were washed through the column (it is important to not have reducing agent in solution with octamers or nucleosomes after this point). Labeled octamer was checked for integrity on a denaturing protein gel, and stored in the dark on ice at 0°C until used. Labeled octamers are stable on ice for at least a month, although we generally use them before then.

Reconstitutions

Nucleosomes were reconstituted with the uniquely end labeled DNAs and OP histone octamers as described [57]. Reconstitutions contained 20,000- 200,000cpm ^{32}P labeled DNA,

0.2mg/ml core particle DNA (CPDNA) for buffering, 0.2mg/ml OP histone octamer, 0.5mM phenylmethanesulphonylfluoride (PMSF) and 1mM benzamadine (BZA) as proteinase inhibitors in 0.5x TE. Nucleosomes were not purified away from free DNA and aggregates, since we show by native gel that there is very little aggregation, and intact nucleosomes are enriched in solution after the mapping reaction.

Mapping

OP-nucleosomes are activated for mapping by rapid sequential addition of 100μM $CuCl_2$, 6mM 3-Mercaptopropionic acid (MPA, Acros Chemicals stock concentration ~11.7M) a reducing agent, and 6mM H_2O_2 (Sigma, 30% solution ~9.6M) a free radical source (the reaction is not highly sensitive to a 2x increase in concentration of MPA and H_2O_2, as the reaction proceeds as expected with 2X excess of activators). We nucleosome mapping solution contains 40mM Tris pH 7.5, 5mM NaCl, 20mM $MgCl_2$. Tris acts as a free radical mop eliminating significant background cutting, $MgCl_2$ allows solutions to be enriched for nucleosomes after cutting as nucleosomes self-assemble at moderate concentrations of $MgCl_2$, and low concentration NaCl stabilizes the nucleosome. Since nucleosome reconstitutions are not purified, and we cannot see what happens to unlabeled CPDNA, the exact concentration of nucleosomes was not calculated for the reaction. We typically measured that enough counts from ^{32}P would remain in solution to see full length DNA, and cut DNA products after mapping, enriching, and sequencing the DNA (at least 200-2000cpm). We used high concentrations of metal, reducing agents, and peroxide in comparison to the nucleosome solutions, so that there is full occupancy of OP-nucleosomes with Cu^{2+}.

A time course for mapping was done, using 30 sec, 1min, 5 min, and 10 min to determine the optimal time for mapping. The reaction is fast, and we found ~20% of nucleosomes had backbone cleavage by 30-60 seconds, which is sufficient for our experimental analysis. By 5-10 minutes nucleosome integrity was reduced by the high occurrence of double stranded DNA breaks resulting from free radicals diffusing away from the OP label site (Figure 2). We wanted to avoid over cutting, both to increase the fraction of nucleosomes that survived the reaction, and because diffuse cut sites makes data analysis less precise. Mapping reactions were quenched by addition of $1/10^{th}$ volume of 28mM 2-9-dimethyl-1,10-phenanthroline (Neocuproine, Acros Organics) in a solution of 30% DMSO and water. Mapping reactions are typically 20-25μL volume. This allows us to use 15-20μL volumes for a preliminary nucleosome location or moving assay, add the mapping chemistry, while still leaving a small volumes to conserve sample, and for loading on the sequencing gel. Neocuproine is very similar in structure and function to 1,10-phenanthroline, but because it is free in solution it sequesters the Cu^{2+} away from DNA to stop the mapping reaction. It was first dissolved in DMSO, and then mixed to a final concentration of 28mM in a 30% DMSO (in water) solution to increase solubility. Neocuproine should be dissolved fresh for each experiment just prior to beginning the reaction, since it precipitates out of solution over time.

After mapping, we enriched solutions for whole nucleosomes to reduce the noise from background cutting from Cu and peroxide in solution, free DNA, or nucleosomes that were cut too far and subsequently fell apart. 20mM $MgCl_2$ in solution facilitates nucleosome self-association, which helps nucleosomes to precipitate out of solution by centrifugation. We spin at 50,000 rpm 1 hour in the TLA 100.3 rotor in the Beckman Optima TL Ultracentrifuge, this requires high quality eppendorf tubes that can withstand that g force. Enriched nucleosomes were

Figure 2

Native gel of the time course for mapping nucleosomes. Lane 1: 50bp ladder, lane 2: unmapped nucleosomes, lane 3: quenched nucleosome mapping reaction, lane 4: 1 nucleosomes mapped 1 min, lane 5: nucleosomes mapped 5 min. Nucleosomes in solution are somewhat destabilized by mapping chemicals, and as the reaction proceeds, double stranded breaks in the DNA increase, causing nucleosomes fall apart completely.

Figure 2

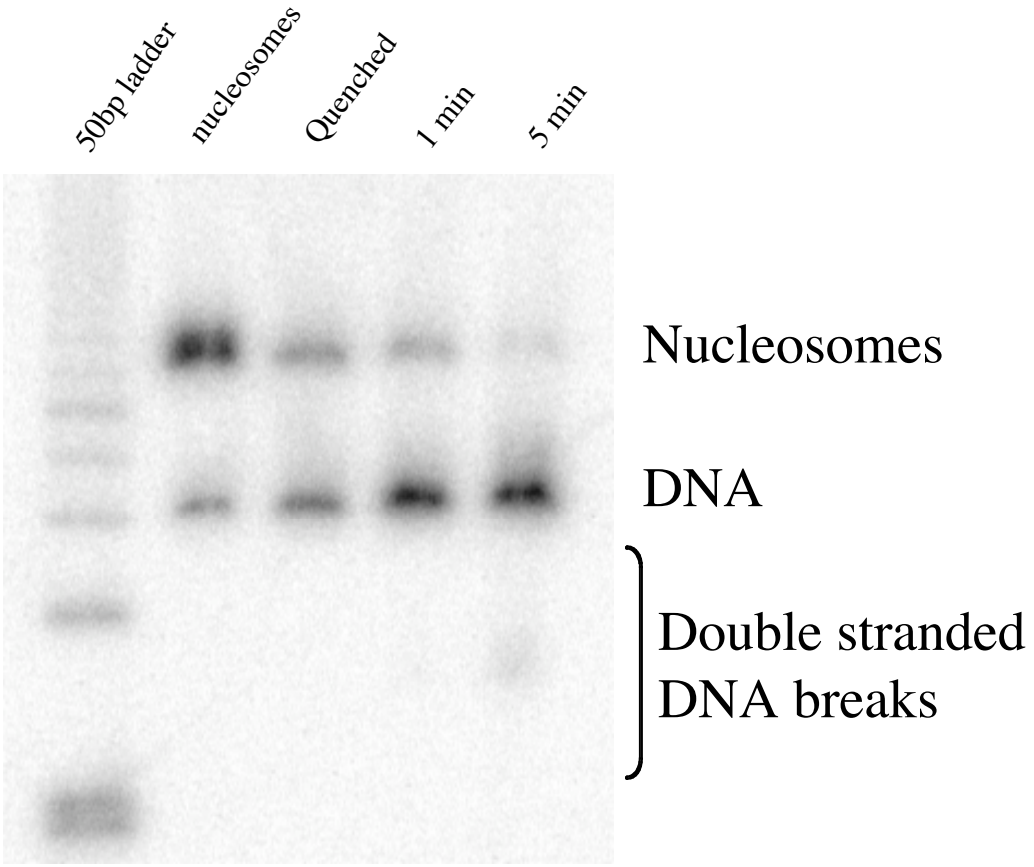
50bp ladder
nucleosomes
Quenched
1 min
5 min
Nucleosomes
DNA
Double stranded
DNA breaks

resuspended in low concentration TE (Figure 3) or in formamide gel loading buffer, or formamide loading buffer with proteinase K. DNAs were denatured at 95°C for 5-10 minutes before loading on the gel. We removed DNAs from 95°C block, spun briefly to collect sample, and load while still warm onto gels pre-run to increase temperature to 48-52°C.

Sequence standards

To accurately determine migration of DNA through a gel, the standards for comparison must be the same length, composition, and labeled similarly. For mapping, we need to know with basepair resolution the migration of the DNA through the gel, compared to the appropriate size standard. For this reason, we used 601-147 or 601-278 DNA as the template for a sequencing standard using the Sanger method and Sequenase cycle sequencing kit (GE Healthcare). Almost all sequencing kits come ready to use with 7-deaza-dGTPs. This modification does not affect the migration of DNA in the gel, but allows easier denaturing of the DNA both during cycle sequencing and gel running.

Sequencing Gels

For nucleotide resolution of the mapping cut site, we ran mapping products on a sequencing sized 8% denaturing polyacrylamide gel (1x Tris Borate EDTA (TBE), 8% acrylamide, 60g/140ml Urea (~30%) 1µl/ml TEMED, 4µl/ml (300µl/70ml) 10% APS). Gels were pre-run at constant wattage, 72-73W in practice, (certain power supplies are not capable of maintaining the voltage required to run the gels at this wattage, so be certain you use a power supply that can handle at least 1500V) until the temperature reached 48-52°C. After loading samples, gels were run at the same wattage until DNAs had separated far enough. They were

Figure 3

A) Native gel of nucleosomes labeled on the left (L) or right (R) end show very little free DNA before mapping. B) Native gel after mapping shows that some nucleosomes have disassembled (lane 1). We can enrich solutions for intact nucleosomes by pelleting nucleosome aggregates from solution in 20mM $MgCl_2$ solutions, whereas DNA is fully soluble at this concentration $MgCl_2$. Lane 2 shows precipitated nucleosomes resuspended in 0.5xTE, lane 3 shows free DNA (and small amounts of nucleosomes) which remain in the supernatant after centrifugation, and lane 4 shows naked DNA for comparison.

Figure 3

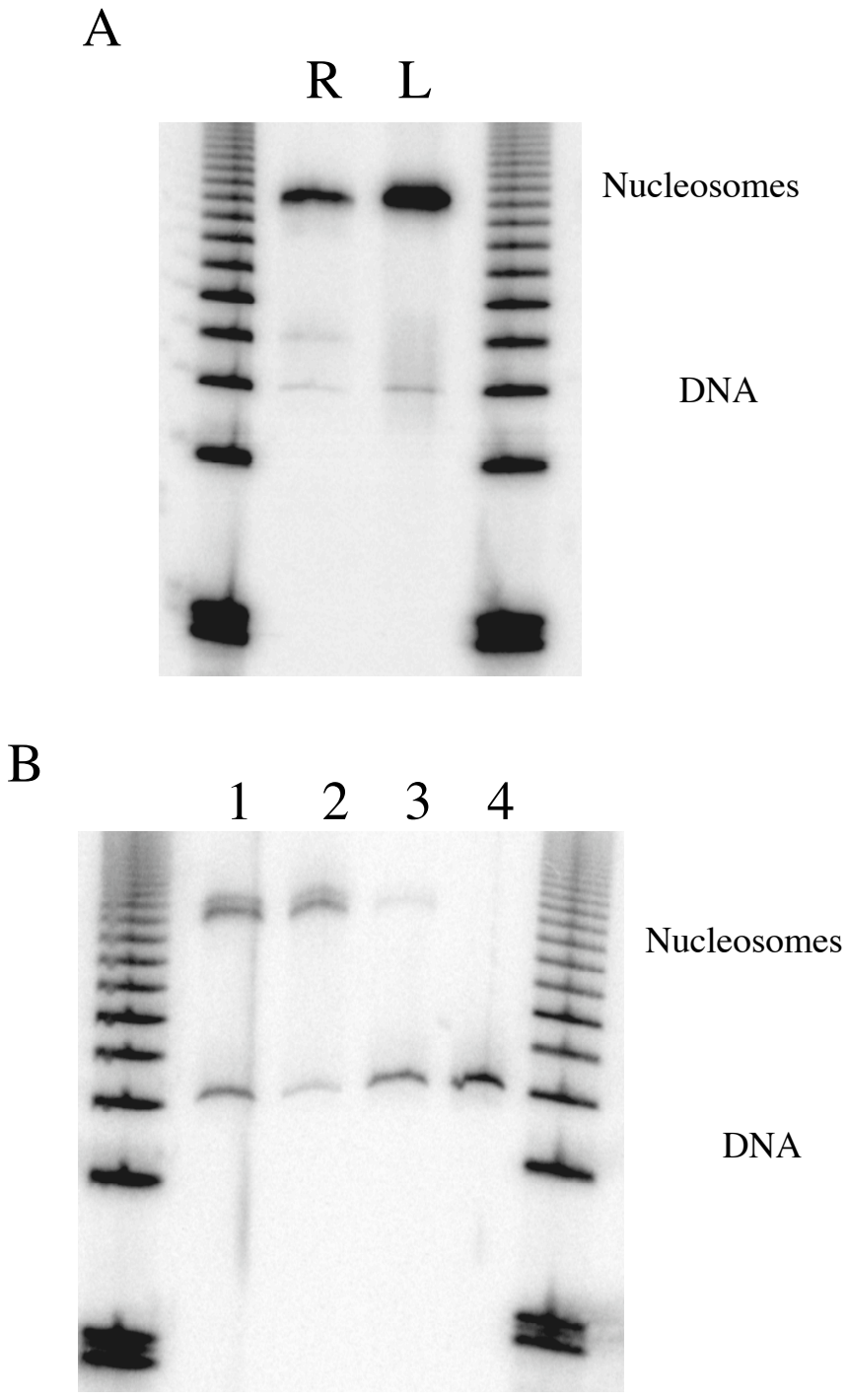

then dried down (without soaking in acetic acid solution, since the thin gels dry fine), and exposed to phosphorimager plates for analysis.

Gel analysis

Mapping products should show two main cutting sites (Figures 1 and 4). The mapping agent is closest to the backbone ~70 and ~80bp from the DNA ends. Since DNAs are uniquely end labeled, if cutting occurs at both sides you see more cut sites for the shorter ~70bp cut site. DNAs cut at ~80bp will only been seen if there is no cutting 70bp from the end, thus these bands are much less intense. Additionally, each cut site consists of one higher intensity band flanked on either side by minor additional sites that define one central cut site, and diffusion of hydroxyradicals from that site along the DNA. Figure 5 shows representative dyad mapping of 147-601 nucleosomes from the right end. Aligning cut sites with the sequence show that the cut sites do lie on either side of the known dyad position for this sequence. The shorter band has a higher intensity for the middle peak, making the OP location easy to determine. However, for the longer cut bands, information content is weakened by low signal, giving a range of possible center locations for the OP. For this reason, dyad mapping should be done from the left and right ends simultaneously. Preliminary experiments show that the left and right mapping information align well (data not shown), and all mapping experiments should use data from the left and right ends to more accurately define the dyad. The cut sites on either side of the dyad give a ~10bp frame around the nucleosome dyad, which, with data from the left and right end, gives us an exact dyad location.

Figure 4

8% Denaturing gels of cut nucleosome products and sequence standards from the right end labeled DNA. Sequence lanes are loaded in order: A C G T. Lane 1: quenched mapping reaction. Lane 2-6: various cut nucleosome products. You can see that most DNA is still full length, but there are two main cutting products. The major product is ~70bp, with a minor cut site at ~79 bp. Major bands are flanked by lower intensity neighboring DNA cut sites.

Figure 4

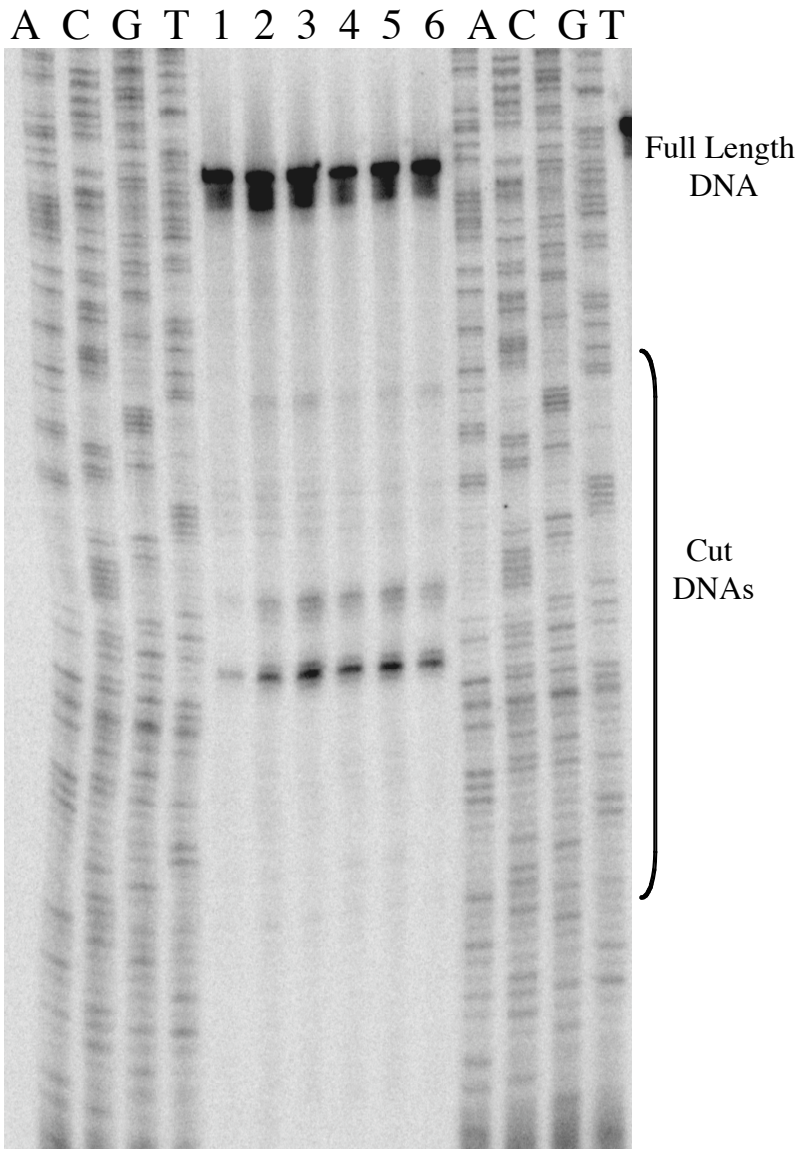

Figure 5

Analysis of the mapping cleavage sites flanking the nucleosome dyad with DNAs labeled on the right end of the nucleosome. Dyad resolution is possible by mapping left and right end labeled DNA simultaneously. Sequence is read from the standards and aligned with the mapped nucleosome cut sites. A) Here we have shown lines representing the DNA strands after mapping ending at their corresponding bands in the gel. B) Without mapping information from the left end, the mapped dyad location is off by one basepair, this discrepancy is likely due to the poor resolution of bands at cut ~80bp.

Figure 5

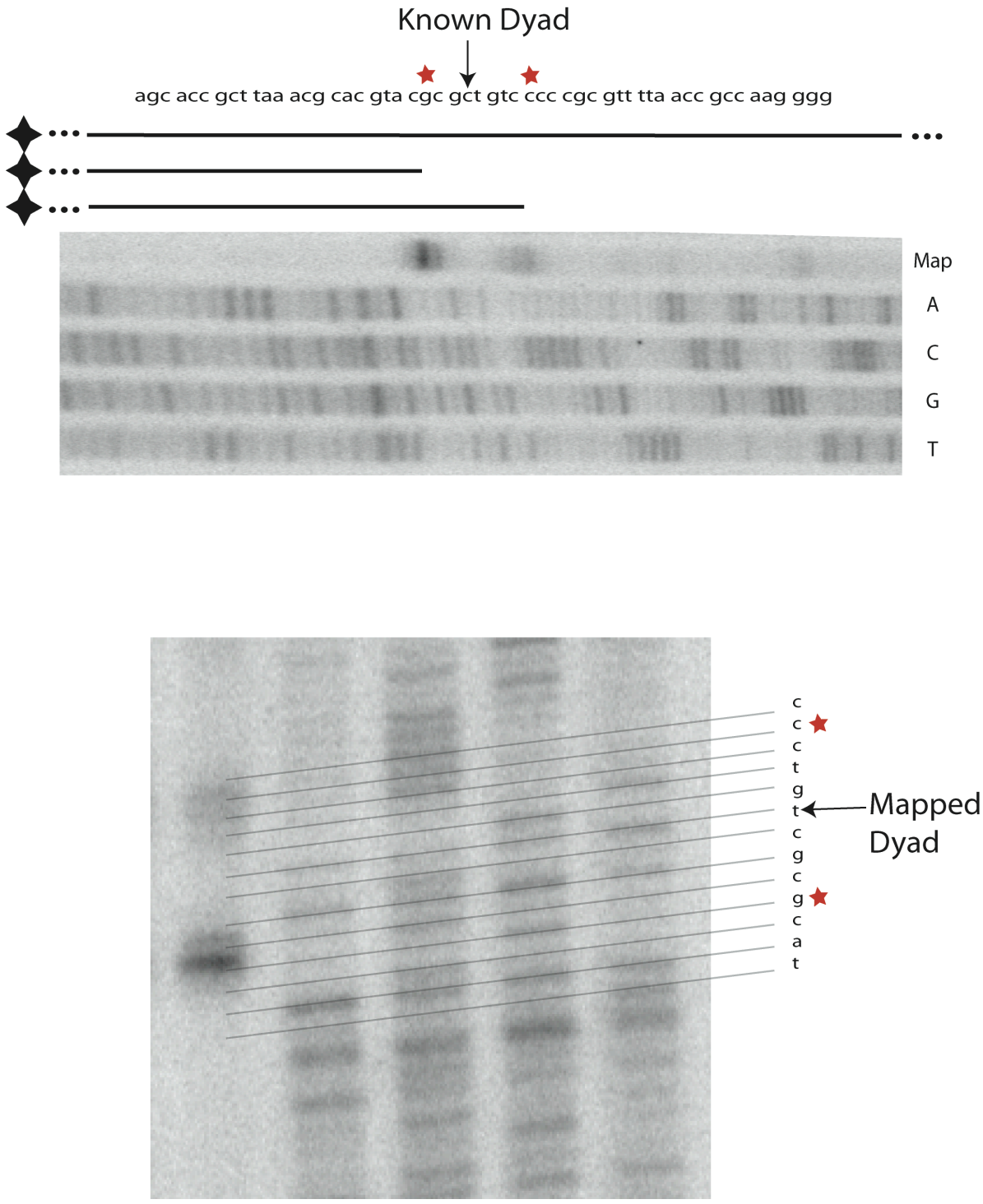
Known Dyad
agc acc gct taa acg cac gta cgc gct gtc ccc cgc gtt tta acc gcc aag ggg
Map
A
C
G
T
c
c
c
t
g
t
c
g
c
g
c
a
t
Mapped
Dyad

Applications

This mapping method can be applied to several situations where exact nucleosome translational position is desired. It can be used to monitor changes in nucleosome position induced by polymerases, remodeling proteins, or histone chaperones, and may be used to map the native location of nucleosomes *in vivo*. For *in vitro* nucleosome mapping experiments, DNAs must have a reasonably specific nucleosome positioning sequence to reduce noise from variant locations. Nucleosome relocation by protein machinery can be determined by mapping before and after addition and reaction of the protein (or protein complex) of interest. Specifically, this method is ideally suited for studies with chromatin remodeling complexes, which move nucleosomes from one location to another; mapping by this method would give the step size of remodeler induced movement, a critical parameter for understanding the mechanisms of nucleosome remodeling factors.

Additionally, the method can be modified so that OP is attached to nucleosomes that are extracted from living cells, potentially allowing base pair resolution mapping of *in vivo* nucleosome locations. For this method, mutant H4 must be expressed endogenously, which can be done by replacing one or more copies of the native histone H4 with an S47C mutant. Studies are currently underway to show that this does not affect cell viability. Once the H4S47C mutant is endogenously expressed, it can be incorporated into chromatin along with (or possibly even instead of) the wild type H4. Chromatin can be extracted and cut with micrococcal nuclease (Sigma) to make single nucleosomes, or left intact. The mutant cysteine residue can be labeled with OP in the nucleosome context, and then dyad location mapped. For labeling, nucleosomes should be reduced with TCEP as before, and labeled according to previous experiments, except that solutions should have low salt concentrations (so as to prevent spontaneous nucleosome

relocation). Excess OP should be removed, and nucleosomes can be mapped as before to cleave the backbone near the dyad. The cutting site for these genomic mapped nucleosomes can be resolved by primer extension with primers designed for known nucleosome locations *in vivo* (Yvonne Fondufe Mittendorf personal communication), or, potentially, by parallel sequencing after S1 nuclease cleavage. This experiment may reveal whether nucleosomes in vivo occupy exact locations, or sets of related nearby locations (perhaps differing by 10 bp steps).

Conclusion

Here we present an easy and reliable method for mapping, with basepair resolution, the translational position of the histone octamer on DNA. The method is quick and efficient, and has many practical applications for important question in the chromatin field. It can be used to define the dyad location of nucleosomes, before and after chromatin remodeling activity, or passage of polymerases, or other nucleosome perturbations.

Chapter 6

Chromatin remodeling by ISWI/ACF

Chromatin remodeling by ISWI/ACF

Introduction

Organization of DNA into nucleosomes, and higher order chromatin folding, occludes many DNA target sites from their binding proteins. We have shown that nucleosomes spontaneously unwrap DNA to expose buried target sites [11]. However, as discussed earlier in Chapter 4, as targets are moved further inside nucleosomes, the rate of unwrapping DNA from the nucleosome is significantly slowed. This results in a potentially delayed response time for gene activation, or necessitates the help of remodeling complexes to expose buried DNA.

SWI/SNF related chromatin remodeling complexes are the primary molecular machinery responsible for assembly and disassembly of chromatin, internucleosomal spacing, nucleosome movement, and remodeling [35]. There are three main classes of SWI/SNF remodelers, all of which have been shown to be involved in positively or negatively regulating gene expression. SWI/SNF complexes activate transcription by remodeling or disrupting nucleosomes. ISWI (Imitation SWItch) containing complexes are involved in transcription regulation through both chromatin assembly and nucleosome mobilization. Mi2/CHD complexes repress transcription by nucleosome movement and by complexing with histone deacteylases to promote silenced chromatin [34, 35, 37, 38]. While many studies have shed light on the questions of which remodelers act where, when and why, we still do not understand how any of the remodeling complexes move or remodel nucleosomes.

The ISWI containing complex ACF (ATP-dependent Chromatin-assembly Factor) is the primarily machine responsible for organizing and packaging chromatin into a tightly packaged,

silenced state by creating ordered, regularly spaced nucleosomes [52, 101]. ISWI exists in the context of three different complexes in vivo in *Drosophila*, but has been shown to have nucleosome remodeling activity in vitro on its own [46]. This allows a more simplified model system for study of nucleosome remodeling activity, as well as a comparison of the function and mechanism of ISWI alone and in the context of its in vivo complexes.

Mechanistic analyses of ISWI have addressed the substrate requirements for remodeling, and include in vitro solution studies that show cooperative binding of ISWI and ACF to DNA and nucleosomes in solution [51, 52]. This cooperative binding suggests that ISWI acts as a functional dimer, perhaps pulling from both sides of the nucleosome to center and space nucleosomes on a stretch of DNA [50]. However, the SWI/SNF complexes, such as RSC, appear to have only one active unit in each complex, suggesting that the remodeling mechanism may not require dimerization [102].

Previous studies have shown that ISWI activity depends on the amount of linker DNA that extends beyond the edge of the nucleosome, however ISWI can interact with nucleosomes without additional linker DNA [50, 51, 103]. This requirement for additional linker DNA agrees with recent proposed mechanisms for chromatin remodeling. These models suggest that remodelers anchor on the histone octamer (for ISWI, near the H4 tail [104]), with an extended arm that binds linker DNA to pull a bulge of DNA into the nucleosome. This bulge could then be propagated through the nucleosome by a translocase domain, to move the nucleosome along the DNA [24, 52, 105] (Figure 1).

Mechanistic studies have investigated the nature of nucleosome remodeling by ISWI complexes, by monitoring remodeler dependent changes in nucleosome position on DNA. However additional information can be gained by comparison of the catalytic subunits of

Figure 1

The mechanism of chromatin remodeling is likely conserved between families of remodelers, but modified by the specifics of the catalytic subunit, and additional modifying proteins in the complex. Schematic of remodeling taken from P. Becker 2005 [24] shows that nucleosome relocation is proposed to proceed through bulge propagation through the nucleosome. Remodeling complexes bind the histone core at some internal location (H), and an extended arm (L) reaches out to pull in DNA from the linker region forming a bulge of excess DNA inside the nucleosome. This bulge is propagated through the nucleosomes by the translocase domain (T). The star is shown to mark relative movement of DNA through the nucleosome.

Figure 1

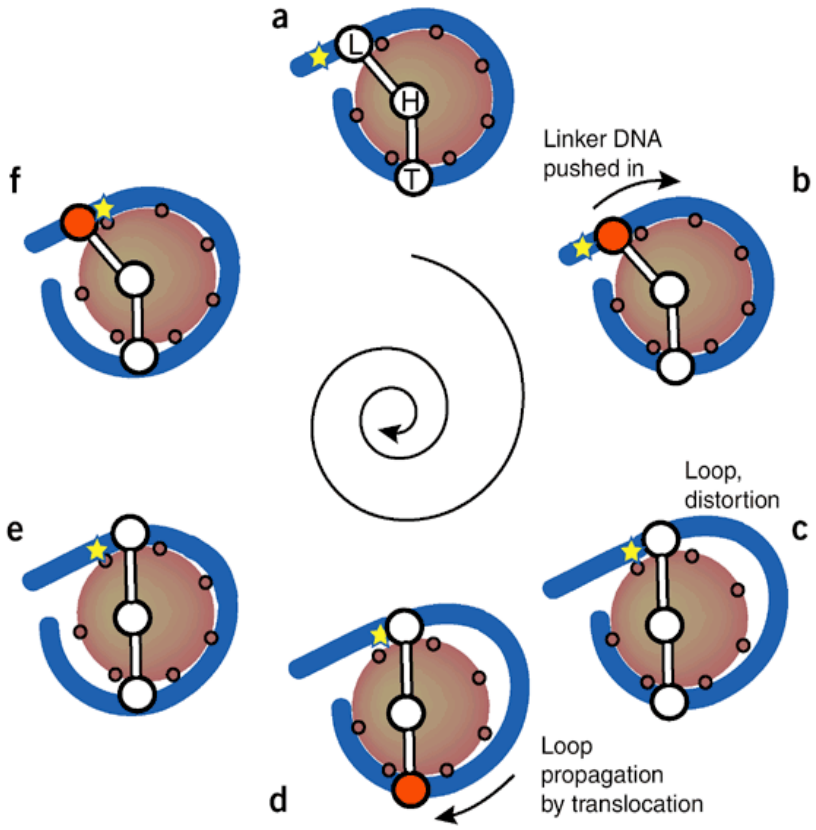
a
L
H
T
Linker DNA
pushed in
b
c
Loop,
distortion
d
Loop
propagation
by translocation
e
f

remodeling complexes to the closely related DEAD box family of ATPases [39-41]. Studies of sequence similarity reveal that ISWI and the other remodeler ATPase subunits are closely related to this protein superfamily that contains DNA translocases and helicases. Although very little is known about the mechanism of SWI/SNF related proteins, much insight can be gained by structural and mechanical comparisons to this larger family of ATPases.

There are currently two different models for how DNA is pulled into the nucleosome, the twisting and looping models. These are discussed in detail in [42]. The looping model of movement allows remodelers to capture spontaneous unwrapping events of DNA away from the histone core to pull in a loop of DNA [24]. Studies of ISWI remodeling show that DNA maintains the same orientation towards the histone octamer before and after remodeling [106]. These results are most easily understood if nucleosomes move in steps of multiples of ~10 base pairs (the DNA helical repeat). Consistent with this view, high resolution mapping of nucleosome movement from remodelers show step sizes of ~10 bp. However complications arise from the use of periodic nucleosome positioning sequences in these studies [45, 107]. These DNA sequences themselves have a 10 bp sequence periodicity, which make it most probable that nucleosomes will find a thermodynamically favorable location every 10 bp, potentially skewing the relative populations of intermediate states towards these energy minima. Thus, even if the true mechanism involved steps of just one or a few base pairs, intermediates might pile up at steps of 10 bp because these accord with helical repeats of the DNA, and are therefore more energetically stable. This issue can be lessened by allowing the remodeling complex to move only one step (at the most), before stopping the reaction.

The twisting model suggests that spontaneous twist fluctuations may form inside the nucleosome, and then propagate all the way around, resulting in net movement of the

nucleosome by a single base pair. Because of the helical symmetry of DNA, twist fluctuations are equivalent to bulges but with a bulged length of just one base pair. This model has been challenged by studies showing that nicks, gaps [43], and large adducts on the DNA backbone [52] have no effect on remodeling.

Studies with gapped DNAs reveal that remodelers have directional DNA translocase activity [105, 108]. This discovery potentially challenges the bulge model of remodeling, since it is not easily understood how a DNA translocase can take steps of 10 bp, while steps of 1-3 bp are accomplished by other closely related translocating enzymes in this enzyme superfamily [109].

Taken together, these step-size studies have so far failed to yield definitive answers for the mechanism of ISWI dependent nucleosome movement. We still do not know how far ISWI can move a nucleosome in one remodeling step, what the ISWI or substrate requirements are, or the energy cost for remodeling. Answering these questions requires that we define the end product of remodeling, the unit step-size of nucleosome movement, and the ATP and substrate requirements for a remodeling step. We set out to determine the substrate requirement of ISWI and ACF, using ATPase assays with γ^{32}P-ATP, monitoring hydrolysis with thin layer chromatography plates. The unit step-size of nucleosome movement will be mapped before and after ISWI remodeling, under limiting ATP conditions, to determine how far ISWI moves the nucleosome in one ATP turnover step. The nucleosome mapping reaction uses a new procedure that we developed, taking advantage of a histone mutation and chemical modification near the nucleosome dyad to define the center of the nucleosome. Understanding the mechanism of remodeling by ISWI will be a major advance in chromatin biochemistry.

Materials and Methods

Nucleosomes

Nucleosomes for the mapping reaction were reconstituted from recombinant histones containing H3C110A, H2A, H2B, and H4S47C. The histone octamer was labeled with N-(1,10-phenanthrolin-5-yl)iodoacetamide (OP, Invitrogen) though cysteine conjugation on the H4S47C mutation (as in chapter 5). DNAs were uniquely end labeled with ^{32}P off the 5' end by PCR with kinased primers. Reconstitutions contained labeled histone octamer with either left or right end labeled DNAs as described (Chapter 5) [57].

ISWI and ACF

ISWI and ACF were expressed and purified from cultured Sf9 cells in collaboration with Peter Becker's group. Sf9 cells were transfected with baculovirus that contain expression vectors for ISWI, N-terminally FLAG tagged ISWI, Acf-1, and C-terminally FLAG tagged Acf-1. For expression and purification of ISWI alone we used FLAG ISWI for expression. For purification of the ACF complex, we used either FLAG ISWI with Acf-1 or ISWI with Acf-1 FLAG for purification of only ACF complexes that bind natively. We used M2 anti- FLAG beads for affinity chromatography purification as described [30, 47, 110]. Purified ISWI/ACF was stored at –80ºC in 20mM HEPES pH 7.6, 1.5mM $MgCl_2$, 200mM KCl, 0.5mM EDTA, 0.05% NP-40, 10% glycerol, 0.2mM PMSF, and 1mM DTT (HEMG 200) until used.

ATPase assays

ATPase assays testing ISWI/ACF enzymatic activity were buffered with 50mM Tris pH 7.5, 50mM KCl, .5mM ßME, 0.1mg/ml BSA (3x) or with 40mM Tris pH 7.5, 20mM $MgCl_2$,

5mM NaCl (5x). Reagents were mixed as described, ISWI/ACF was diluted in HEMG 200 for use, activators such as DNA were stored in TE before use. Unlabeled ATP for reactions was mixed 1:1 with $MgCl_2$ before use.

γ^{32}PATP for reactions was purified away from free phosphate and ADP by gel extraction. Crude γ^{32}PATP (from MDBiomedicals or Amersham) was run on a 24% mini-acrylamide gel in 1xTBE. γ^{32}PATP was mixed with ficol loading buffer without dye, and loaded with dye standards on the sides, use both bromophenol blue and xylene cyanol. The gel was run until bromophenol blue was 1/4 down the gel (45 min-1hr). Fiducial marks are added at the corners of the gel for alignment and it was covered in saran wrap, and exposed briefly (30 sec-1min) to a phosphorimager plate. γ^{32}PATP band was cut from the gel (the slow migrating main band) and ATP was gel extracted by soaking the cut gel slice in 0.5xTE overnight (no crushing necessary, ATP is small and will diffuse). ATP was removed from the gel slice by centrifugation in the microspin column (Amicon-Millipore Ultrafree 0.22μM), alloquoted and stored at –20°C for ATPase assays.

ATP hydrolysis was quantified by resolving free phosphate from ATP on Cellulose PEI thin layer chromatography plates (Flexo Scientific). ATP was resolved in a buffer of 1M Formic Acid, 0.5M LiCl, which was allowed to run up the plates to within a cm of the top. TLC plates were dried and imaged on the phosphorimager plates. No fiducial marks were necessary, since free phosphate resolves as a small species that runs with the buffer, and ATP remains behind as a slower migrating mark consisting of free ATP, and ATP still bound by ISWI.

Results and Discussion

To define the active oligomeric state of ISWI and ACF, we measured their ATPase activities as a function of enzyme concentration. We used γ^{32}P-ATP to monitor free phosphate production as ISWI hydrolyzed ATP, the source of energy it uses to move nucleosomes. The free $\gamma^{32}P_i$ was separated from γ^{32}P-ATP on TLC plates and was quantified by phosphorimager analysis. By titrating the concentration of nucleosome or DNA substrates in each reaction, we defined activation curves for each substrate; and for fixed substrate, we determined the dependence of the ATPase reaction rate on the concentration of enzyme.

In assays where the concentration of ISWI or ACF was held constant at 5-10nM, and the concentration of activators was varied from 0 to 300nM (Figure 2), we find a striking difference in the ability of naked DNA, nucleosomes, and chromatin to activate ISWI and ACF ATPase activity. We find that long strings of nucleosomes such as chromatin, where nucleosomes are present in high number and there is room for the enzyme to processively move along the DNA, maximally activate ISWI and ACF. The ATPase activity of ACF is more sensitive to the presence of DNA flanking nucleosomes than is ISWI alone. For ACF, the ATPase activity stimulated by core particles and naked DNA are the same, but the ATPase activity of ISWI is activated more by core particles than naked DNA (Figure 2). Both ISWI and ACF have very little, if any ATPase activity in the absence of an activator, showing that their ATPase turnover mechanism is closely linked to substrate binding [111]. This confirms previous results on ACF and ISWI stimulation, as well as on their nucleosome spacing activities, which sense how much DNA is on either side of the nucleosome, and centers the nucleosome in the middle of the DNA [36, 50, 104, 112, 113].

It has been hypothesized that the nucleosome centering activity is accomplished by cooperative binding of two ACF molecules on both sides of one nucleosome. If the enzymes

Figure 2

ISWI and ACF are unequally activated by remodeling substrates. A) All experiments are done with 5nM ISWI or ACF, and 20μM ATP, titrating concentrations of activators as shown. We find that ISWI is maximally activated by native chromatin structure. ISWI is activated to the same levels by naked DNA and nucleosomes, but at a higher affinity for nucleosomes than for naked DNA. ISWI is sensitive to linker DNA for activation, and the addition of histones to naked DNA increases recognition of the molecule, but without full activation. B) ACF is also maximally activated by chromatin, but is only minimally stimulated by DNA or nucleosomes with no additional flanking DNA. This shows that ACF is more sensitive to substrate and the presence of linker DNA for activity.

Figure 2

A

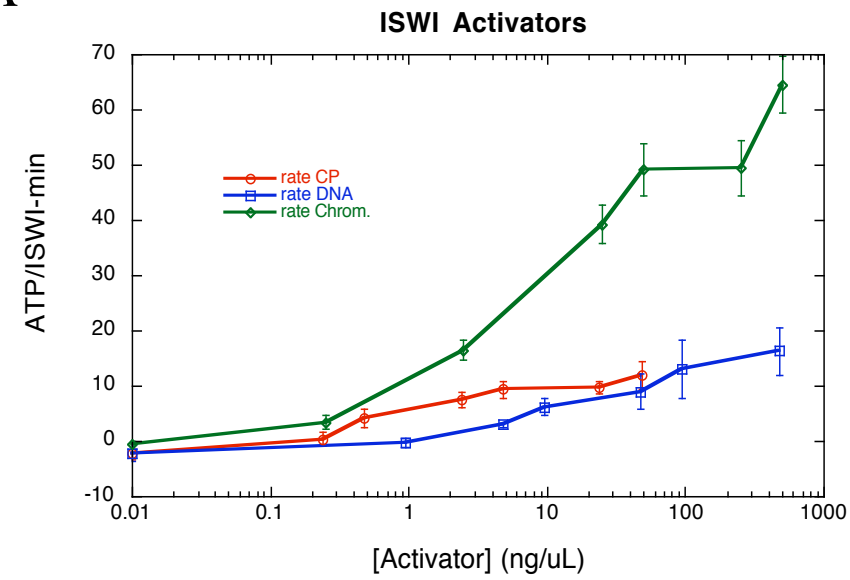
ISWI Activators
ATP/ISWI-min
[Activator] (ng/uL)
rate CP
rate DNA
rate Chrom.
70
60
50
40
30
20
10
0
-10
0.01
0.1
1
10
100
1000

B

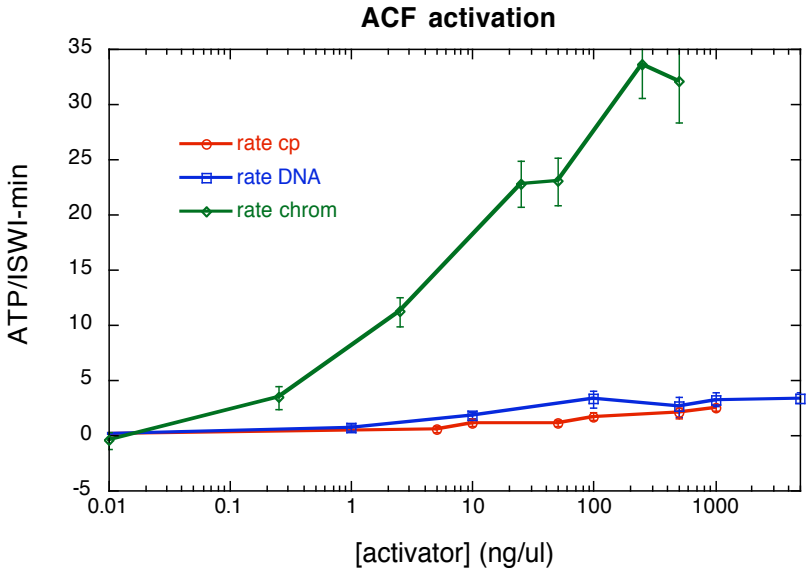
ACF activation
ATP/ISWI-min
[activator] (ng/ul)
rate cp
rate DNA
rate chrom
35
30
25
20
15
10
5
0
-5
0.01
0.1
1
10
100
1000

Figure 3

A) ISWI and B) ACF have K_m values ~100μM for ATP, similar to most molecular machines. We used ATP titration assays to determine the concentration of ATP at which ISWI was reasonably active for titrations with activators, and cooperativity assays. Titrations were done with 50ng/μl chromatin and 200nM ISWI or 50ng/μL chromatin with 5nM ACF (to conserve reagents).

Figure 3

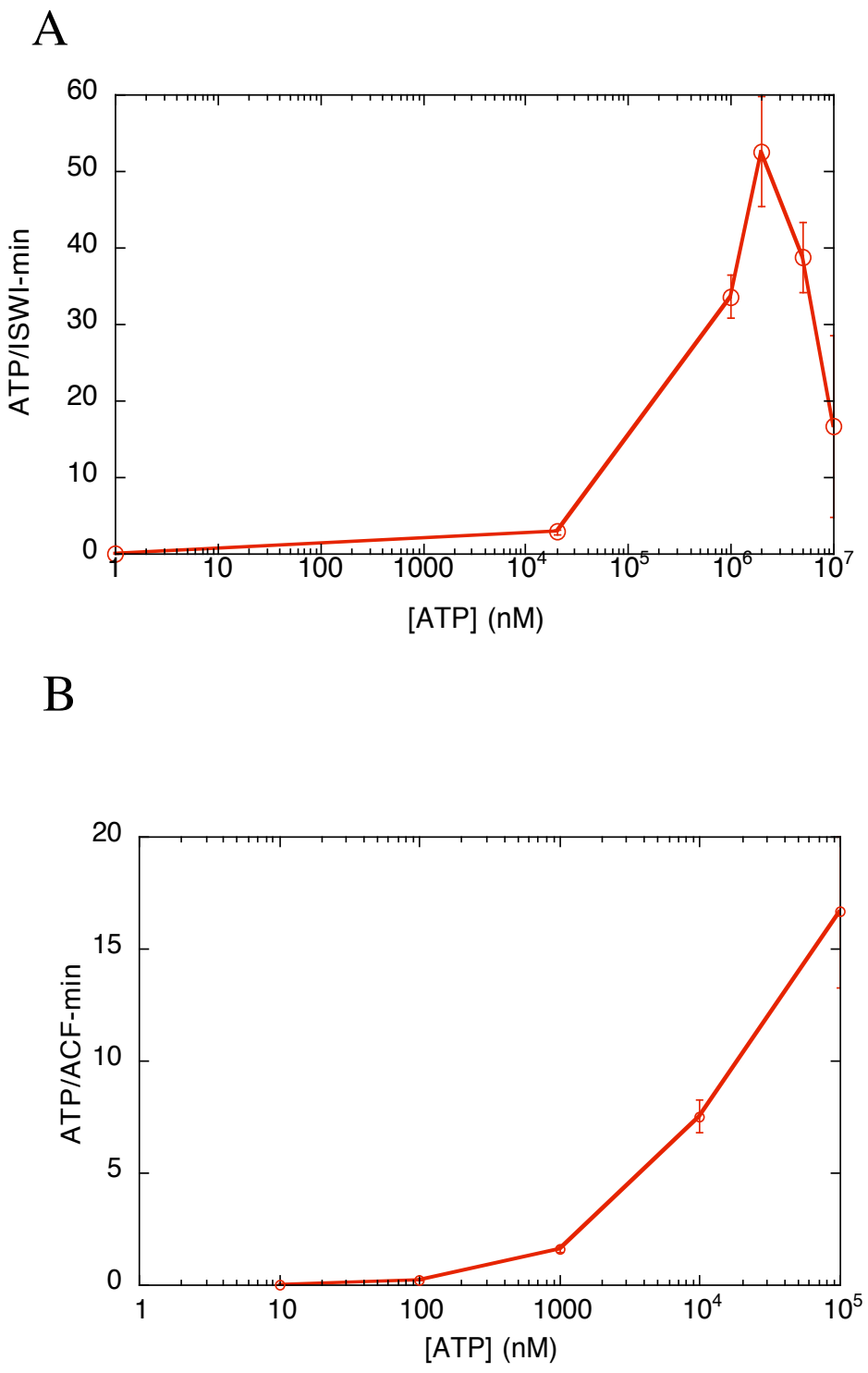
A
ATP/ISWI-min
60
50
40
30
20
10
0
1
10
100
1000
10^4
10^5
10^6
10^7
[ATP] (nM)
B
ATP/ACF-min
20
15
10
5
0
1
10
100
1000
10^4
10^5
[ATP] (nM)

pull the nucleosome in opposite directions, the average location of the nucleosome would be centered on the DNA [50]. In fact, cooperative binding of ISWI to DNA and nucleosomes has been shown by fluorescence anisotropy assays of ISWI binding in vitro [51]. ACF has also been shown, by two color fluorescence cross correlation experiments, to bind DNA in a complex consisting of two ISWI and two Acf-1 proteins, binding four DNAs [52].

We tested whether dimerization is essential for ISWI activity by monitoring the dependence of ISWI's enzymatic ATPase activity on the concentration of ISWI in solution, over the same range of concentrations in which ISWI was shown to bind cooperatively to DNA. Here we hold the concentration of activator and ATP constant, and increase the concentration of enzyme in solution while monitoring the ATPase activity. In contrast to the experiments that suggested a role for dimerization in ISWI action, we show that the ATPase activity of ISWI alone or in complex with Acf-1 is independent of enzyme concentration (Figure 4). If ISWI were a functional dimer, we would expect the ATPase activity per enzyme to increase with concentration since this would increase the likelihood that ISWI could dimerize. Our data show that ISWI is not dependent on dimerization for activity, as the rate of ATPase activity does not increase with increasing ISWI. This agrees with studies of the SWI/SNF remodeling factors such as RSC remodeling complex, which show only one active remodeling enzyme in complex with the nucleosome [102, 114]. These data suggest that although ISWI does cooperatively bind DNA, it may be able to function as a monomer.

Our ATPase assays also define conditions in which ISWI or ACF turn over very slowly – only a few ATPs per minute, per enzyme molecule. We plan to use this information to define the intrinsic step length of ISWI and ACF – that is, the distance in base pairs that a nucleosome is moved when ISWI or ACF hydrolyze a single ATP. ISWI or ACF will be pre-bound to

Figure 4

A) ISWI and B) ACF are not functional Dimers. As the concentration of enzyme increases, the rate of ATPase per enzyme remains the same or decreases, but does not increase. This shows that ISWI is not an obligate dimer in the ATPase domain, despite its ability to cooperatively bind substrates. ISWI titration with 100nM CP, 20μM ATP. ACF titration with 20μM ATP, 50ng/μL chromatin.

Figure 4

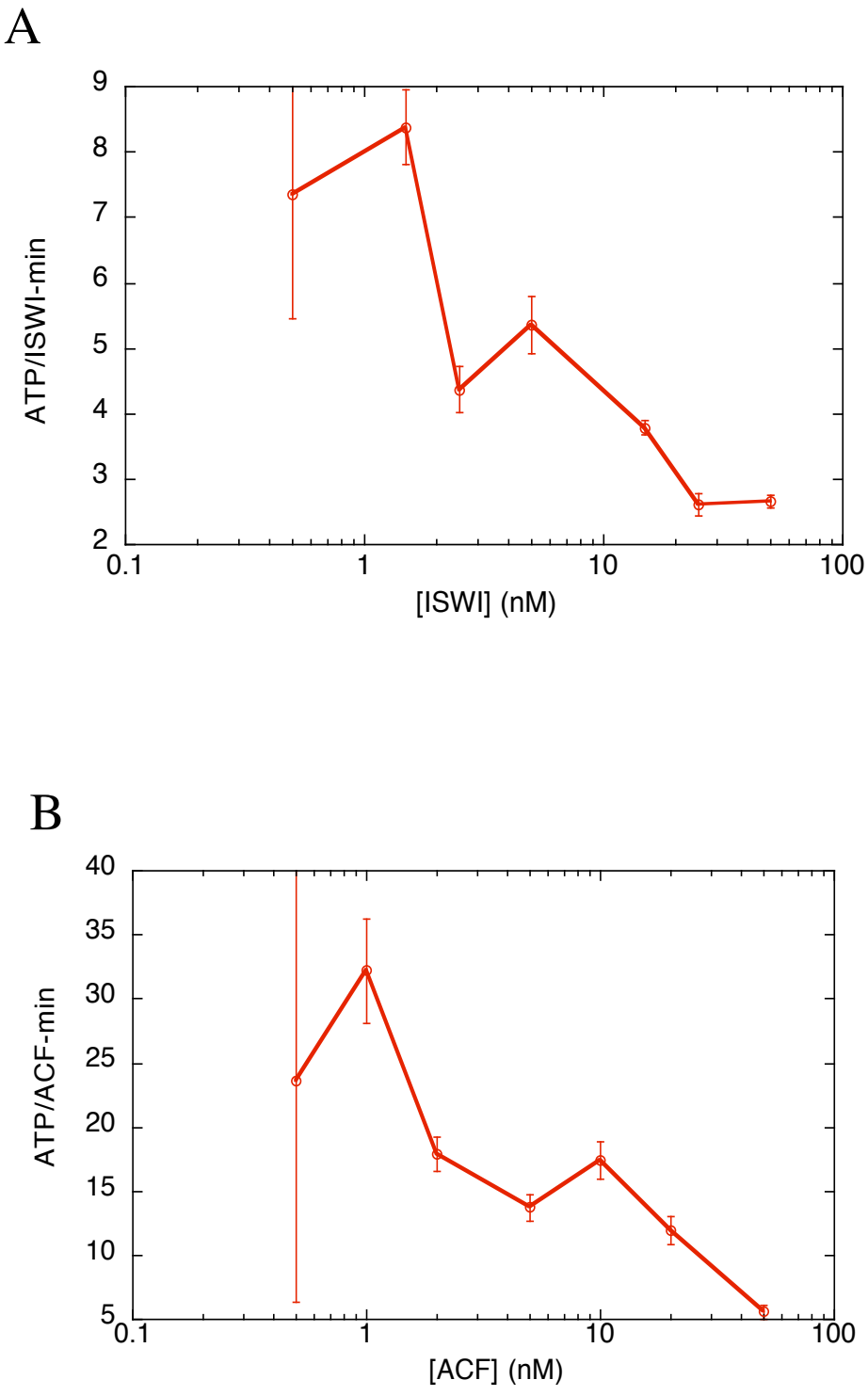
A
ATP/ISWI-min
9
8
7
6
5
4
3
2
0.1
1
10
100
[ISWI] (nM)
B
ATP/ACF-min
40
35
30
25
20
15
10
5
0.1
1
10
100
[ACF] (nM)

nucleosomes, then rapidly mixed with ATP, followed shortly thereafter by addition of a non-hydrolysable ATP analog, to stop any further ATPase activity. This quencher will be added after only a short time, such that every enzyme has gone through zero or at most one ATPase turnover. The exact new nucleosome locations that result will be mapped as described in Chapter 5, to reveal the individual step size of ISWI induced nucleosome movement. Although these experiments have not yet been done, the method has been worked out, and the mapping reactions are underway.

We find that the chromatin remodeling complex ACF, and ISWI alone, do not function as dimers in vitro. The ATPase activity of these enzymes is independent of their oligomeric state, but is sensitive to substrate requirements. This shows that, while ISWI may bind cooperatively to the nucleosome, this property is either happenstance, or perhaps is related to aspects of nucleosome rearrangement that are independent of the ATPase activity; but in any case enzyme dimerization is not linked to ATP turnover. Our studies of the ATPase activity have defined the conditions that, together with our new strategy for mapping nucleosome locations, will allow us to measure the step size for ATP-dependent nucleosome translocation catalyzed by ISWI on its own and in the ACF complex. Knowing the step size of ISWI is central to understanding the mechanisms of nucleosome remodeling.

Chapter 7

Conclusions

Conclusions

Our studies, together with a wealth of biochemical and structural data from previous studies, show that the compaction of DNA into chromatin poses an enormous energetic and kinetic barrier for proteins trying to bind DNA target sites inside the nucleosome [1, 7, 8, 75, 115]. Here we studied two mechanisms used to expose the buried DNA, and studied the intrinsic nucleosome structural stability that allows invasion without loss of epigenetic information. Using FRET systems that are sensitive to structural changes between DNA and histones, and to loss or exchange of tagged histones, we have been able to study the intricacies of nucleosome conformational changes in response to DNA unwrapping, protein binding, and transcription. We have also developed a new biochemical method to probe nucleosome structural changes induced by chromatin remodelers during a single enzymatic turnover. From these studies we have gained a more thorough understanding of the spontaneous and catalyzed mechanisms by which nucleosomal DNA is made accessible.

Our work on the intrinsic structural stability of the nucleosomes shows that the histone octamer is a stably associated with nucleosomal DNA. It is stable against loss or exchange of histones, even when much or all of the nucleosomal DNA is unwrapped by protein binding or by transient passage of an RNA polymerase. This stability of the octamer facilitates retention of gene-silencing or activating epigenetic marks on the histones, which can only be removed or modified by specific chromatin modifying complexes.

Earlier biochemical and FRET based assays prove that DNA spontaneously unwraps from the histone core to expose buried targets to solution [6, 8, 11]. These studies show that there is decreased accessibility to DNA buried inside the nucleosome, but that this DNA nevertheless

does remain accessible a small fraction of the time. Experiments using FRET dye pairs that directly monitor nucleosome structural changes provide a basis for probing spontaneous conformational fluctuations of DNA buried deep inside the nucleosome. We have extended this FRET based method to study how, and how quickly, deeply buried DNA is unwrapped to reveal buried sites. The site exposure model hypothesizes that DNA is progressively unwrapped from one end, and that DNA must be unwrapped for proteins to occupy their target sites [8]. Consistent with this idea, we find that, for typical regulatory factors, occupancy of a target site is possible only when DNA is unwrapped all the way through to the target site, even when that site is located far inside the nucleosome.

Previous *in vitro* and *in vivo* biochemical studies prove that occupancy of one DNA binding protein in a nucleosome increases the occupancy of a second DNA binding protein at its own site inside that same nucleosome [12, 22]. This cooperativity is thought to arise from collaborative competition: the binding of a protein to an outer more site in the nucleosome is thought to destabilize the wrapping of DNA further inside the nucleosome, but such destabilization has not been directly observed or tested. We used FRET to test this idea directly. We find that binding of target sites near the nucleosome edge does indeed destabilize the DNA further inside the nucleosome. Collaborative competition may be one of the main mechanisms that cells use to increase the accessibility of buried DNA target sites. For example, at promoters, important regulatory protein binding sites often occur in clusters of multiple sites [23]. Collaborative competition could facilitate access to and occupancy of buried nucleosomal target sites, even if all of the sites are covered by a nucleosome.

Our studies of spontaneous nucleosomal site exposure, for sites buried at increasing distances inside the nucleosome, show that mechanisms for easing repression of buried sites are

in fact necessary. While DNA at the edges of nucleosomes is spontaneously available many times per second [19], we find that the rate of unwrapping decreases by an order of magnitude or more for each additional 10 bp that a target site is moved further in from the nucleosome ends. Our data help to paint a picture of spontaneous DNA unwrapping events. Near the nucleosome edges, DNA is in rapid equilibrium between a fully wrapped and partially unwrapped state, which allows easy and rapid access to targets. As you move progressively further into the nucleosome, it become less likely that a spontaneous unwrapping event will extend far enough to expose the target site. This increases the lifetime of the closed (inaccessible) state of buried DNA target sites, and decreases the rate of spontaneous unwrapping to, and the lifetime of, the open (accessible) state. It follows that target site location within a nucleosome can be an important source of variability in the response time of a particular cell to signaling.

Recent studies watching gene activation in real time in single living cells highlight the consequences of such a time delay in access to buried targets [21]. In a population of genetically identical cells, the delay in activation between different individuals is often many minutes, and sometimes as long as a cell lifecycle time. This range of times corresponds well with the time delays we find for binding targets buried inside nucleosomes. Differences in nucleosome positioning between individuals in the population could be primarily responsible for the time delay in gene activation seen in these single cell studies.

Our studies show that spontaneous site accessibility suffices to provide access to target sites buried far inside nucleosomes, but only if saturating occupancy of the binding site is not required, and you can wait a long time. This is not always the case. Thus, in vivo, there must be mechanisms for speeding accessibility, so that targets can be fully bound on a biologically

relevant timescale. We have shown that cooperative binding of targets inside the nucleosome is one such mechanism. Chromatin remodelers provide another mechanism.

Chromatin remodelers increase accessibility by moving or removing nucleosomes from DNA [24]. Remodelers are also involved in decreasing accessibility of DNA by tightly packaging and spacing nucleosomes, to restrict access and silence DNA. We have begun studying the mechanism by which these remodelers make nucleosomal DNA accessible, by investigating the mechanistic reaction steps that allow remodelers to move nucleosomes along DNA.

Our studies of the chromatin remodeling complex ACF, and of ISWI alone, focus on the mechanism by which these remodelers move nucleosomes along DNA. The intrinsic spacing and packaging activity that ACF shows in vivo and in vitro, together with evidence of cooperative binding to substrates, suggested that it may function as a dimer [51, 52]. However, we definitively show that the ATPase activity of ISWI and ACF are not dependent on dimerization. Thus, while ISWI binds cooperatively to the nucleosome, and ACF binds two or distinct DNA fragments [52], these properties are not linked to the fundamental ATPase catalytic cycle.

In addition to these mechanistic discoveries, this work has produced two useful technological advances. Our stopped-flow FRET methodology provides a powerful and versatile tool with which to elucidate rates and detailed conformational changes as they occur in biological macromolecular complexes and machines. This method is ideally suited for analysis of intrinsic properties of chromatin and of the machines that control chromatin assembly, disassembly, and function. Careful experimental set-up allows detection of two color fluorescence changes simultaneously from extraordinarily dilute (nM) samples, on the

millisecond or longer timescale. The stopped flow instrument can be used to determine binding and dissociation kinetics, and rates of enzymatic and chemical reactions.

We have also developed a new method for mapping nucleosome translational position with basepair resolution. The method is quick and efficient, and has many practical applications for critical questions in the chromatin field. This method takes advantage of histone mutant H4S47C to position chemical mapping reagents in very close proximity to the DNA flanking the nucleosome dyad symmetry axis. This reagent can be activated to produce free radicals that are highly localized to the DNA backbone flanking the dyad. Cut sites in the DNA backbone resulting from this chemistry can be used to define the dyad position with basepair resolution. This method can be used to define the distance along the DNA (step size) that ISWI translocates a nucleosome during a single ISWI or ACF ATPase catalytic cycle. The step size is fundamental to the mechanism of nucleosome movement, and give clues to how the remodeling complexes work.

Chromatin is not a haphazard conglomeration of DNA and histones, rather it is a tightly packaged, ordered, and controlled molecular assembly. Changes in chromatin packaging are under tight regulation so that DNA remains ordered and protected, and genes are properly regulated. Our studies show that this regulation of structure is facilitated by the stability of the histones with individual nucleosomes. Additionally, there are rules, with penalties, for proteins invading the nucleosome structure spontaneously. As proteins try to probe further inside the nucleosome, the energetic and time cost of accessing sites rise sharply, significantly affecting gene regulation. We show two mechanisms for increasing the accessibility of nucleosomal DNA above the levels that can be achieved by such simple spontaneous binding: cooperative binding of proteins within a nucleosome, and catalyzed nucleosome movement. All three of these

mechanisms of nucleosome accessibility -spontaneous unwrapping, cooperative binding, and remodeling– help regulate access to critical targets in chromatin.

References:

1. Luger, K., et al., *Crystal structure of the nucleosome core particle at 2.8 A resolution*. Nature, 1997. **389**(6648): p. 251-60.

2. Felsenfeld, G. and M. Groudine, *Controlling the double helix*. Nature, 2003. **421**(6921): p. 448-53.

3. Felsenfeld, G., et al., *Chromatin boundaries and chromatin domains*. Cold Spring Harb Symp Quant Biol, 2004. **69**: p. 245-50.

4. Gaszner, M. and G. Felsenfeld, *Insulators: exploiting transcriptional and epigenetic mechanisms*. Nat Rev Genet, 2006. **7**(9): p. 703-13.

5. Holmquist, G.P. and T. Ashley, *Chromosome organization and chromatin modification: influence on genome function and evolution*. Cytogenet Genome Res, 2006. **114**(2): p. 96-125.

6. Anderson, J.D., A. Thastrom, and J. Widom, *Spontaneous access of proteins to buried nucleosomal DNA target sites occurs via a mechanism that is distinct from nucleosome translocation*. Mol Cell Biol, 2002. **22**(20): p. 7147-57.

7. Anderson, J.D. and J. Widom, *Sequence and position-dependence of the equilibrium accessibility of nucleosomal DNA target sites*. J Mol Biol, 2000. **296**(4): p. 979-87.

8. Polach, K.J. and J. Widom, *Mechanism of protein access to specific DNA sequences in chromatin: a dynamic equilibrium model for gene regulation*. J Mol Biol, 1995. **254**(2): p. 130-49.

9. Bucceri, A., K. Kapitza, and F. Thoma, *Rapid accessibility of nucleosomal DNA in yeast on a second time scale*. Embo J, 2006. **25**(13): p. 3123-32.

10. Peterson, C.L., *Chromatin remodeling: nucleosomes bulging at the seams*. Curr Biol, 2002. **12**(7): p. R245-7.

11. Li, G. and J. Widom, *Nucleosomes facilitate their own invasion*. Nat Struct Mol Biol, 2004. **11**(8): p. 763-9.

12. Polach, K.J. and J. Widom, *A model for the cooperative binding of eukaryotic regulatory proteins to nucleosomal target sites*. J Mol Biol, 1996. **258**(5): p. 800-12.

13. Saha, A., J. Wittmeyer, and B.R. Cairns, *Chromatin remodelling: the industrial revolution of DNA around histones*. Nat Rev Mol Cell Biol, 2006. **7**(6): p. 437-47.

14. Smith, C.L. and C.L. Peterson, *ATP-dependent chromatin remodeling*. Curr Top Dev

Biol, 2005. **65**: p. 115-48.

15. Kireeva, M.L., et al., *Nucleosome remodeling induced by RNA polymerase II: loss of the H2A/H2B dimer during transcription*. Mol Cell, 2002. **9**(3): p. 541-52.

16. Thastrom, A., et al., *Histone-DNA Binding Free Energy Cannot Be Measured in Dilution-Driven Dissociation Experiments*. Biochemistry, 2004. **43**(3): p. 736-741.

17. Anderson, J.D. and J. Widom, *Poly(dA-dT) promoter elements increase the equilibrium accessibility of nucleosomal DNA target sites*. Mol Cell Biol, 2001. **21**(11): p. 3830-9.

18. Anderson, J.D., P.T. Lowary, and J. Widom, *Effects of histone acetylation on the equilibrium accessibility of nucleosomal DNA target sites*. J Mol Biol, 2001. **307**(4): p. 977-85.

19. Li, G., et al., *Rapid spontaneous accessibility of nucleosomal DNA*. Nat Struct Mol Biol, 2005. **12**(1): p. 46-53.

20. Raser, J.M. and E.K. O'Shea, *Control of stochasticity in eukaryotic gene expression*. Science, 2004. **304**(5678): p. 1811-4.

21. Raser, J.M. and E.K. O'Shea, *Noise in gene expression: origins, consequences, and control*. Science, 2005. **309**(5743): p. 2010-3.

22. Miller, J.A. and J. Widom, *Collaborative competition mechanism for gene activation in vivo*. Mol Cell Biol, 2003. **23**(5): p. 1623-32.

23. Kim, J.D., et al., *Identification of clustered YY1 binding sites in imprinting control regions*. Genome Res, 2006. **16**(7): p. 901-11.

24. Becker, P.B., *Nucleosome remodelers on track*. Nat Struct Mol Biol, 2005. **12**(9): p. 732-3.

25. Stern, M., R. Jensen, and I. Herskowitz, *Five SWI genes are required for expression of the HO gene in yeast*. J Mol Biol, 1984. **178**(4): p. 853-68.

26. Carlson, M., B.C. Osmond, and D. Botstein, *Mutants of yeast defective in sucrose utilization*. Genetics, 1981. **98**(1): p. 25-40.

27. Hirschhorn, J.N., et al., *Evidence that SNF2/SWI2 and SNF5 activate transcription in yeast by altering chromatin structure*. Genes Dev, 1992. **6**(12A): p. 2288-98.

28. Peterson, C.L., *Multiple SWItches to turn on chromatin?* Curr Opin Genet Dev, 1996. **6**(2): p. 171-5.

29. Tsukiyama, T. and C. Wu, *Chromatin remodeling and transcription*. Curr Opin Genet Dev, 1997. **7**(2): p. 182-91.

30. Deuring, R., et al., *The ISWI chromatin-remodeling protein is required for gene expression and the maintenance of higher order chromatin structure in vivo*. Mol Cell, 2000. **5**(2): p. 355-65.

31. Wittmeyer, J., A. Saha, and B. Cairns, *DNA translocation and nucleosome remodeling assays by the RSC chromatin remodeling complex*. Methods Enzymol, 2004. **377**: p. 322-43.

32. Jaskelioff, M., et al., *Rad54p is a chromatin remodeling enzyme required for heteroduplex DNA joint formation with chromatin*. J Biol Chem, 2003. **278**(11): p. 9212-8.

33. Gelbart, M.E., et al., *Genome-wide identification of Isw2 chromatin-remodeling targets by localization of a catalytically inactive mutant*. Genes Dev, 2005. **19**(8): p. 942-54.

34. Langst, G. and P.B. Becker, *Nucleosome remodeling: one mechanism, many phenomena?* Biochim Biophys Acta, 2004. **1677**(1-3): p. 58-63.

35. Varga-Weisz, P.D. and P.B. Becker, *Chromatin-remodeling factors: machines that regulate?* Curr Opin Cell Biol, 1998. **10**(3): p. 346-53.

36. Boyer, L.A., et al., *Functional delineation of three groups of the ATP-dependent family of chromatin remodeling enzymes*. J Biol Chem, 2000. **275**(25): p. 18864-70.

37. Peterson, C.L., *Chromatin remodeling enzymes: taming the machines. Third in review series on chromatin dynamics*. EMBO Rep, 2002. **3**(4): p. 319-22.

38. Varga-Weisz, P.D. and P.B. Becker, *Regulation of higher-order chromatin structures by nucleosome-remodelling factors*. Curr Opin Genet Dev, 2006. **16**(2): p. 151-6.

39. Yu, X., et al., *What is the structure of the RecA-DNA filament?* Curr Protein Pept Sci, 2004. **5**(2): p. 73-9.

40. Ye, J., et al., *RecA-like motor ATPases--lessons from structures*. Biochim Biophys Acta, 2004. **1659**(1): p. 1-18.

41. Cordin, O., et al., *The DEAD-box protein family of RNA helicases*. Gene, 2006. **367**: p. 17-37.

42. Flaus, A. and T. Owen-Hughes, *Mechanisms for nucleosome mobilization*. Biopolymers, 2003. **68**(4): p. 563-78.

43. Lorch, Y., B. Davis, and R.D. Kornberg, *Chromatin remodeling by DNA bending, not twisting*. Proc Natl Acad Sci U S A, 2005. **102**(5): p. 1329-32.

44. Langst, G. and P.B. Becker, *ISWI induces nucleosome sliding on nicked DNA*. Mol Cell, 2001. **8**(5): p. 1085-92.

45. Zofall, M., et al., *Chromatin remodeling by ISW2 and SWI/SNF requires DNA translocation inside the nucleosome*. Nat Struct Mol Biol, 2006. **13**(4): p. 339-46.

46. Corona, D.F., et al., *ISWI is an ATP-dependent nucleosome remodeling factor*. Mol Cell, 1999. **3**(2): p. 239-45.

47. Ito, T., et al., *ACF consists of two subunits, Acf1 and ISWI, that function cooperatively in the ATP-dependent catalysis of chromatin assembly*. Genes Dev, 1999. **13**(12): p. 1529-39.

48. Ito, T., et al., *ACF, an ISWI-containing and ATP-utilizing chromatin assembly and remodeling factor*. Cell, 1997. **90**(1): p. 145-55.

49. Tsukiyama, T., et al., *ISWI, a member of the SWI2/SNF2 ATPase family, encodes the 140 kDa subunit of the nucleosome remodeling factor*. Cell, 1995. **83**(6): p. 1021-6.

50. Yang, J.G., et al., *The chromatin-remodeling enzyme ACF is an ATP-dependent DNA length sensor that regulates nucleosome spacing*. Nat Struct Mol Biol, 2006. **13**(12): p. 1078-83.

51. Chin, J., et al., *Fluorescence anisotropy assays for analysis of ISWI-DNA and ISWI-nucleosome interactions*. Methods Enzymol, 2004. **376**: p. 3-16.

52. Strohner, R., et al., *A 'loop recapture' mechanism for ACF-dependent nucleosome remodeling*. Nat Struct Mol Biol, 2005. **12**(8): p. 683-90.

53. Clegg, R.M., *Fluorescence resonance energy transfer and nucleic acids*. Methods Enzymol, 1992. **211**: p. 353-88.

54. Park, Y.J., et al., *A new fluorescence resonance energy transfer approach demonstrates that the histone variant H2AZ stabilizes the histone octamer within the nucleosome*. J Biol Chem, 2004. **279**(23): p. 24274-82.

55. White, C.L. and K. Luger, *Defined structural changes occur in a nucleosome upon Amt1 transcription factor binding*. J Mol Biol, 2004. **342**(5): p. 1391-402.

56. Lowary, P.T. and J. Widom, *New DNA sequence rules for high affinity binding to histone octamer and sequence-directed nucleosome positioning*. J Mol Biol, 1998. **276**(1): p. 19-42.

57. Thastrom, A., P.T. Lowary, and J. Widom, *Measurement of histone-DNA interaction free energy in nucleosomes*. Methods, 2004. **33**(1): p. 33-44.

58. Sambrook, J., E.F. Fritsch, and T. Maniatis, *Molecular cloning : a laboratory manual. 1.* 2nd ed. 1989, Cold Spring harbor, N.Y.: Cold Spring Harbor Laboratory Press. Pagination multiple.

59. Luger, K., T.J. Rechsteiner, and T.J. Richmond, *Expression and purification of recombinant histones and nucleosome reconstitution*. Methods Mol Biol, 1999. **119**: p. 1-16.

60. Little, J.W., et al., *Cleavage of LexA repressor*. Methods Enzymol, 1994. **244**: p. 266-84.

61. Lee, N.K., et al., *Accurate FRET measurements within single diffusing biomolecules using alternating-laser excitation*. Biophys J, 2005. **88**(4): p. 2939-53.

62. Rachofsky, E.L. and W.R. Laws, *Kinetic models and data analysis methods for fluorescence anisotropy decay*. Methods Enzymol, 2000. **321**: p. 216-38.

63. Kouzarides, T., *Chromatin modifications and their function*. Cell, 2007. **128**(4): p. 693-705.

64. Kusch, T. and J.L. Workman, *Histone variants and complexes involved in their exchange*. Subcell Biochem, 2007. **41**: p. 91-109.

65. Park, Y.J., et al., *Nucleosome assembly protein 1 exchanges histone H2A-H2B dimers and assists nucleosome sliding*. J Biol Chem, 2005. **280**(3): p. 1817-25.

66. Fan, J.Y., et al., *The essential histone variant H2A.Z regulates the equilibrium between different chromatin conformational states*. Nat Struct Biol, 2002. **9**(3): p. 172-6.

67. Roth, S.Y., et al., *Stable nucleosome positioning and complete repression by the yeast alpha 2 repressor are disrupted by amino-terminal mutations in histone H4*. Genes Dev, 1992. **6**(3): p. 411-25.

68. Gottesfeld, J.M. and K. Luger, *Energetics and affinity of the histone octamer for defined DNA sequences*. Biochemistry, 2001. **40**(37): p. 10927-33.

69. Zhu, Z. and D.J. Thiele, *A specialized nucleosome modulates transcription factor access to a C. glabrata metal responsive promoter*. Cell, 1996. **87**(3): p. 459-70.

70. Bao, Y., C.L. White, and K. Luger, *Nucleosome core particles containing a poly(dA.dT) sequence element exhibit a locally distorted DNA structure*. J Mol Biol, 2006. **361**(4): p. 617-24.

71. Kulaeva, O.I., D.A. Gaykalova, and V.M. Studitsky, *Transcription through chromatin by RNA polymerase II: histone displacement and exchange*. Mutat Res, 2007. **618**(1-2): p. 116-29.

72. Workman, J.L., *Nucleosome displacement in transcription*. Genes Dev, 2006. **20**(15): p. 2009-17.

73. Studitsky, V.M., et al., *Chromatin remodeling by RNA polymerases*. Trends Biochem Sci, 2004. **29**(3): p. 127-35.

74. Studitsky, V.M., et al., *Mechanism of transcription through the nucleosome by eukaryotic RNA polymerase*. Science, 1997. **278**(5345): p. 1960-3.

75. Bednar, J., et al., *The nature of the nucleosomal barrier to transcription: direct observation of paused intermediates by electron cryomicroscopy*. Mol Cell, 1999. **4**(3): p. 377-86.

76. Protacio, R.U. and J. Widom, *Nucleosome transcription studied in a real-time synchronous system: test of the lexosome model and direct measurement of effects due to histone octamer*. J Mol Biol, 1996. **256**(3): p. 458-72.

77. Luger, K., T.J. Rechsteiner, and T.J. Richmond, *Preparation of nucleosome core particle from recombinant histones*. Methods Enzymol, 1999. **304**: p. 3-19.

78. Studitsky, V.M., D.J. Clark, and G. Felsenfeld, *A histone octamer can step around a transcribing polymerase without leaving the template*. Cell, 1994. **76**(2): p. 371-82.

79. Protacio, R.U., et al., *Effects of histone tail domains on the rate of transcriptional elongation through a nucleosome*. Mol Cell Biol, 2000. **20**(23): p. 8866-78.

80. Protacio, R.U., K.J. Polach, and J. Widom, *Coupled-enzymatic assays for the rate and mechanism of DNA site exposure in a nucleosome*. J Mol Biol, 1997. **274**(5): p. 708-21.

81. Jessen, W.J., et al., *Active PHO5 chromatin encompasses variable numbers of nucleosomes at individual promoters*. Nat Struct Mol Biol, 2006. **13**(3): p. 256-63.

82. Albert, I., et al., *Translational and rotational settings of H2A.Z nucleosomes across the Saccharomyces cerevisiae genome*. Nature, 2007. **446**(7135): p. 572-6.

83. Segal, E., et al., *A genomic code for nucleosome positioning*. Nature, 2006. **442**(7104): p. 772-8.

84. Peterson, C.L. and C. Logie, *Recruitment of chromatin remodeling machines*. J Cell Biochem, 2000. **78**(2): p. 179-85.

85. Corey, L.L., et al., *Localized recruitment of a chromatin-remodeling activity by an activator in vivo drives transcriptional elongation*. Genes Dev, 2003. **17**(11): p. 1392-401.

86. Tomschik, M., et al., *Fast, long-range, reversible conformational fluctuations in nucleosomes revealed by single-pair fluorescence resonance energy transfer*. Proc Natl Acad Sci U S A, 2005. **102**(9): p. 3278-83.

87. Tims, H.S. and J. Widom, *Stopped-flow fluorescence resonance energy transfer for analysis of nucleosome dynamics*. Methods, 2007. **41**(3): p. 296-303.

88. Widengren, J., R. Rigler, and U. Mets, *Triplet-State Monitoring by Fluorescence*

Correlation Spectroscopy. Journal of Fluorescence, 1994. **4**(3): p. 255-258.

89. Zhao, M., et al., *Afterpulsing and its correction in fluorescence correlation spectroscopy experiments*. Appl Opt, 2003. **42**(19): p. 4031-6.

90. Widengren, J., et al., *Strategies to improve photostabilities in ultrasensitive fluorescence spectroscopy*. J Phys Chem A, 2007. **111**(3): p. 429-40.

91. Torres, T. and M. Levitus, *Measuring Conformational Dynamics: A New FCS-FRET Approach*. J Phys Chem B, 2007. **111**(25): p. 7392-400.

92. Clegg, R.M., *Fluorescence resonance energy transfer*. Curr Opin in Biotech, 1995. **6**: p. 103-110.

93. Mustard, J.A. and J.W. Little, *Analysis of Escherichia coli RecA interactions with LexA, lambda CI, and UmuD by site-directed mutagenesis of recA*. J Bacteriol, 2000. **182**(6): p. 1659-70.

94. Thastrom, A., et al., *Sequence motifs and free energies of selected natural and non-natural nucleosome positioning DNA sequences*. J Mol Biol, 1999. **288**(2): p. 213-29.

95. Flaus, A. and T.J. Richmond, *Base-pair resolution mapping of nucleosomes in vitro*. Methods Mol Biol, 1999. **119**: p. 45-60.

96. Flaus, A. and T.J. Richmond, *Base-pair resolution mapping of nucleosome positions using site-directed hydroxy radicals*. Methods Enzymol, 1999. **304**: p. 251-63.

97. Flaus, A., et al., *Mapping nucleosome position at single base-pair resolution by using site-directed hydroxyl radicals*. Proc Natl Acad Sci U S A, 1996. **93**(4): p. 1370-5.

98. Pan, C.Q., et al., *Structure of the Escherichia coli Fis-DNA complex probed by protein conjugated with 1,10-phenanthroline copper(I) complex*. Proc Natl Acad Sci U S A, 1994. **91**(5): p. 1721-5.

99. Sigman, D.S., et al., *Nuclease activity of 1,10-phenanthroline-copper in study of protein-DNA interactions*. Methods Enzymol, 1991. **208**: p. 414-33.

100. Sambrook, J., E.F. Fritsch, and T. Maniatis, *Molecular cloning : a laboratory manual*. 2nd ed. 1989, Cold Spring Harbor, N.Y.: Cold Spring Harbor Laboratory. 3 v.

101. Eberharter, A., et al., *Acf1, the largest subunit of CHRAC, regulates ISWI-induced nucleosome remodelling*. Embo J, 2001. **20**(14): p. 3781-8.

102. Asturias, F.J., et al., *Electron microscopic analysis of the RSC chromatin remodeling complex*. Methods Enzymol, 2004. **376**: p. 48-62.

103. Kagalwala, M.N., et al., *Topography of the ISW2-nucleosome complex: insights into*

nucleosome spacing and chromatin remodeling. Embo J, 2004. **23**(10): p. 2092-104.

104. Clapier, C.R., et al., *Critical role for the histone H4 N terminus in nucleosome remodeling by ISWI*. Mol Cell Biol, 2001. **21**(3): p. 875-83.

105. Saha, A., J. Wittmeyer, and B.R. Cairns, *Chromatin remodeling through directional DNA translocation from an internal nucleosomal site*. Nat Struct Mol Biol, 2005. **12**(9): p. 747-55.

106. Schwanbeck, R., H. Xiao, and C. Wu, *Spatial contacts and nucleosome step movements induced by the NURF chromatin remodeling complex*. J Biol Chem, 2004. **279**(38): p. 39933-41.

107. Kassabov, S.R., et al., *High-resolution mapping of changes in histone-DNA contacts of nucleosomes remodeled by ISW2*. Mol Cell Biol, 2002. **22**(21): p. 7524-34.

108. Whitehouse, I., et al., *Evidence for DNA translocation by the ISWI chromatin-remodeling enzyme*. Mol Cell Biol, 2003. **23**(6): p. 1935-45.

109. Dumont, S., et al., *RNA translocation and unwinding mechanism of HCV NS3 helicase and its coordination by ATP*. Nature, 2006. **439**(7072): p. 105-8.

110. Tsukiyama, T., et al., *Characterization of the imitation switch subfamily of ATP-dependent chromatin-remodeling factors in Saccharomyces cerevisiae*. Genes Dev, 1999. **13**(6): p. 686-97.

111. Smith, C.L. and C.L. Peterson, *A conserved Swi2/Snf2 ATPase motif couples ATP hydrolysis to chromatin remodeling*. Mol Cell Biol, 2005. **25**(14): p. 5880-92.

112. Tsukiyama, T. and C. Wu, *Purification and properties of an ATP-dependent nucleosome remodeling factor*. Cell, 1995. **83**(6): p. 1011-20.

113. Brehm, A., et al., *dMi-2 and ISWI chromatin remodelling factors have distinct nucleosome binding and mobilization properties*. Embo J, 2000. **19**(16): p. 4332-41.

114. Asturias, F.J., et al., *Structural analysis of the RSC chromatin-remodeling complex*. Proc Natl Acad Sci U S A, 2002. **99**(21): p. 13477-80.

115. Bondarenko, V.A., et al., *Nucleosomes can form a polar barrier to transcript elongation by RNA polymerase II*. Mol Cell, 2006. **24**(3): p. 469-79.